PHD THESIS

FUNGAL EICOSANOID BIOSYNTHESIS INFLUENCES THE VIRULENCE OF CANDIDA PARAPSILOSIS

TANMOY CHAKRABORTY

SUPERVISOR:

DR. ATTILA GÁCSER
ASSOCIATE PROFESSOR

DOCTORAL SCHOOL IN BIOLOGY

UNIVERSITY OF SZEGED
FACULTY OF SCIENCE AND INFORMATICS
DEPARTMENT OF MICROBIOLOGY

2018

SZEGED

TABLE OF CONTENTS

ABBREVIATIONS

15-k-PGE_2	15-keto-Prostaglandin E_2
AIDS	Acquired immune deficiency syndrome
BLAST	Basic Local Alignment Search Tool
BPS	Bathophenanthrolinedisulfonic acid
BSA	Bovine serum albumin
CFU	Colony forming unit
CGD	Candida Genome Database
CR	Congo red
CW	Calcofluor white
DMSO	Dimethyl sulfoxide
DNA	Deoxyribonucleic acid
DTT	Dithiothreitol
EDTA	Ethylene diamine tetra-acetic acid
ELISA	Enzyme-linked immunosorbent assay
EtBr	Ethidium Bromide
FBS	Fetal bovine serum
GFP	Green fluorescent protein
GM-CSF	Granulocyte macrophage colony-stimulating factor
HIV	Human immunodeficiency virus
IL10	Interleukin 10
IL1β	Interleukin 1 beta
IL8	Interleukin 8
LB	Luria-Bertani medium
LC/MS	Liquid chromatography/Mass spectrometry
LDH	Lactate dehydrogenase
LiAc	Lithium acetate

LXA_4	LipoxinA_4
$MgCl_2$	Magnesium chloride
NAT	Nourseothricin N-acetyltransferase
ORF	Open reading frame
PAGE	Polyacrylamide gel electrophoresis
PBMC	Peripheral blood mono-nuclear cells
PBMC-DM	Peripheral blood mono-nuclear cells derived macrophages
PBS	Phosphate buffered saline
PCR	Polymerase chain reaction
PGD_2	Prostaglandin D_2
PGE_2	Prostaglandin E_2
PS	Penicillin-Streptomycin
qPCR	Quantitative real time polymerase chain reaction
RNA	Ribonucleic acid
RPMI	Roswell Park Memorial Institute medium
RT	Room temperature
SDS	Sodium Dodecyl Sulphate
TE	Tris-EDTA
TMB	Tetramethylbenzidine
TNFα	Tumor necrosis factor alpha
TRIS	Tris- (hydroxymethyl) aminomethane
XTT	2-methoxy-4-nitro-5-sulfophenyl)-5-[(phenylamino)-carbonyl]-2H-tetrazolium
YNB	Yeast nitrogen base
WGA-TRITC	Wheat germ agglutinin conjugated to tetramethylrhodamine isothiocyanate-dextran
FITC	Fluorescein isothiocyanate

LIST OF FIGURES

Introduction

Results

LIST OF TABLES

Introduction

1.1 Eicosanoid lipid mediators

Eicosanoids are bioactive lipid molecules, generally act locally affecting either on the cells producing them (autocrine function), or nearby cells (paracrine function). The name eicosanoid is derived from the Greek word 'eicosa' which means 'twenty', refers to the presence of 20 carbon atoms in these molecules. The preferred IUPAC (International Union of Pure and Applied Chemistry) name is 'icosanoid', although, this is largely ignored in the scientific literature. In most cases they are different from systemic hormones, because eicosanoids have much shorter half-lives than hormones. They control various functions, mainly during inflammation or in immunity, and also act as messengers in the central nervous system. Inhibition of the formation or the receptor-mediated actions of classical eicosanoids such as prostaglandins by aspirin and other non-steroidal anti-inflammatory drugs (NSAIDs) still remains the best strategy to alleviate pain, swelling, fever and asthmatic conditions [1].

1.1.1 Different classes of eicosanoids

Eicosanoids are either derived from omega-3 (ω-3) or omega-6 (ω-6) essential fatty acids such as eicosapentaenoic acid (EPA) (an ω-3 fatty acid with 5 double bonds); arachidonic acid (AA) (an ω-6 fatty acid, with 4 double bonds) or dihomo-gamma-linolenic acid (DGLA) (an ω-6, with 3 double bonds). Eicosanoids are divided into three main classes: prostanoids (prostaglandins, prostacyclins, thromboxanes), leukotrienes and lipoxins (Fig 1) [2].

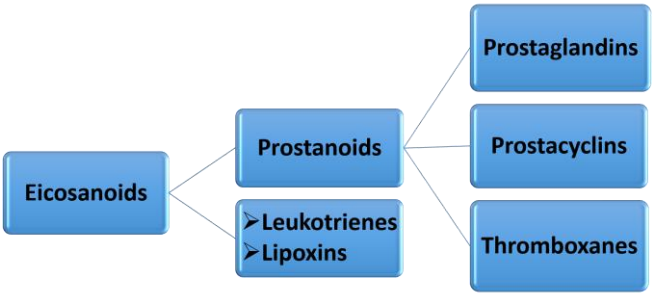

Fig 1: Classification of eicosanoids

Eicosanoids can be separated into three main groups, which are prostanoids, leukotrienes and lipoxins.

The prostanoids (prostaglandins, thromboxanes and prostacyclins) have distinctive ring

structures in the center of the molecule (Fig 2), while the hydroxyeicosatetraenes (HETE) are apparently simpler in structure, being precursors for families of more complex molecules, such as leukotrienes and lipoxins. Leukotrienes and prostanoids are sometimes termed as "classic eicosanoids", whereas hepoxilins, resolvins, isofurans, isoprostanes, lipoxins, epi-lipoxins and epoxyeicosatrienoic acids (EETs) can be termed as "non-classic" eicosanoids [3,4].

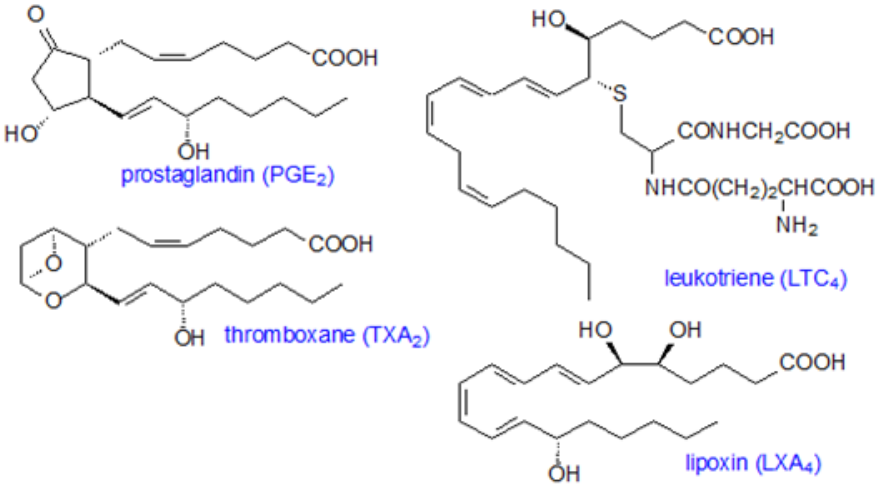

Fig 2: Chemical structure of key eicosanoids
Chemical structures of prostaglandin E_2, thromboxane A_2, leukotriene C_4 and lipoxin A_4.

1.1.2 Eicosanoid biosynthesis and receptor signaling

Eicosanoid production is initiated by phospholipases that mediate the release of arachidonic acid from the cell membrane. They arise from the oxidation of arachidonic acid and related PUFAs by cyclooxygenases (COX) [5], lipoxygenases (LOX) [6] and cytochrome P450 (CYP) enzymes, or via non-enzymatic free radical mechanisms. Their activity is generally facilitated by binding to G-protein coupled receptors (GPCRs) and peroxisomal proliferator-activated receptors (PPARs) on the surface of different cells. Eicosanoid biosynthetic pathways and their corresponding receptors are shown in Fig 3.

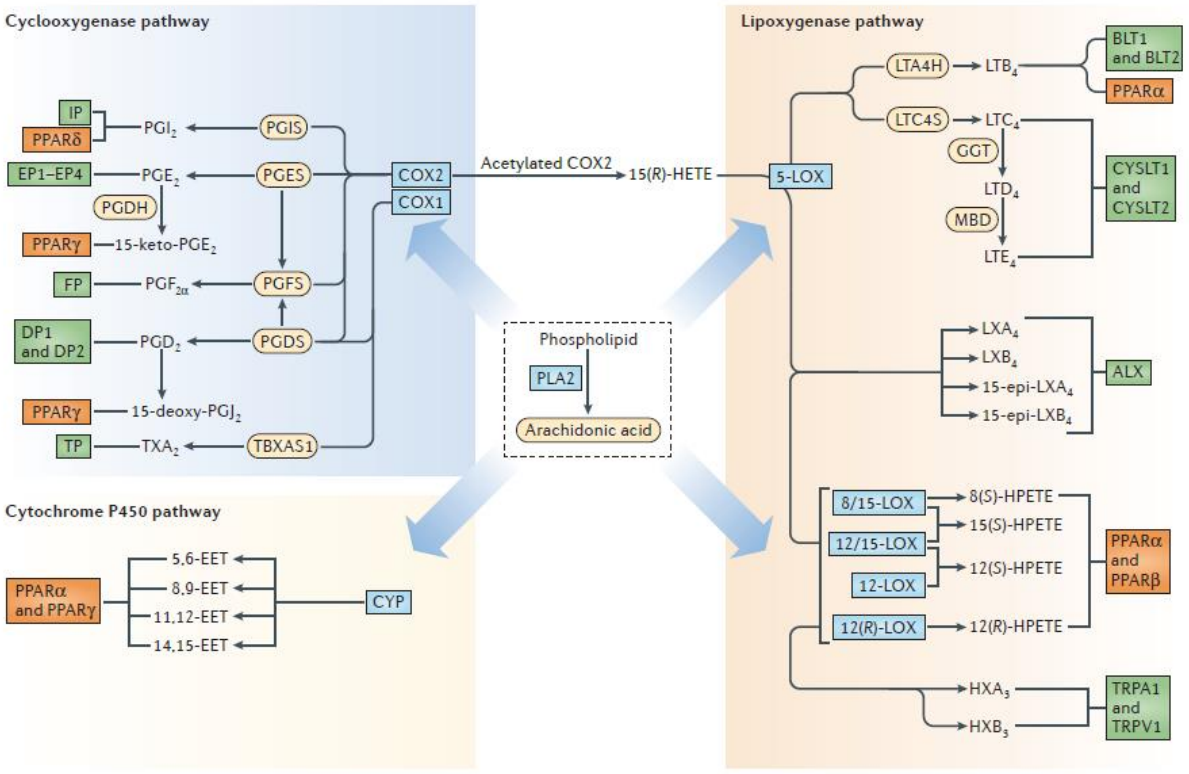

Fig 3: Eicosanoid biosynthetic pathways and receptors of different eicosanoids. Schematic presentation of phospholipase A2 (PLA2), cyclooxygenase 1 (COX1), COX2, 5-lipoxygenase (5-LOX), 8-LOX, 12-LOX, 15-LOX and cytochrome P450 (CYP) pathways of eicosanoid biosynthesis from arachidonic acid. Orange and green boxes are showing the corresponding receptors for the eicosanoids [4].

There are at least nine prostaglandin receptors that have been identified in humans and mouse (EP1–EP4 for PGE_2; DP1 and DP2 for PGD_2) and the receptors that bind $PGF_{2\alpha}$, PGI_2, and TxA_2 (FP, IP, and TP, respectively). All of these receptors belong to the GPCR family of transmembrane proteins and each is encoded by different genes [7,8]. Four leukotriene binding receptors were also identified which belong to the same family. Peroxisomal proliferator-activated receptors (PPARs) can also be activated by a variety of eicosanoids; PPAR-α by LTB_4 and 8(S)-HETE, PPAR-γ by 15-deoxy-delta-12,14-PGJ_2 (a dehydration metabolite of PGD_2), and PPAR-δ by prostacyclin analogs [1,4]

1.1.3 Pro-inflammatory function

The functional significance of eicosanoid lipid mediators in infection and immune regulation is revealed by experiments performed with knock out mice. The early events of the inflammation such as vasodilation and increased permeability of post-capillary venules are generally elicited by prostaglandins and leukotrienes at the site of inflammation. The signs of inflammation include heat, swelling, redness, pain and loss of function [9]. Although eicosanoids derived from the enzymatic action of COX pathways control a wide range of processes, eicosanoids from the 5-LOX pathway are more relevant during inflammation to promote bronchoconstriction [10] and leukocyte recruitment to the sites of tissue damage [11,12]. In some cases, this natural phenomenon of leukocyte recruitment to a site of acute inflammation can be fatal to the host during toxic or septic shock. It has been shown that, prostaglandins produced via COX1 (also known as PTGS1) during inflammasome activation contribute to excessive vascular leakage that is lethal in mice [9]. However, the role of COX1 derived PGE_2 is more complicated during inflammation as PGE_2 acts both as a pro-inflammatory and an anti-inflammatory cytokine depending on the context. For example, in neurons, the binding of PGE_2 to its cognate G protein-coupled receptors (GPCRs) causes pain associated with inflammation, but autocrine EP signaling by PGE_2 in macrophages (and possibly in other leukocytes) can downregulate the production of tumor necrosis factor (TNF) and upregulate IL-10 secretion, leading to a net reduction in inflammatory signaling [13]. While the functions of 5-LOX-derived leukotrienes in asthma and allergy are well understood, biological functions of the intermediate metabolites 8-hydroperoxyeicosatetraenoic acid (8-HPETE), 12-HPETE and 15-HPETE, as well as their hydroxyeicosatetraenoic acid (HETE) products, have not yet been defined [14].

1.1.4 Anti-inflammatory function

An effective host defense mechanism in response to infection by pathogens involves inflammation in order to eliminate the invading pathogen. This event is followed by the systemic and local production of endogenous mediators that counterbalance these proinflammatory events and restore tissue homoeostasis [12]. In recent years, studies have uncovered new endogenous anti-inflammatory lipid mediators that have potent immunomodulatory and anti-inflammatory effects. These anti-inflammatory/pro-resolving

lipid mediators can be divided into two classes: the lipoxins and the cyclopentenone prostaglandins (cyPGs) [15]. Lipoxins are usually generated *in vivo* by the action of lipoxygenase or the concerted action of lipoxygenase (5-LO, 15-LO, and 12-LO) and cyclooxygenase enzymes, whereas the cyPGs are spontaneous prostaglandin metabolites that are formed by cyclooxygenases [2].

Lipoxins have a short half-life and act in nanomolar concentrations. Their mechanism of action involves blocking of neutrophil migration across postcapillary venules and inhibiting neutrophil entry into inflamed tissues in animal models [16]. They also promote the phagocytic clearance of apoptotic cells by macrophages, which might further contribute to the resolution of inflammation [17]. Cyclopentenone prostaglandins are also produced by cyclooxygenase 2 enzymes. Studies have shown that although COX2 mainly drives the onset of inflammation through the production of the pro-inflammatory prostaglandin E2 (PGE_2), it also helps in the resolution of inflammation through the synthesis of anti-inflammatory cyPGs such as 15deoxyΔ12,14PGJ_2 (15dPGJ_2) [18]. It has been shown that 15dPGJ_2 can inhibit TNF-stimulated expression of adhesion molecules such as the vascular cell adhesion molecule 1 (VCAM1) and the intercellular adhesion molecule 1 (ICAM1) by primary human endothelial cells [4]. Suppression of pro-inflammatory signaling pathways, including nuclear factor-κB (NF-κB), AP1 and signal transducers and activators of transcription (STATs) in macrophages by 15dPGJ_2 has also been described in recent years [19]. Synthetic analogues of these pro-resolving molecules have been shown as promising therapeutic agents in several disease models [20].

1.1.5 Role of eicosanoids (PGE_2) in antifungal immunity

Fungal infection can also induce the production of lipid mediators in different host cells. It has been shown that during *C. albicans* infection, the binding of dectin-1,2 receptor to the fungal cell wall β-glucan activates the cytosolic phospholipase A_2 ($cPLA_2\alpha$) production in resident mouse peritoneal and alveolar macrophages [21,22]. cPLA2 releases arachidonic acid (AA) that is further processed into a number of bioactive lipid mediators such as prostaglandins and leukotrienes. It has also been established that the MyD88 pathway is also involved in this process [22]. β-glucan in the cell wall of *Candida* species also induces PGE_2 production by human dendritic cells and primary macrophages that has been reported to play a role in the Th17 cell response during infection [23,24]

1.2 Eicosanoid production by human fungal pathogens

Human fungal pathogens belonging to different families can produce a variety of eicosanoids from external arachidonic acid. These include *C. albicans*, *C. parapsilosis*, *C. dubliniensis*, *C. tropicalis*, *Cryptococcus neoformams*, *Aspergillus fumigatus*, *Histoplasma capsulatum* and *Paracoccidioides brasiliensis*. A summary of the oxylipins produced by fungi is provided in Table 1.

Table 1. Eicosanoids in human fungal pathogens

Species	Eicosanoid	References
Aspergillus fumigatus	cysteinyl leukotrienes; LTB_4; PGD_2; PGE_2; $PGF_{2\alpha}$; prostaglandins	Noverr et al., 2002; Tsitsigiannis et al., 2005a
Aspergillus nidulans	hydroxylated C18 fatty acids (psi factors); prostaglandins	Mazur et al., 1990, 1991; Tsitsigiannis et al., 2005
C. albicans	1-OH-3,7,11-trimethyl-2,6,10-dodecatriene; 3(*R*)-HTDE; 3-OH-PGE2; 3,18 di-HETE; cysteinyl leukotrienes; LTB_4; PGD_2; PGE_2; $PGF_{2\alpha}$	Alem & Douglas, 2004, 2005; Ciccoli et al., 2005; Deva et al., 2000, 2001; Ells, 2008; Erb-Downward & Huffnagle, 2007; Erb-Downward & Noverr, 2007; Nickerson et al., 2006; Nigam et al., 2011; Noverr et al., 2001, 2002; Oh et al., 2001; Shiraki et al., 2008
C. dubliniensis	3,18 di-HETE	Ells, 2008
C. glabrata	PGE_2	Shiraki et al., 2008
C. tropicalis	PGE_2	Shiraki et al., 2008
C. parapsilosis	PGE_2, PGD_2	Grozer et al, 2015
Cryptococcus neoformans	3-OH 9:1; cysteinyl leukotrienes; LTB_4; PGD_2; PGE_2; $PGF_{2\alpha}$	Erb-Downward & Huffnagle, 2007; Erb-Downward & Noverr, 2007; Noverr et al., 2001,

		2002; Sebolai et al., 2007
Histoplasma capsulatum	cysteinyl leukotrienes; LTB_4; PGD_2; PGE_2; $PGF_{2\alpha}$	Noverr et al., 2002
Paracoccidioides brasiliensis	PGE_X	Biondo et al., 2010; Bordon et al., 2007

1.2.1 Eicosanoid biosynthetic pathways in the human fungal pathogens

Although the production of eicosanoids by human pathogenic fungi was reported almost three decades ago, the exact process of their biosynthesis is still not properly understood. The situation becomes more complicated by the fact that extensive searches in fugal genome databases have not revealed any sequences that have significant similarity with mammalian cyclooxygenases or lipoxygenases [25]. One exception is, the *Aspergillus spp*. where the psi factor-producing oxygenases (Ppo proteins), are a well characterized class of cyclooxygenase-like enzymes [26,27]. Interestingly, experiments performed with COX/LOX inhibitors to explore probable pathways or identify enzymes in different fungal species have diverse effects on prostaglandin synthesis. For example, prostaglandin synthesis was inhibited in *C. albicans*, *Cr. neoformans* and *P. brasiliensis* in the presence of indomethacin or aspirin and in some cases the pretreatment also resulted in reduced viability [28,29].

After the *in silico* identification of cyclooxygenase homologues in *Aspergillus spp*., it has been shown that deletion of the *ppoA*, *ppoB* and *ppoC* genes significantly reduced the amount of PGE_2 production in both *A. nidulans* and *A. fumigatus* [27]. While in case of *C. albicans* strains lacking a fatty acid desaturase gene *OLE2* or multicopper oxidase gene *FET3* showed a highly reduced ability to form PGE_2 [30]. *Cr. neoformans* also showed the same reduction of PGE_2 production when the multicopper oxidase gene *LAC1* (laccase) was deleted from the genome [31]. Recently, it was shown that the fungus *Paracoccidioides brasiliensis* also utilizes both exogenous and endogenous AA for the synthesis of PGE_X [29,32], although the biosynthetic pathways involved in this mechanism are still unknown (Fig 4).

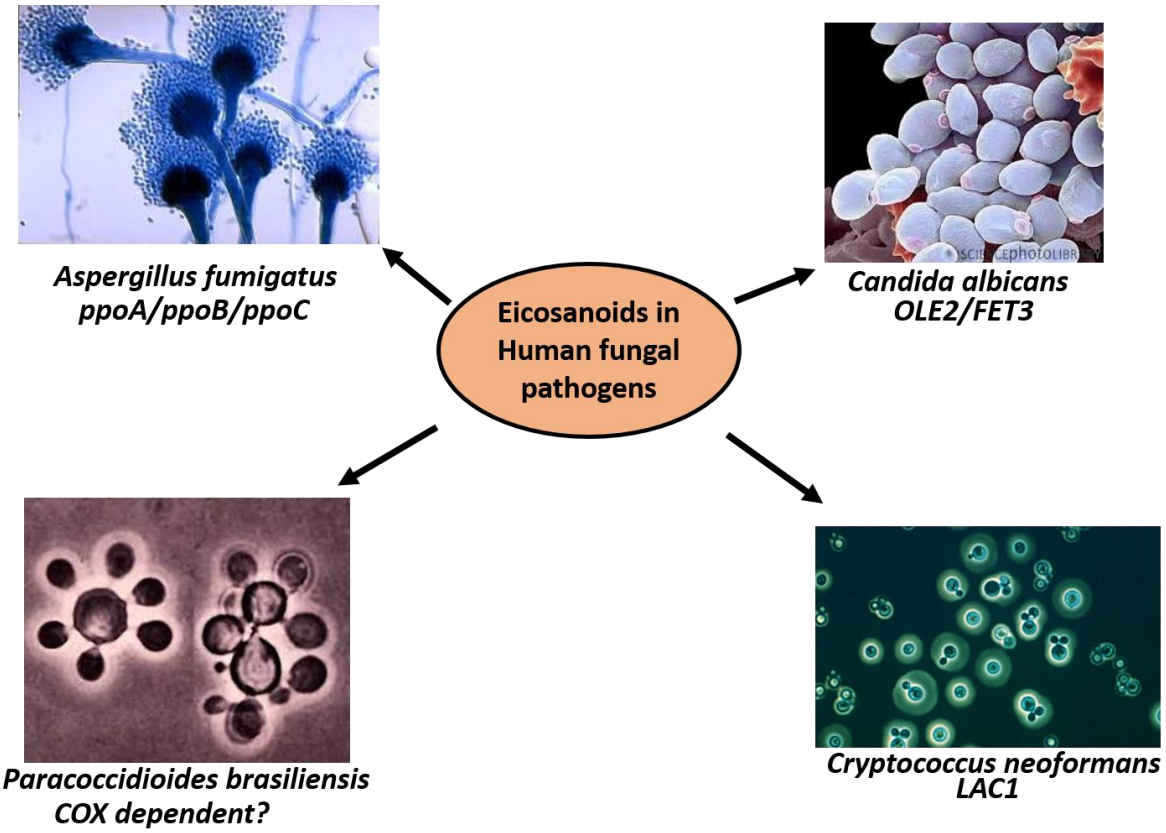

Fig 4: Genes identified for prostaglandin production in human fungal pathogens
Genes involved in prostaglandin biosynthetic pathways in the human fungal pathogens *C. neoformans* (*LAC1/LAC2*), *C. albicans* (*FET3/OLE2*) and *A. fumigatus* (*ppoA/ppoB/ppoC*).

1.2.2 Role of fungal lipid mediators in pathogenesis

The fungal prostaglandins play important roles in development and pathogenesis [33]. It has been shown that PGE_2 induces yeast to hyphal transition in *C. albicans*, an important virulence trait of the fungi [34–36]. In case of *Cr. neoformans*, the deletion mutants of the cryptococcal phospholipase B (*PLB*) or the cryptococcal laccase (*LAC*) enzyme, that have been identified as PGE_2 production regulators, are less virulent in mice compared to the wild type strain [37,38]. The fungal prostaglandins produced by these two species have also been confirmed to have immunomodulatory functions [39]. In contrast, in *A. nidulans* the triple *ppo* mutant was found to be hypervirulent in a mouse model of invasive aspergillosis. Although, the deletion of the *PPO* genes in *Aspergillus fumigatus* decreases spore production, reduces the ability to colonize peanut seeds and alter the production of secondary metabolites. Besides classical eicosanoids, *C. albicans* also produces farnesol, a

non-classical eicosanoid molecule. This was the first reported quorum-sensing molecule with nonbacterial origin. It plays an important role in biofilm formation in *C. albicans* [40] and functions as a mating factor in *Cr. neoformans* [41]. *Cr. neoformans* also produces PGE_2, which plays an important role in antifungal immune response. It inhibits interferon regulatory factor 4 function and interleukin-17 expression in T Cells during infection [42].

1.3 *Candida parapsilosis,* a significant neonatal pathogen

The increased incidence and high mortality rate of fungal infections have become a serious concern in hospitals since the early 1990s [43]. Among different pathogenic fungi, *Candida* spp. remain the most prevalent cause of invasive fungal infections, exceeding invasive aspergillosis and mucormycosis [44,45]. Although, *C. albicans* is still the most common cause of invasive candidiasis, bloodstream infections caused by non-*albicans Candida* species such as *C. glabrata*, *C. krusei*, *C. auris*, *C. parapsilosis*, and *C. tropicalis*, altogether have risen to account for approximately one-half of all candidemia cases (Fig 5) [44,46].

C. parapsilosis is ubiquitous in nature and also found on human skin as a commensal. It can also be frequently isolated from the gastrointestinal tract [47]. It is the leading cause of invasive fungal infections in premature infants [48]. Among non-*albicans Candida* spp., the incidence of *C. parapsilosis* is increasing in this particular patient group and in some hospitals it even outnumbers *C. albicans* infections [49]. *C. parapsilosis* is known for its presence in the hospital environment and ability to grow in total parenteral nutrition. It also can form biofilms on catheters and other implanted devices [50,51]. Risk factors that are associated with *C. parapsilosis* driven neonatal candidiasis includes low birth weight (<1500 g), prematurity, prior colonization, the use of parenteral nutrition, intravascular catheters and prolonged treatment with antibiotics or steroids [52]. *C. parapsilosis* cells are generally oval, round, or have cylindrical shapes and can form white, creamy, shiny, and smooth or wrinkled colonies on Sabouraud D-Glucose agar. Unlike *C. albicans* and *C. tropicalis*, *C. parapsilosis* does not form true hyphae and exists in either a yeast or a pseudohyphal form [53].

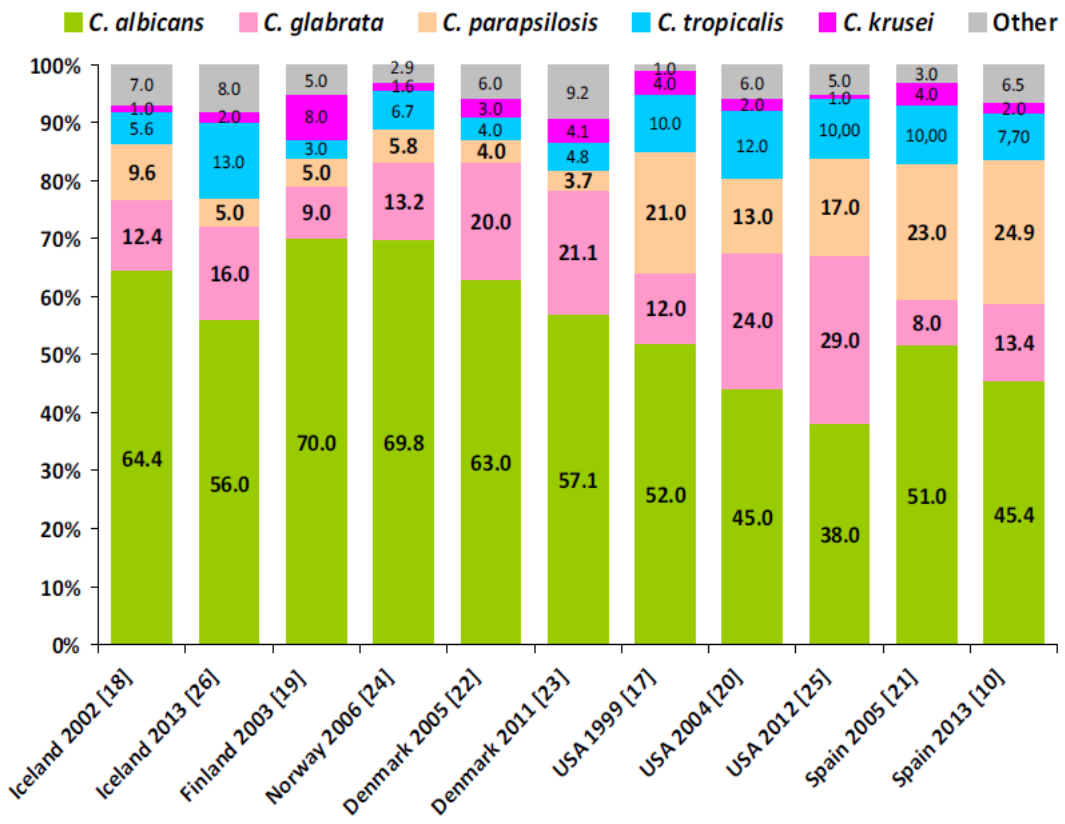

Fig 5: Distribution of *Candida* species in a population-based study with data acquired from different countries

Graph showing the proportion of different *Candida* species in different countries. While *C. albicans* is the most frequently isolated fungi from invasive candidiasis patients, *C. parapsilosis* remains the second or third most isolated species [44].

1.3.1 Classification of *C. parapsilosis*

Kingdom: Fungi

Phylum: Ascomycota

Subphylum: Saccharomycotina

Class: Saccharomycetes

Order: Saccharomycetales

Family: *Ascomycetes*

Genus: *Candida*

Species: *parapsilosis*

1.3.2 CTG clade of ascomycetes fungi

This group of fungi belongs to *Ascomycetes* family, where the universal leucine codon CUG is predominantly translated to serine is called CTG clade species [54]. There are at least 75 *Candida* species in this group with *Pichia stipitis*, *Debaryomyces hansenii* and *Lodderomyces elongisporus* (Fig 6) [55]. There are two distinct CTG sub-clades: one where the fungal species has a defined sexual cycle (*Candida lusitaniae*, *Candida guilliermondii*, *Debaromyces hansenii*) and the other one where the fungal species predominantly reproduce asexually (*Candida albicans*, *Candida dubliniensis*, *Candida tropicalis*, *Candida parapsilosis* and *Lodderomyces elongisporus*). This unusual codon translation is mediated by a Ser-tRNA$_{CAG}$ that can be recognized by two aminoacyl-tRNA synthetases: seryl- and leucyl-tRNA synthetase. The hydrophilic nature of serine compared to the hydrophobic leucine generates an array of proteins with different structure and function. Comparative genomic analysis of the orthologous genes from the CTG clade and the non-CTG clade species demonstrate that the original CUG codons are present in the genome of the ancestor of a CTG clade species. It has been reported that the CUG present in the genome of the CTG clade species evolved recently from Ser rather than Leu codons [56]. This mistranslation of the CUG codon generates an enhanced protein diversity which helps to expand the capacity of these organisms to different environmental conditions, suggesting that CUG ambiguity is a major generator of phenotypic diversity [57].

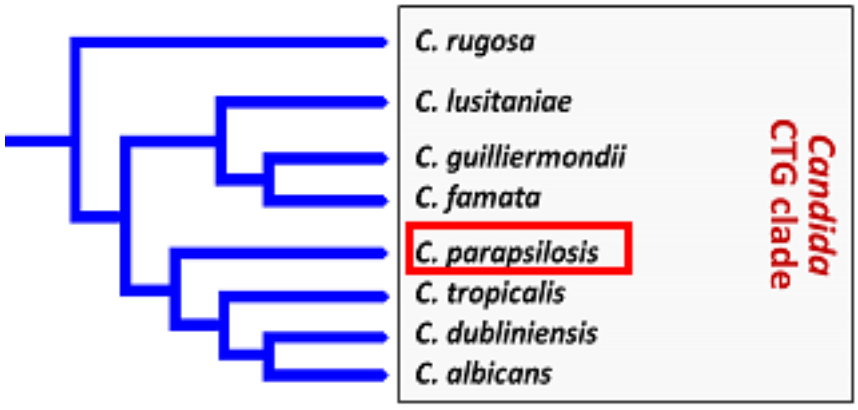

Fig 6: Phylogenetic tree showing the CTG clade of *Ascomycetes* fungi.
C. parapsilosis belongs to the CTG clade of Ascomycetes fungi, where the universal leucine codon CUG is predominantly translated to serine. The image has been adapted and modified from Papon *et al.*, 2013 [58]**.**

1.4 *C. parapsilosis* pathogenicity and virulence factors

Virulence factors associated with invasive *Candida* infections include many different factors. The virulence factors identified in *C. albicans* are adherence, hyphal morphogenesis, biofilm formation and the presence of secreted hydrolytic enzymes such as lipases, phospholipases and secreted aspartyl proteases. Although, extensive research has been done on *C. albicans* pathogenicity mechanisms, relatively less is known about the virulence determinants of *C. parapsilosis*. The key virulence traits of *C. parapsilosis* are shown schematically in Fig 7.

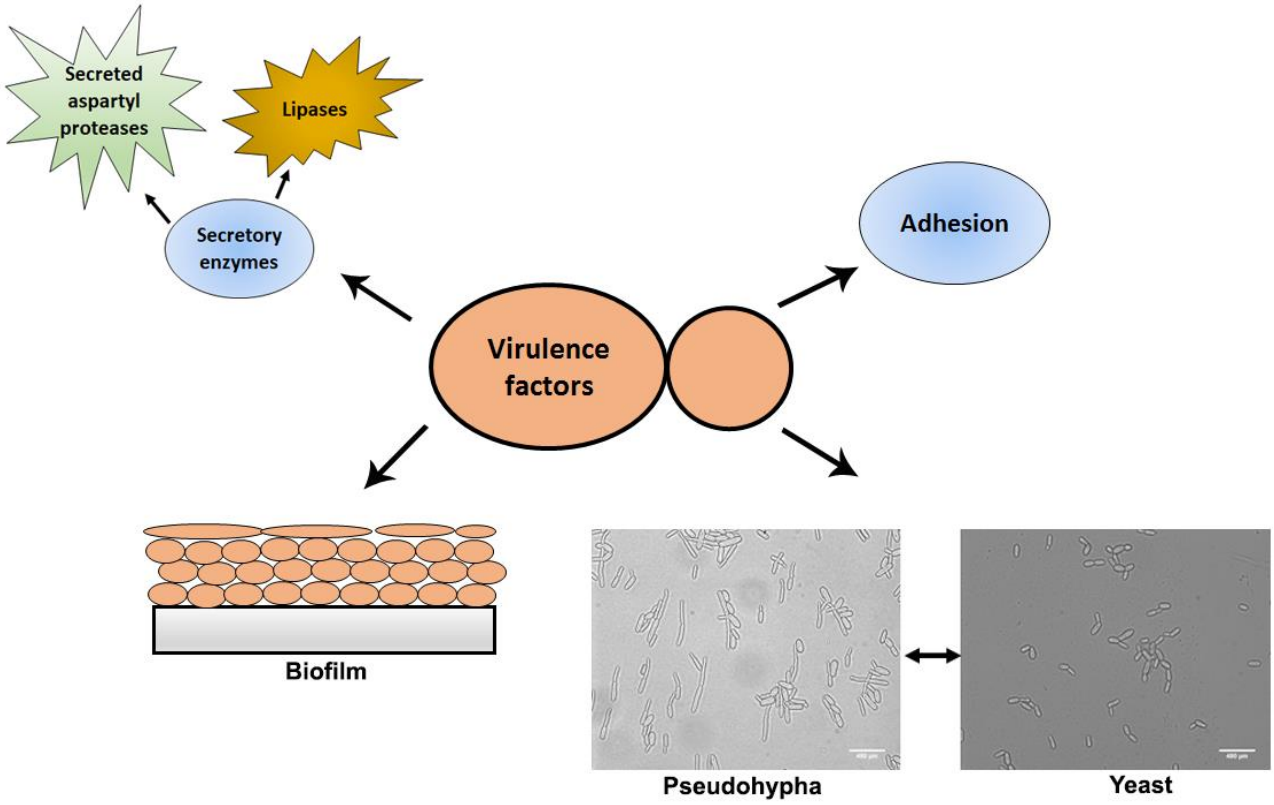

Fig 7: An overview of key virulence factors in *C. parapsilosis*
The key virulence traits of *C. parapsilosis* include adhesion, secretion of extracellular enzymes, yeast to pseudohyphal switch and biofilm formation.

1.4.1 Yeast to pseudohypha switch

Unlike *C. albicans*, *C. parapsilosis* does not form true hyphae, instead appears in a yeast or pseudohyphal form. Pseudohypha is comprised of a series of conjoined elongated yeast cells that have visible constrictions at septal sites. Although, the molecular mechanisms behind the morphogenetic transition is still unknown, it has been shown previously that amino acids (particularly citrulline) stimulate yeast to pseudohypha formation in *C. parapsilosis* [59]. Recently, two genes were identified that could regulate this morphological transition. Homozygous deletion mutant of the gene CPAR2_200390 appeared to form pseudohypha more rapidly compared to the wild type strain, whereas deletion of the CPAR2_501400 ORF resulted in a yeast-locked form. The *CPAR2_200390Δ/Δ* strain showed increased survival compared to the wild type strain with mouse macrophage infection [60]. However, they are less virulent in *Galleria mellonella* and mouse model of systemic infection [60]. The above facts show that, CPAR2_200390 plays a role in morphology as well as in cell wall homeostasis regulation and also contributes to virulence.

1.4.2 Biofilm formation

One of the most important virulence determinants of *C. parapsilosis* is its ability to form biofilm. Biofilms are complex three-dimensional structures formed by microorganisms on abiotic or biotic surfaces and are held together by an extracellular matrix. The different stages of biofilm formation include adhesion, maturation and dispersal. In contrast to the closely related species *C. albicans*, *C. parapsilosis* produces quantitatively less and structurally less complex biofilms [61]. However, certain pseudohypha forming strains of *C. parapsilosis* form more complex biofilms compared to the strains predominantly present in a yeast form [53]. *C. parapsilosis* has the ability to form biofilms on diverse medical devices, including central and peripheral venous catheters, hemodialysis and peritoneal dialysis catheters, intracardiac prosthetic devices, and prosthetic joints [62]. Like many other *Candida* species, the biofilm forming capacity of *C. parapsilosis* confers significant resistance to different antifungal drugs [63] and host immune response.

In a recent study, a complex network of six transcription factors (Efg1, Tec1, Bcr1, Ndt80, Rob1 and Brg1) have been identified that regulate biofilm formation in *C. albicans* [64].

Among these six transcription factors, the homologue of *EFG1* and *BCR1* also regulate biofilm formation in *C. parapsilosis*, as the deletion of these two genes results in a significant reduction in biofilm formation on abiotic surfaces [61,65]. Other than these two transcription factors, six additional genes (*CZF1*, *GZF3*, *UME6*, *CPH2*, *ACE2* and *MKC1*) were also found to play role in biofilm formation in *C. parapsilosis* [66].

1.4.3 Adhesion

Before colonization and infection, *Candida* cell adhere to host surfaces like epithelial cells or endothelium [67]. The ability to adhere also to abiotic surfaces such as catheters or prosthetic devices enables *Candida* cells to form biofilm. The most important proteins enabling the adhesion property of the fungal cells are the Als (Agglutinin-like sequence) proteins [68]. In *C. albicans*, 8 *ALS* genes (*ALS1-7* and *ALS9*) were identified which encode large cell surface glycoproteins [69]. Studies have also confirmed the role of *ALS1* and *ALS3* in *C. albicans* virulence [69]. On the contrary, we lack detailed information about adhesion mechanisms present in *C. parapsilosis*. Recent analysis of the *ALS* gene family in different clinical and environmental isolates of *C. parapsilosis* showed that the presence of *ALS* genes varies in these isolates [70]. Recently, Bertini et al. identified a gene in *C. parapsilosis*, CPAR2_404800 (ortholog of *C. albicans* ALS genes) that regulates adhesion, as its disruption significantly reduced the fungi's ability to adhere to human buccal epithelial cells. The deletion mutant was also less virulent in *in vivo* infection model [71,72].

1.4.4 Secreted enzymes

Microbial pathogens including fungi secrete a variety of extracellular enzymes, which play an important role in virulence. These include aspartic proteinases (Saps), phospholipases, and lipases.

Secreted aspartic proteinases:

Secreted aspartic proteinases are important virulence factors of *C. albicans*. While, *C. albicans'* genome contains ten different secreted aspartic proteinases (*SAP1-SAP10*) [73,74], only 3 have been identified in *C. parapsilosis* (*SAPP1*, *SAPP2* and *SAPP3*) [75]. This explain why *C. parapsilosis* displays less SAP activity compared to *C. albicans* [76].

Interestingly, *C. parapsilosis* isolates derived from different host niches display different SAP activity. Of these, isolates obtained from the skin or the vagina show increased SAP activity compared to those isolated from the blood [77]. In a recent study it has been shown that two copies of *SAPP1* are present in the *C. parapsilosis* genome [78]. Secreted aspartyl proteases play a role in pathogenesis via facilitating invasion and host tissue colonization by disrupting host mucosal membranes [79]. They also degrade host immune related proteins such as immunoglobulin G heavy chains, α2-macroglobulin, C3 protein, β-lactoglobulin, lactoperoxidase, collagen, and fibronectin [80]. Although, the function of the three *SAPP* genes is not completely understood in *C. parapsilosis*, the role of the Sapp1p has been well described. Deletion of both *SAPP1* genes (*SAPP1a* and *SAPP1b*) resulted in increased susceptibility to killing by human macrophages and the mutant were also sensitive to the presence of human serum, suggesting that *C. parapsilosis* Sapp1s acts similarly to *C. albicans* Saps [78].

Lipases and phospholipases:

Lipases are a class of enzymes that catalyze both the hydrolysis and synthesis of triacylglycerols [81]. Lipases secreted by microbial pathogens play a role in nutrient acquisition by liberation of free fatty acids from lipid molecules, promote adhesion to host surfaces and induce inflammatory response [82]. In *C. albicans*, ten lipase genes have been reported [83]. *LIP5*, *LIP6*, *LIP8* and *LIP9* were found to be expressed during experimental infection of mice and Lip8p was identified as a virulence factor [84]. Whereas, in *C. parapsilosis* two lipase genes (*LIP1* and *LIP2*) have been identified to date and only *LIP2* codes for an active protein [85]. It has been shown that fungal lipases act as major virulence determinant, in *C. parapsilosis*, as the mutant strain lacking lipase activity formed thinner and less complex biofilms, had reduced growth in lipid-rich media, was more efficiently ingested and killed by human monocyte derived dendritic cells, caused less damage to reconstituted human oral epithelium and was less virulent *in vivo* [86]. It has also been found that human macrophages stimulated with the *C. parapsilosis* $lip^{-/-}$ strain produced more pro-inflammatory cytokines such as TNFα, IL-1β, and IL-6 compared to the wild-type strain [87,88].

The role of phospholipases in the virulence of *C. parapsilosis* has not yet been clarified.

1.5 Prostaglandin production by *C. parapsilosis*

C. parapsilosis, like other pathogenic fungal species, is able to produce different types of prostaglandins in the presence of exogenous arachidonic acids. The prostaglandin profile of *C. parapsilosis* is similar to that of *C. albicans*, with PGE_2 and PGD_2 being predominantly produced (Fig 8). Although, unlike in case of *C. albicans*, the fatty acid desaturase homologue gene *OLE2*, does not play a role in their synthesis [89].

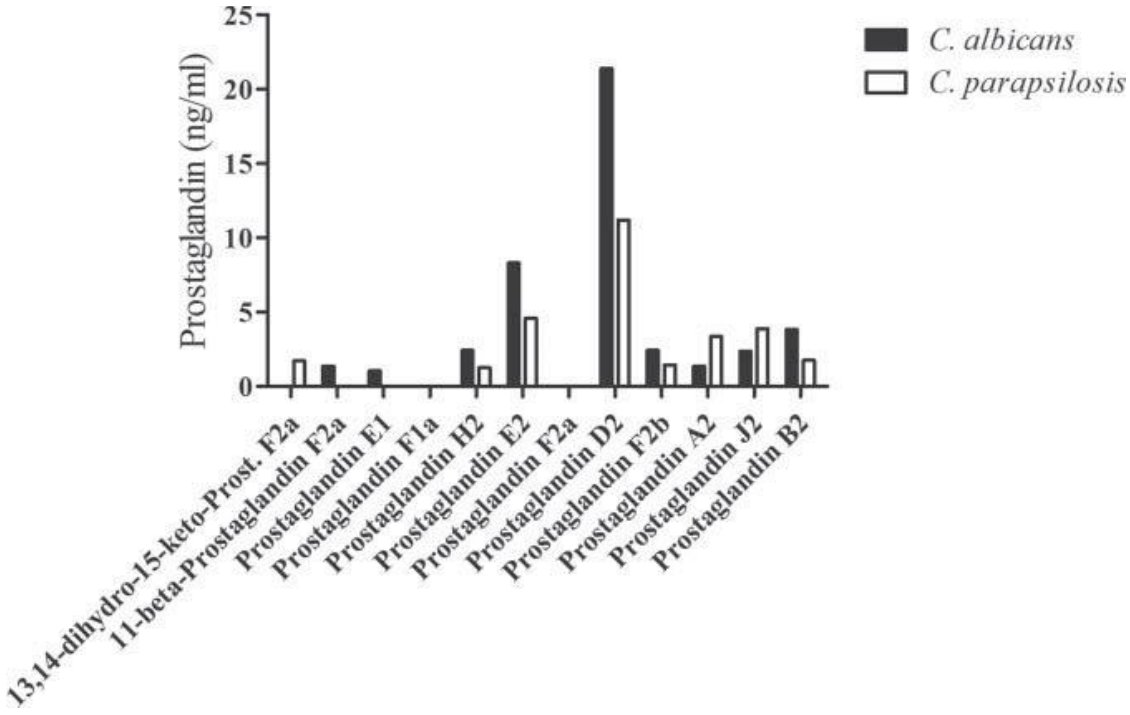

Fig 8: Prostaglandin profile of *C. parapsilosis and C. albicans*
Comparison of the prostaglandin profiles of *C. albicans* and *C. parapsilosis* by LC/MS analysis [89].

1.6 Antifungal immune response against *Candida spp.*

The majority of our knowledge regarding host defenses against *Candida* spp. is based on investigations performed with *C. albicans*. There are three main steps involved in the innate immune response against *C. albicans* infection. The first step in this cascade is the recognition of different PAMPs (**P**athogen **A**ssociated **M**olecular **P**attern) present on the fungus by several PRRs (**P**attern **R**ecognition **R**eceptor) present on the surface of host

immune cells. The main PAMPs recognized by the host are found in the fungal cell wall. The outer layer is mainly composed of O- and N-linked glycoproteins, the majority of which (approx. 80–90%) consists of mannose, whereas the inner cell wall layer contains chitin, β-1,3-glucan and β-1,6-glucan [90]. The PRRs involved in this process include the Toll-like receptors (TLRs), C-type lectin receptors (CLRs), NOD-like receptors (NLRs) and RIG-I-like receptors (RLRs) (Fig 9) [91].

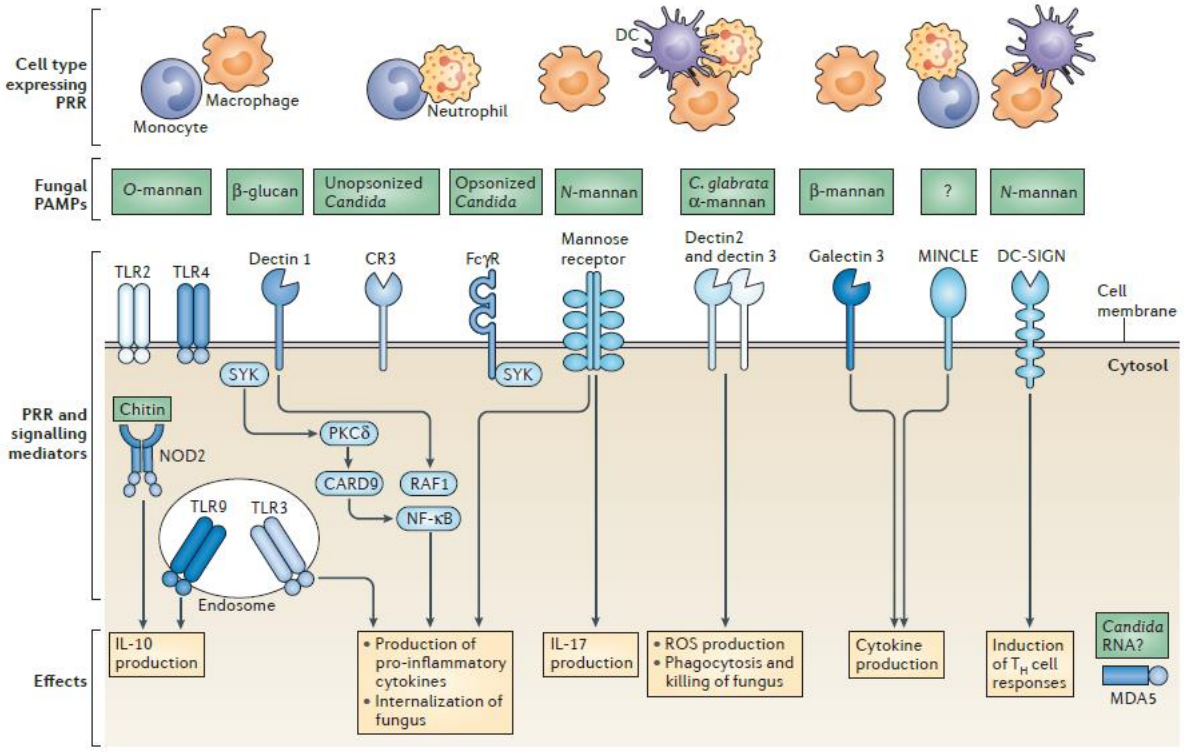

Fig 9: Recognition of different PAMPs of *Candida* species by host PRRs present in innate immune cells
Various receptors present on the surface of different innate immune cells such as TLR2, TLR4, dectin1, CR3, FcγR, mincle recognizes fungal cell wall components such as mannan and β-glucan leads to induction of antifungal immune response [90].

After the recognition, a chain of effector mechanisms ultimately lead to the clearance of the fungus. Different immune and non-immune cells are involved in the antifungal immune response. This includes epithelial cells, monocytes and macrophages, neutrophils, natural killer cells and dendritic cells. Epithelial cells mainly act as a physical barrier against tissue invasion by invading fungi. Tissue-resident macrophages produce inflammatory cytokines and chemokines that recruit and activate other immune cells at the site of infection.

Neutrophils are one of the most potent killers of *Candida*, which can kill fungal cells by both oxidative (reactive oxygen species) and non-oxidative (lysozyme, lactoferrin, elastase, β-defensins, gelatinases and cathepsin G) effector mechanisms. In addition to neutrophils, monocytes and macrophages, natural killer (NK) cells and dendritic cells also contribute to the rapid innate immune response against invading *Candida* cells [90].

1.6.1 Antifungal immune response against *C. parapsilosis*

The role of innate immune response and inflammasome activation during *C. albicans* infection is well known. Although, very limited knowledge is available regarding the immune response against *C. parapsilosis*. Previously, it has been shown that Dectin 1 is involved in the immune recognition of *C. parapsilosis* and it induces different T-cell responses in human primary macrophages compared to *C. albicans* [92]. It has also been reported that like *C. albicans*, *C. parapsilosis* activates the NLRP3 inflammasome, which in turn produces IL-1β in the human macrophage cell line (THP1) and also in primary human macrophages. The secretion of IL-1β induced by *C. parapsilosis* was also strongly dependent on TLR4, Syk, caspase-8 and NADPH-oxidase, while TLR2 and IRAK played a minor role in IL-1β release. Interestingly, while *C. albicans* induced a robust IL-1β release after a very short incubation time, *C. parapsilosis* was not able to stimulate the production of IL-1β after this short incubation period. Furthermore, *C. parapsilosis* was phagocytosed to a lesser extent, and induced significantly lower ROS production and lysosomal cathepsin B release compared to *C. albicans* [93].

1.7 Importance of micronutrients in human fungal pathogens

The importance of trace metals in mammalian biology is well understood. Trace metals such as iron, copper, zinc and manganese also play a pivotal role in the viability of different human bacterial and fungal pathogens as well as protozoan parasites. Their importance during the infection comes from the fact that these metals serve as cofactors for the functioning of a wide variety of enzymes including those with direct roles in virulence, such as metal-dependent superoxide dismutases (SODs), metalloproteases or melanin-producing

laccases. Therefore, an important host defense strategy against invading microbial pathogens is the 'nutritional immunity' [94]. One mechanism of nutritional immunity is when metals are actively restricted (e.g. bound to carrier proteins) from uptake by microbes. Another type of nutritional defense is when the concentration of metallic ions is locally increased to a toxic threshold to inhibit microbial growth [95].

Most research on metal homoeostasis in human pathogenic fungi has been focused on iron uptake. Iron plays a diverse role in cellular processes including respiration, mostly via incorporation of iron or the iron-containing prosthetic group heme into the active centers of key enzymes. Similar to iron, copper is also required for many biochemical reactions, although it rapidly becomes highly toxic at increased levels. Copper containing enzymes include the mitochondrial cytochrome c oxidase required for the respiratory electron transport chain, and cytoplasmic or cell-wall associated Cu-SOD that protect fungal cells from externally and internally generated oxidative stress [95]. After iron, zinc is the second most abundant trace metal in the host. Zinc is the structural co-factor of ubiquitously found zinc finger DNA-binding proteins in fungi [96]. It has been reported that about 8% of the yeast proteome is thought to bind zinc [97] and more than 400 yeast genes are required for growth under zinc limitation [98].These include proteins for endoplasmic reticulum (ER) function, oxidative stress resistance regulation, protein folding, vesicular trafficking and chromatin modification.

1.7.1 Iron homoeostasis and uptake mechanisms in *Candida albicans*

C. albicans is an opportunistic human fungal pathogen that can cause severe life-threatening infections in immunocompromised patients. As the fungus encounters many host niches, it has evolved complex mechanisms to survive and to tolerate iron limitations in the host. *C. albicans* acquires iron from three different sources within the host. These include hemoglobin (the oxygen binding protein of red blood cells), the transferrin family of proteins (transferrin and lactoferrin) and siderophores produced by other bacteria and fungi (Fig 10) [99].

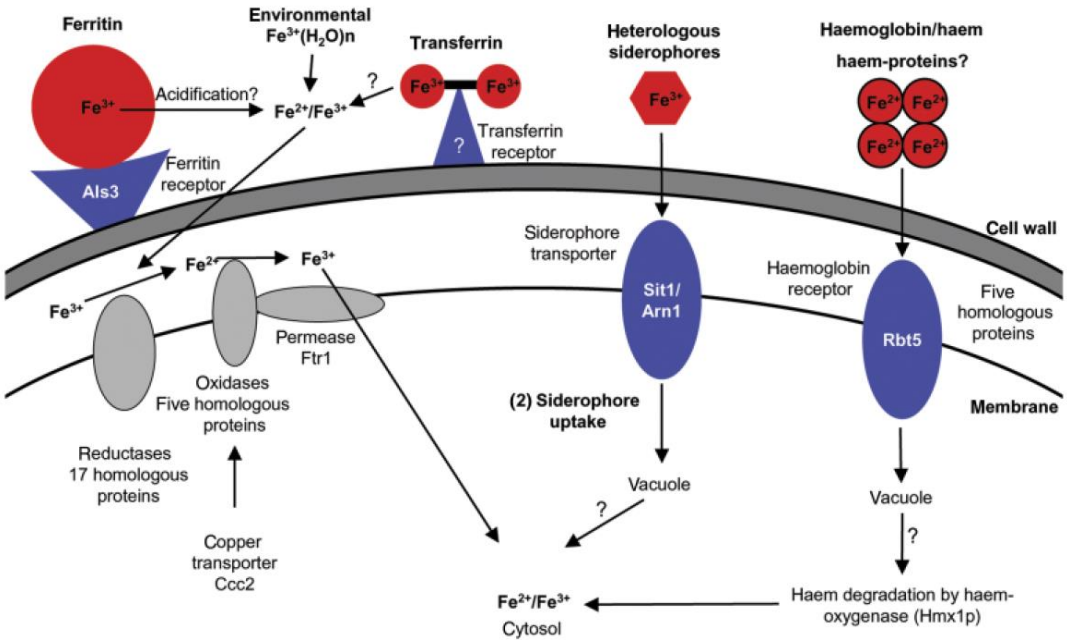

Fig 10: Iron uptake mechanisms in *C. albicans*
Different strategies used by *C. albicans* for exploitation of iron within host [100]**.**

There are five hemoglobin receptor genes that have been identified in *C. albicans*, namely *RBT5, RBT51, WAP1/CSA1, CSA2* and *PGA7* [101]. Two of these (*RBT5* and *RBT51/PGA10*) have been characterized *in vitro* as possessing hemoglobin-binding properties [102]. Although the molecular mechanisms of hemolysis by *C. albicans* is not fully understood, it has been reported that the haem oxygenase Hmx1 promotes the release of Fe^{2+} from hemoglobin. Although production of siderophore by *C. albicans* is still not proven, it can acquire siderophores of other microorganism by a membrane siderophore transporter. Homologue of yeast siderophore transporter Sit1/Arn1 mediate the uptake of a of siderophores in *C. albicans* [103]. Other than siderophores and hemoglobin, *C. albicans* can acquire iron from transferrin proteins with the help of the hypha associated protein Als3 [104]. Although, the iron releasing mechanism from transferrin is still not clearly understood. It has been suggested that the mechanism is pH dependent.

C. albicans uses the reductive pathway to utilize iron from the above-mentioned iron sources inside the host. This system is located on the plasma membrane and comprised of three different components. The first component being Cfl1/Fre1 and Cfl95/Fre10/Rbt2, two surface ferric reductases that reduce insoluble extracellular ferric (Fe^{3+}) ions into soluble ferrous (Fe^{2+}) ions [105]. The second component of the reductive pathway consists of

multicopper oxidases, as the ferrous ion spontaneously generates toxic free radicals, the multi copper oxidases oxidize the Fe^{2+} to Fe^{3+}. Five putative multicopper oxidases have been identified in the *C. albicans* genome. A *C. albicans* homozygous deletion strain lacking *FET3* is defective in *in vitro* high-affinity iron uptake. The third component comprises of iron permeases, that form a protein complex with multicopper oxidases and transport Fe^{3+} inside the cell. It has been reported that the high-affinity iron permease gene *FTR1* is induced and essential for growth upon iron deprivation and also necessary for iron acquisition from ferritin and transferrin [104–106]. Other than *FTR1*, two other putative iron permease genes (*FTH1* and *FTH2*) can also be found in the *C. albicans* genome.

1.7.2 Role of iron in commensalism and in the pathogenicity of *Candida albicans*

The iron concentration of the gut remains relatively high throughout the gastrointestinal tract [107]. Gastrointestinal commensals such as *C. albicans* thus face the risk of potential iron-associated toxicity (toxic free radicals generated in the Fenton reaction) [108], at least in some regions of the gut. *C. albicans* evolved a survival strategy to defend against iron-related toxicity in areas of iron excess, while retaining the capacity for aggressive iron uptake in host niches under iron depletion. In presence of high iron concentration, Sfu1 represses genes for iron uptake factors, including components of the hemoglobin uptake system and the reductive iron uptake system. It also downregulate the Sit1 siderophore transporter [103]. *SFU1* is also essential for defense against high iron concentrations *in vitro* and for normal commensal fitness in the mammalian gut [109]. The Hap43/CBP complex directly represses *SFU1* and genes for nonessential iron-utilizing processes, such as aerobic respiration and iron-sulfur cluster assembly under iron-depleted conditions [110–112]. Under these conditions, Sef1 directly activates *HAP43*, genes for all three modes of iron uptake, as well as virulence genes thought to act independently of iron. Sef1 also affects fitness in a gastrointestinal infection model, suggesting that at least some regions of the gut are effectively depleted of iron [113]. However, Sef1 is phosphorylated by the protein kinase, Ssn3, and transported into the nucleus, where it induces the transcription of iron uptake genes [113] under iron depleted condition.

Iron homoeostasis also plays a crucial role in *C. albicans* virulence. Although, a *C. albicans* strain lacking the multicopper oxidase gene *FET3* is defective in high-affinity iron uptake *in vitro*, it was as virulent as the wild-type strain in a mouse model of systemic infection, probably due to the activity of other multicopper oxidases during infection [114]. However, *Candida* cells lacking the high affinity iron transporter gene *FTR1* lost their ability to damage oral epithelial cells and were completely avirulent in mice [106], which demonstrated that this permease is crucial for *C. albicans* virulence.

2 Objectives

Over the last few years, various fungal species have been reported to produce bioactive lipid mediators. It has also been shown that the human pathogenic fungus, *C. parapsilosis* produces immunomodulatory prostaglandin molecules (PGD_2, PGE_2) from exogenously supplied arachidonic acid. However, the biosynthetic pathways are still unknown. Therefore, the objectives of the current study are as following:

1. Explore the fungal prostaglandin biosynthesis pathways in *C. parapsilosis*.
2. Finding the role of fungal eicosanoid molecules in virulence of *C. parapsilosis.*

Trace metal iron plays an important role in commensalism and also regulates the pathogenicity of the human fungal pathogen *C. albicans.* However, the molecular mechanisms of iron uptake and their role in *C. parapsilosis*' virulence is still unexplored. Thus, our further aims of this study are:

1. Analyze the role of a putative multi copper oxidase encoding gene, *CPAR2_603600* in iron metabolism.
2. Decipher the role of *CPAR2_603600* in morphology regulation and biofilm formation.

3 Materials and methods

3.1 Strains

All *Candida parapsilosis* strains used in this study are listed in supplementary table S1 and the oligonucleotide primers are listed in supplementary table S2.

3.2 Media and growth conditions

All strains were grown in YPD (1% D-Glucose, 1% peptone and 0.5% yeast extract) at 30 °C. For colony selection 2% agar was added to the media. NAT^R transformants were selected on YPD plates with 100 μg/ml nourseothricin. Transformants with *LEU2* and *HIS1* marker were selected on synthetic complete media (SC; 2% D-Glucose, 0.95% yeast nitrogen base, mixture of amino acid, 2% agar) without leucine and histidine. For biofilm analysis cells were grown on Spider media (1% peptone, 1% yeast extract, 1% mannitol, 0.5% NaCl and 0.2% K_2HPO_4) at 37 °C.

3.3 RNA extraction

For RNA sequencing, the *C. parapsilosis* GA1 strain was grown overnight in 2 ml of YPD media at 30 °C with continuous shaking applied at 180 rpm. The next day cells were washed 3 times with 1xPBS and then counted using a Burker's chamber. Cell concentration was adjusted to 2×10^7 cells per 10 ml 1xPBS supplemented with 500 μM of arachidonic acid (diluted in ethanol) in triplicates. As a control, cells were also grown in 10 ml 1xPBS supplemented with ethanol only, as it is the dissolving agent used for arachidonic acid solubilization. After 3 hours of growth at 30 °C, RNA was isolated using the Ribopure Yeast RNA isolation Kit (Ambion) following the manufacturer's instructions. For validating the RNA sequencing data, *C. parapsilosis* CLIB and GA1 cells were grown as described above and RNA extraction was performed using the same kit.

3.4 Reverse Transcription PCR

A total of 500 ng RNA was used for cDNA synthesis. The cDNA was synthesized using the

Revert Aid first Strand cDNA Synthesis Kit (Thermo Scientific) according to the manufacturer's instructions.

3.5 Real time PCR

Real time PCR was performed in a final volume of 20 µl using Maxima SYBR Green/Fluorescein qPCR Master Mix (2X) (Thermo Scientific). The reaction was performed in Thermal Cycler (Bio-Rad C1000 Thermal Cycler) using the following protocol: 95 °C for 3 minutes, 95 °C for 10 seconds, 60 °C for 30 seconds, 65 °C for 5 seconds for 50 cycles. Fold change in mRNA expression was calculated by ΔΔCt method (Real–Time PCR applications guide BIO-Rad). *TUB4* gene was used as a housekeeping gene for an internal control.

3.6 RNA sequencing

RNA-seq library preparation and sequencing, paired-end reads (Illumina Truseq V2 PolyA, not -stranded, V3-150, 2×75bp, 25M read) were generated from three biological replicates of induced and non-induced *C. parapsilosis* cells. RNA sequencing was done in collaboration with Dr. László Bodai (Department of Biochemistry and Molecular Biology**,** University of Szeged, Szeged, Hungary).

3.7 RNA sequencing analysis

For initial quality assessment and data preprocessing, we used FastQC 0.10.1 [http://www.bioinformatics.bbsrc.ac.uk/projects/fastqc/] quality assessment and Trimmomatic v0.32 [115], where preset conditions were applied for quality cutoff to remove low quality regions from the raw data [parameters used LEADING:3 TRAILING:3 SLIDINGWINDOW:4:15 MINLEN:36.]. Mapping was carried out against the reference genome obtained from the Candida Genome Database. We used the splice junction sensitive mapper Tophat 2.01.13 [116] with default settings, and mapped by applying the bowtie 2.2.4 [117] short read mapper. The counts per gene were estimated by using flux-capacitor [118]. To estimate differential expression, we used the R package Deseq2 [119] with a cutoff of log2fold change of 1.5. Gene Ontology enrichment was performed using the CGD

database [120]. RNA sequencing data analysis was performed in collaboration with Prof. Toni Gabaldon and Dr. Ernst Thuer (Centre for Genomic Regulation, Barcelona Institute of Science and Technology, Barcelona, Spain).

3.8 Transformation of *Candida parapsilosis*

All the deletion mutants and fluorescently labeled strains were constructed using chemical transformation. A single colony was inoculated in 2 ml YPD and grown for overnight at 30 °C at 180 rpm. Then the culture was diluted to an OD_{600} of 0.2 in 30 ml YPD broth. This was grown at 30 °C to an OD_{600} of 0.8-1. The culture was collected by centrifuging at 4000 rpm for 5 min and the pellet was re-suspended in 3 ml of ice cold water. The re-suspended pellet was again centrifuged at 4000 rpm for 5 min and the pellet was re-suspended in 1 ml of ice cold TE-LiOAC (0.1M lithium acetate, 10mM tris and 1mM EDTA). After centrifugation the final pellet was dissolved in 200-300 µl of ice cold TE-LiOAC. A transformation mix was prepared with 100 µl competent *Candida* cells, 10 µl boiled and cooled salmon sperm DNA (10 mg/ml), 25-30 µl (2-5 µg) fusion PCR product and kept for 30 minutes. Finally, 700 µl PLATE (0.1M lithium acetate, 10mM tris, 1mM EDTA and 40% PEG 4000) was added to the transformation mix and kept at 30 °C for overnight. Next day the cells were heat shocked at 44 °C for 15min, collected by centrifugation and washed with 1ml of YPD media. Again after the centrifugation, the cells were re-suspended in 1ml of YPD followed by incubation at 30 °C at 200 rpm for 2-3 hours. After the incubation, the cells were centrifuged and dissolved in 100 µl of YPD, then plated on the respective agar plates.

3.9 Construction of deletion strains

To delete the six target genes in *C. parapsilosis* the fusion PCR technique was used, as described previously by Holland *et al*. Approximately 500bp upstream and downstream sequence of the target genes were amplified with primer pairs 1, 3 and 4, 6 using DreamTaq polymerase (Thermo Scientific). Selection markers *LEU2* and *HIS1* were amplified with primer pairs 2 and 6 from the plasmids pSN40 (*LEU2*) and pSN52 (*HIS1*) [121]. All the PCR products were purified using Qiagen PCR Purification kit according to the manufacturer's instruction. Finally, the 5′ flanking region, 3′ flanking region and the marker

fragment were fused with the Phusion Taq polymerase (Thermo Scientific) with the primer pair 1 and 6. The resulting disruption cassette was used for transformation. *LEU2* was always used for the deletion of the 1st allele and *HIS1* for the 2nd allele.

The integration of the cassette was verified by PCR of both ends of the deletion construct using primer pairs 5′Chk, Leu2Chk1 or His1Chk1 for the 5′ region and 3′Chk, Leu2Chk2 or His1 Chk2 for the 3′ region. Schematic presentation of the gene deletion strategy in *C. parapsilosis* is shown on Fig 11.

PCR conditions:

5′& 3′ Flanking PCR

94 °C-5 min
94 °C-30 s
55 °C-45 s ×30
72 °C-1 min
72 °C-7 min

Marker PCR

94 °C-5 min
94 °C-30 s
45 °C-45 s ×30
72 °C-2 min
72 °C-7 min

Fusion PCR

98 °C-30 s
98 °C-10 s
60 °C-45 s ×30
72 °C-3 min
72 °C-10 min

Colony Check PCR

94 °C-5 min
94 °C-30 s
53 °C-45 s ×30
72 °C-1.5 min
72°C-7 min

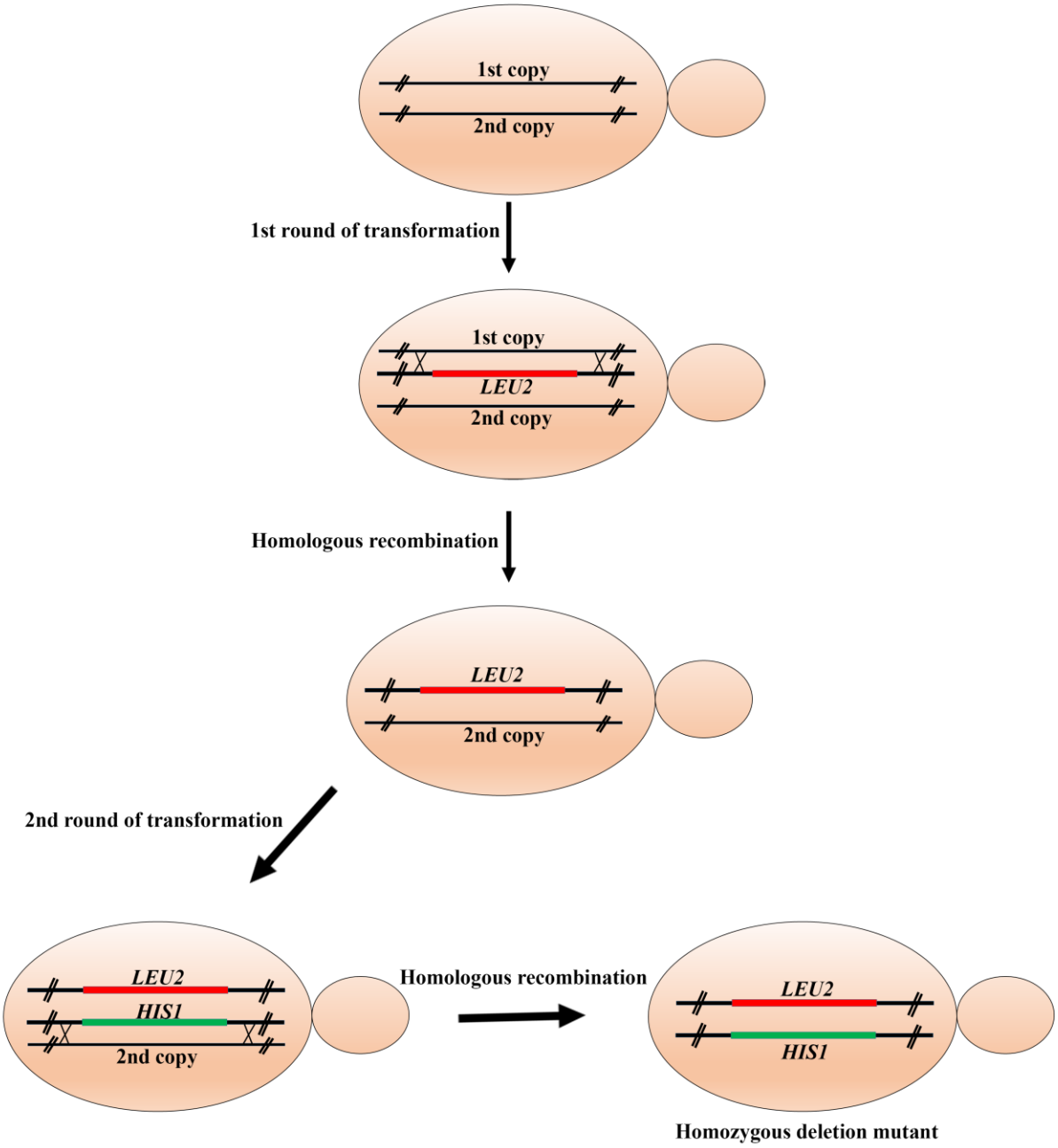

Fig 11: Schematic presentation of the gene deletion strategy in *C. parapsilosis*

3.10 Genomic DNA isolation from yeast

For total genomic DNA isolation, a single colony was inoculated in YPD broth and grown overnight at 30 °C with shaking (180 rpm). Next day, the cells were harvested by centrifugation at 5000 rpm for 5 min. The supernatant was discarded and the cell pellet was dissolved in 500 µl of lysis buffer (1% SDS, 50 mM EDTA, 100 mM TRIS-Cl pH8). Then,

the 2 ml Eppendorf tube was filled with acid washed glass beads (with 0.5mm diameter) up to 1ml and vigorously vortexed for 3 minutes. 275 µl of 7M ammonium acetate was added to the mixture followed by heat shock at 65 °C for 5 minutes and incubation on ice for 5 more minutes. Then 500 µl of chloroform: isoamyl alcohol (24:1) solution was added to denature the proteins and the tube was centrifuged at 13000 rpm for 10 minutes. The denatured proteins were collected in the organic phase or at the interphase, while nucleic acids remained in the aqueous phase. The DNA from the aqueous phase was collected in a new Eppendorf tube, 500 µl of isopropanol was added and incubated on ice for at least 30 minutes. Afterwards, samples were centrifuged at 13000 rpm for 10 minutes. The precipitated DNA was washed with 500 µl 70% ethanol (13000 rpm for 10 minutes) and the obtained pellet was air dried. Genomic DNA was dissolved in RNase supplemented distilled water. Finally, 1 µl of the DNA solution was analyzed on a 0.8% agarose gel with EtBr (10 µl from 0.5 mg/ml stock) to check DNA quality and quantity under UV light.

3.11 Construction of the mCherry plasmid

The mCherry plasmid was constructed using the Invitrogen Gateway® Cloning strategy. Briefly, the mCherry ORF was cloned into the constitutive promoter (CaTDH3-glyceraldehyde-3-phosphate dehydrogenase) containing destination vector pDEST-TDH3-NAT-CpNET5 from the entry vector pEntry-mCherry (construction described elsewhere). Cloning was achieved via the LR clonase reaction using the manufacturer's LR clonase in order to construct the expression vector pDEST-TDH3-mCherry-NAT-CpNET5.

3.12 Construction of fluorescent tagged strains

The expression vector pDEST-TDH3-mCherry-NAT-CpNET5 was digested with *Stu*I restriction enzyme and the digested DNA was used to transform the *C. parapsilosis* strains (*603600*Δ/Δ, *800020*Δ/Δ and *807710*Δ/Δ) using chemical transformation. The mCherry expression was confirmed after checking the strains under fluorescent microscope.

3.13 Phenotypic characterization of *603600Δ/Δ* strain

Growth of the deletion mutants was examined under different conditions, designed to study nutritional, cell wall, osmotic and oxidative stress responses. All deletion mutant strains were grown in 2 ml YPD media at 30 °C overnight. The cultures were then diluted to the desired cell number (10^5 to 10) with 1xPBS after counting using Bruker's chamber. Five microliters from each dilution was plated on different plates and were incubated for 2 days at 30 °C. Growth of the mutant strains was compared to that of the wild type strain. All experiments were performed in duplicate.

3.14 Biofilm formation

In vitro biofilm assay was performed in spider medium containing 96 well polystyrene plates. All *C. parapsilosis* strains were grown overnight in YPD at 30 °C, and then diluted to an OD_{600} of 0.5 in 2 ml spider media. The 96 well flat bottom microtiter plates were pretreated overnight with FBS and then washed 2 times with 1xPBS before plating 100 µl of the prepared cell suspensions ($5X10^5$ cells/100 µl). Plates were kept in 37 °C for 90 mins at 180 rpm for initial adherence of the biofilm. Then, the wells were washed 2 times with 1xPBS and replenished with 100 µl of fresh spider media. The plates were kept at 37 °C for further 48 hours without shaking prior to quantification. Cell free wells with only media were used as controls.

3.15 XTT reduction assay

The biofilms produced by each strain were quantified using the XTT metabolic assay. Briefly, 0.5 mg/ml XTT solution was prepared in 1xPBS, filter sterilized and stored at -70 °C. 10 mM menadione solution in acetone was prepared freshly immediately before use. Prior to the assay 1ul of menadione solution was added to 10 ml of XTT containing 1xPBS. Biofilms were washed 3 times with 1xPBS and then 200 µl of the XTT-menadione solution was added to each well. Plates were then incubated at 37 °C for 2 hours in the dark. After the incubation, 100 ul of the supernatant was transferred into a new 96 well plate and absorbance was measured with a microtiter plate reader at 490 nm. Values of the control

wells were subtracted from the test absorbance values in order to reduce the background interference.

3.16 Crystal violet staining assay

Biofilm formation was also quantified with crystal violet staining assay. In brief, the biofilm coated wells of 96 well flat bottom microtiter plates were washed three times with 200 µl of 1xPBS and air dried for 45 minutes. Then all wells were stained with 100 µl of 0.4% aqueous solution of crystal violet for 45 minutes followed by washing with 200 µl of sterile distilled water. After the washing step, wells were immediately destained with 200 µl of 96% ethanol for 45 minutes. After 45 minutes 100 µl of the destaining solution was taken in a fresh plate and the absorbance was measured in a microtiter plate reader at 595nm.

3.17 Pseudohypha assay by colony morphology

Pseudohypha formation was investigated by examining the colony morphology after spotting. Cells on different pseudohypha inducing media were photographed after 7 days of incubation at 37 °C. Media used for pseudohypha induction were YPD-serum containing medium (0.5% Yeast extract, 1% peptone, 1% D-Glucose and 10% fetal bovine serum), Spider medium (1% peptone, 1% yeast extract, 1% mannitol, 0.5% NaCl and 0.2% K_2HPO_4) [122], YPS (2% peptone 1% yeast extract and 2% sucrose) and Lee's media [123].

3.18 Pseudohypha assay by microscopy

C. parapsilosis strains were grown in 2 ml of YPD at 30 °C overnight with shaking. After the overnight incubation, cells were washed three times with 1xPBS, then approx. 1 O.D cells were transferred into different pseudohypha inducing liquid media and grown for 24 hours at 37°C. Imaging was performed by bright field microscopy.

3.19 Isolation and differentiation of PBMCs

Human PBMCs were isolated from buffy coats of healthy individuals by density gradient centrifugation [124]. Briefly, blood samples were first diluted with 1xPBS (1:1 dilution). The diluted blood was overlaid above the Ficoll solution (Ficoll Paque PLUS-GE Healthcare) and then centrifuged at 900 rpm for 30 minutes at 20 °C. After centrifugation, the mononuclear cell layer was aspirated with a pipette, collected in a separate falcon tube and then washed 3 times with 1xPBS. Finally, cells were suspended in RPMI 1640 medium (Lonza) supplemented with 100 U/ml penicillin and 100 µg/ml streptomycin. Cells were counted and the concentration was adjusted to 5×10^6 cells/ml. For later experiments, 100 µl of 5×10^5 cells in RPMI were added to U-bottom 96-well plates. For macrophage differentiation, cells were added to flat bottom 24-well plates with the concentration of 1ml of 1×10^7 cells per well and incubated for 90 minutes at 37 °C in the presence of 5% CO_2 and 100% humidity. After the incubation, RPMI was removed and cells were washed with 1 ml of 1xPBS. Finally, the cells were re-suspended in X-VIVO 15 media (Lonza) supplemented with 100 U/ml penicillin, 100 µg/ml streptomycin and 10 ng/ml recombinant human granulocyte-macrophage colony-stimulating factor (GM-CSF, Sigma-Aldrich). The media was changed every 2nd day for 7 days. During the study, PBMCs were used for cytokine measurement only.

3.20 Stimulation of PBMCs and PBMC-DMs

For the infection experiments, *C. parapsilosis* strains were grown overnight in 2 ml YPD media, washed 3 times with 1xPBS and adjusted to the proper concentrations used for each experiment. For the infection of both human PBMCs (cytokine measurement only) and PBMC-derived macrophages, the multiplicity of infection (MOI) was 1:5. *Candida* cells were dissolved in 100 µl of either RPMI/PS (PBMC) or GM-CSF-free X-VIVO 15 (PBMC-DM) medium and were added to host cell containing wells.

3.21 Cytokine measurement by ELISA

The concentration of different cytokines was analyzed by commercial ELISA kits according to the manufacturer's instructions. The IL-1β, IL-6, TNFα, IL-10, IL-1ra and IL-8 ELISA kits were obtained from R&D Systems (Abingdon, United Kingdom). For the pro-IL-1β

measurement, macrophages were lysed by repeated freeze-thaw cycles and then the supernatant was collected [125]. The experiments were performed with both PBMCs and macrophages derived from peripheral blood mononuclear cells (PBMC-DMs) from at least five independent donors.

3.22 Sample preparation for analysis of secreted eicosanoids and intracellular eicosanoids

For eicosanoid measurement, 2×10^7 candida cells were inoculated in 10 ml of 1xPBS+100 µM AA in triplicates and incubated at 30 °C for 24 hours. Three tubes with only 1xPBS and 100 µM AA were also incubated which served as the control. 100 µl sample was complemented with 96 µl MeOH and 4 µl internal standards solution (final concentration: 1 ng/ml PGE2-d4, LTB4-d4 and 15-HETE-d8 and 10 ng/ml DHA-d5) and analyzed without further processing.

For secreted oxylipins, the cell supernatant was collected using sterile filtration after centrifugation. For internal oxylipins, the cells were collected after centrifugation and heated at 60 °C in methanolic NaOH (20 µl 10N NaOH+180 µl methanol). Further, 800 µl MeOH (LC-MS grade, Honeywell Riedel-de-Haën) was added to the hydrolyzed cell lysates and the samples were centrifuged (16100 ×g, 4 °C, 5 min.). After sample acidification using formic acid (LC-MS grade, Fluka) the supernatant was complemented with 5 ml H_2O (LC-MS grade, Honeywell Riedel-de-Haën), 4 µl internal standards solution (final concentration: 1 ng/ml PGE_2-d4, LTB_4-d4 and 15-HETE-d8 and 10 ng/ml DHA-d5; all from Cayman Chemicals, Ann Arbor, MI, USA) was added. The samples were mixed and loaded on Waters Sep-Pak C18 cartridges 200 mg, 3 ml (Waters, Milford, MA, USA). Conditioning was done sequentially with 3 ml MeOH and 3 ml water. After samples had been loaded, cartridges were washed with 3 ml water and 3 ml n-hexane (Sigma-Aldrich, St. Louis, MO, USA) and eluted using 3 ml methylformate (spectrophotometric grade, Sigma-Aldrich). Eluates were dried at 40 °C under a gentle stream of nitrogen and reconstituted in 200 µl 40% MeOH, after a final centrifugation step (16100 ×g, 4 °C, 5 min.), samples were transferred to micro vial inserts and transferred to the auto sampler.

3.23 Analysis of lipid mediators by LC/MS

Oxylipins were analyzed using a targeted LC-MS/MS method according to published protocols with a minor modification [126]. The drying temperature was set to 450 °C instead of 400 °C. Supplementary table S5 shows the MRM characteristics for the monitored oxylipins. When concentrations were determined external calibration was carried out with linear regression using a weighting factor of $1/x^2$. Sample preparation for LC/MS analysis and data analysis was done in collaboration with Prof. Martin Giera and Marieke Heijink (Center for Proteomics and Metabolomics, Leiden University Medical Center, Leiden, The Netherlands).

3.24 Phagocytosis competition assay by fluorescent microscopy

GFP (wild type) and mCherry (mutant strains) expressing *C. parapsilosis* strains were grown overnight in YPD at 30 °C at 200 rpm. Next day, the cells were harvested by centrifugation at 3000 rpm for 5 minutes and washed with 1xPBS. PBMC-DMs were infected with a mixture of fungal cells (wild type and a mutant strain, mixed in a ratio of 1:1), and were co-incubated at 37 °C for 2 hours. Then the co-culture was incubated and then washed 2-3 times with 1xPBS prior to visualization under the fluorescent microscope [127]. At least 300 macrophages and 150 yeast cells were counted for each experiment and the experiments were performed with macrophages derived from three independent donors.

3.25 LDH measurement

The lactate dehydrogenase concentration of cell culture supernatant was determined by LDH cytotoxicity detection kit (Takara) according to manufacturer's instruction. Cytotoxicity was calculated after subtracting the absorbance value of the unstimulated control from all the test samples. Cytotoxicity (%)-($OD_{\textbf{Experimental value}}/OD_{\textbf{Positive control}}$) ×100. Supernatant collected from the cells treated with 1% TritonX-100 was used as positive control.

3.26 Killing assay

Human PBMC-DMs (5×10^5/well) were co-incubated with *C. parapsilosis* cells in 24 well plastic culture plates at a MOI of 1:5. As a control, equal amounts of *Candida* cells were incubated in the GM-CSF free X-VIVO 15 media only (500 µl/well). After 3 hours of incubation, macrophages were lysed with 1xPBS+4% TritonX solution. Control wells with yeast cells only were treated similarly. Finally, the lysates and the cells were serially diluted, plated on YPD plates and incubated for 2 days at 30 °C. After 2 days of incubation, the number of CFUs was determined and the recovered CFUs from each strain were compared. The killing efficiency was calculated as follows: (number of live *Candida* cells in control wells - number of live *Candida* cells in co-cultures) / number of live *Candida* cells in control wells × 100. The experiments were performed with PBMC-DMs derived from five independent donors with triplicates.

3.27 Phagosome-lysosome fusion by FACS

For phagosome-lysosome fusion analysis, by quantitative imaging using Amnis Flowsight, the *Candida* cells were labeled with the fluorescent dye pHrodo® (Invitrogen). For labeling, first the yeast cell suspension (100 µl containing 10^9 cells) was treated with 11 µl of Na_2CO_3 (1 M, pH 10) and then 2 µl pHrodo (1 mg/ml in DMSO) was added, followed by incubation for 1hour at room temperature in the dark. After the incubation, the cells were washed 4 times with 1xPBS and adjusted to the proper concentration. Human PBMC derived macrophages were infected with labeled *Candida* cells at a 1:5 ratio and kept for 2 hours to allow phagocytosis. Then the non-phagocytosed *Candida* cells were washed with 1xPBS and macrophages were detached from cell culture plates by using TrypLETM Express solution (Gibco). Finally, the macrophages were collected in FACS buffer (0.5% FBS in 1xPBS), centrifuged and dissolved in 1xPBS, followed by measurement. Data were analyzed by the IDEAS Software (Amnis).

3.28 Morphology analysis in hypoxic condition (5% CO_2) by FACS after cell wall staining

The *Candida* cells were collected from overnight cultures (37 °C, 5% CO_2) from different media and suspended in 1ml of 4% paraformaldehyde followed by 30 minutes of incubation at room temperature, with continuous rotating. Following incubation, cells were washed four times with 1x PBS, and pellets were suspended in 0.5 ml 1% BSA (Sigma – Aldrich), followed by incubation at room temperature for additional 30 minutes with rotation. Then cells were washed three times with PBS and suspended in 200 - 400 µl of the same buffer dependent upon cell concentration (approx. 10^8 /ml cell concentration). Then, 100 µl of the suspension was transferred into a new Eppendorf tube and mixed with 100 µl of freshly prepared CCW fluorescent dye mix (8 µl 2.5 mg/ml ConA-FITC, 1 µl 1 mg/ml CW, 1 µl 1mg/ml WGA-TRITC, 90 µl 1% BSA). Cell suspensions were incubated for 30 minutes at room temperature with continuous rotation. The fluorescently labelled cells were washed three times with 1xPBS and suspended in 100 µl of the same buffer. Finally, the morphology was analyzed by Amnis Flowsight and the pseudohypha was quantified by IDEAS Software (Amnis).

3.29 Bacterial plasmid isolation

Single colonies from LB agar plates were inoculated in 2 ml of LB supplemented with the appropriate antibiotics and grown for overnight at 37 °C with shaking at 200 rpm. Next day, the cells were harvested by centrifugation at 5000 rpm for 5 minutes. The pellet was first resuspended in 100 µl of lysis buffer (50 mM D-Glucose, 10 mM EDTA, 25 mM TRIS, pH7.5), followed by resuspension in 200 µl of alkaline SDS (4.4 ml sterile distilled water, 100 µl 10 M NaOH, 0.5 ml 20% SDS) and 150 µl of 3M potassium acetate solution. The suspension was gently mixed and kept on ice for five minutes. Then the precipitated chromosomal DNA was centrifuged at 13000 rpm for 10 minutes. The supernatant was collected in a fresh Eppendorf tube and 500 µl of 24:1 mixture of chloroform isoamyl alcohol was added, vortexed and centrifuged at 13000 rpm for 10 minutes. The watery layer was collected in a new Eppendorf tube and after addition of 500 µl of isopropanol, tubes

were kept at -20 °C for at least 30 minutes. Samples were then centrifuged (13000 rpm,10 mins) and washed with 70% ethanol (13000 rpm,10 minutes). The pellet was dried and finally dissolved in RNase supplemented distilled water (250 µg/ml, Sigma-Aldrich). The correct plasmid was checked with appropriate restriction enzyme digestion. For isolation of large amount of plasmids, single colony was inoculated in 100 ml of LB with proper antibiotics and after overnight growth (37 °C, 200 rpm) plasmid was isolated using the Plasmid Midi Kit (Geneaid) according to the manufacturer's instructions.

3.30 *E. coli* competent cell preparation and transformation

E. coli competent cells were prepared using the $CaCl_2$-$MgCl_2$ method. Briefly, single colonies of *E. coli* 2T1 cells were inoculated in 5 ml of LB and incubated overnight at 37 °C at 200 rpm. From this pre-culture, cells were re-inoculated in 50 ml of LB grown up to 0.3-0.4 OD. Cells were harvested by centrifugation (4000 rpm, 10 minutes, 4 °C) and washed with pre-cooled wash solution (80 mM $MgCl_2$, 20 mM $CaCl_2$) (4000 rpm, 10 minutes, 4 °C). Finally, the washed cells were resuspended in ice-cold 100 mM $CaCl_2$ solution. The resulting competent cells were stored on ice until usage within 1-2 hours.

Competent *E. coli* cells were mixed with transforming DNA and kept on ice for 45 minutes followed by heat shock at 42 °C for 90 seconds. After the heat shock, cells were recovered in 1ml of LB at 37 °C. Then cells were plated on LB agar plates supplemented with the appropriate antibiotics and the plates were incubated for 12-16 hours.

3.31 Phagocytosis assay using flow cytometry

For phagocytosis analysis by quantitative imaging using Amnis Flowsight, the *Candida* cells were labeled with the fluorescent dye Alexa Fluor 447 carboxylic acid succinyl ester (Invitrogen). For labeling, first the yeast cell suspension (100 µl containing 10^9 cells) was treated with 11 µl of Na_2CO_3 (1 M, pH 10) and then 2 µl Alexa Fluor 447 (1 mg/ml in DMSO) was added followed by incubation for 1 hour at room temperature in the dark. After the incubation, the cells were washed 4 times with 1xPBS and adjusted to the proper concentration. Human PBMC derived macrophages were infected with labeled *Candida* cells at a 1:5 ratio and kept for 2 hours to allow phagocytosis. Then the non-phagocytosed

Candida cells were washed with 1xPBS and macrophages were detached from the cell culture plates by using TrypLETM Express solution (Gibco). Finally, the macrophages were collected in FACS buffer (0.5% FBS in 1xPBS), centrifuged and dissolved in 1xPBS, followed by measurement. Data was analyzed by the IDEAS Software (Amnis).

3.32 Mouse model of systemic *Candida* infection and Fungal burden

An experimental mouse model of disseminated candidiasis was used as reported previously Ifrim et al. [128]. Briefly, groups of five 8–12-weeks-old female Balb/c WT mice (22–27 g. of weight) were infected with 2×10^7 *C. parapsilosis* cells via lateral tail vein injection using syringe with a 32-gauge needle in 100 µl of sterile 1xPBS. A group of control mice was injected with 100 µl of sterile 1xPBS. The mice were maintained with sterile water and pet aliment *ad libitum*. After 3 days of post infection, animals were humanitarianly euthanatized followed by the removal of liver, kidneys and spleen aseptically. Then the organs were weighed and homogenized in sterile 1xPBS in a tissue grinder. Finally, the fungal burden in the organs were determined by plating serial dilutions on three YPD agar plates per organ homogenate. The CFU were determined after 48 hours of incubation at 30 °C and expressed as CFU/g tissue.

3.33 Ethics Statement

The *in vivo* mouse infection experiments were performed by national (1998. XXVIII; 40/2013) and European (2010/63/EU) animal ethics' guidelines. The experimental protocols were approved by the Animal Experimentation and Ethics Committee of the Biological Research Centre of the Hungarian Academy of Sciences and the Hungarian National Animal Experimentation and Ethics Board (clearance number: XVI./03521/2011.), with the University of Szeged granted permission XII./00455/2011 and XVI./3652/2016 to work with mice.

For PBMC isolation blood was collected from healthy individuals. The Institutional Human Medical Biological Research Ethics Committee of the University of Szeged gave approval for the procedure and the respective consent documents. The healthy individuals provided

written informed consent. The experiments were performed in accordance with guidelines and regulations of the Ethics Committee of the University of Szeged and experimental protocols were approved by the same institutional committee.

4 Results

4.1 Identification of differentially regulated genes following arachidonic acid induction

To identify genes involved in the biosynthesis of lipid mediators, we performed global transcriptomic analysis on *C. parapsilosis* GA1 [86] yeast cells following growth in the presence of AA. As a control, equal amounts of cells were grown without the addition of arachidonic acid. Altogether, 151 genes showed significantly altered expression (fold change >1.5) in the presence of AA when compared to control. Out of the 151 genes, 68 genes were upregulated, while 83 genes showed decreased expression levels. Hierarchical clustering and principal component analysis (PCA) (Fig 12) showed that the three replicates from each group clustered together by condition, confirming the reliability of the obtained results.

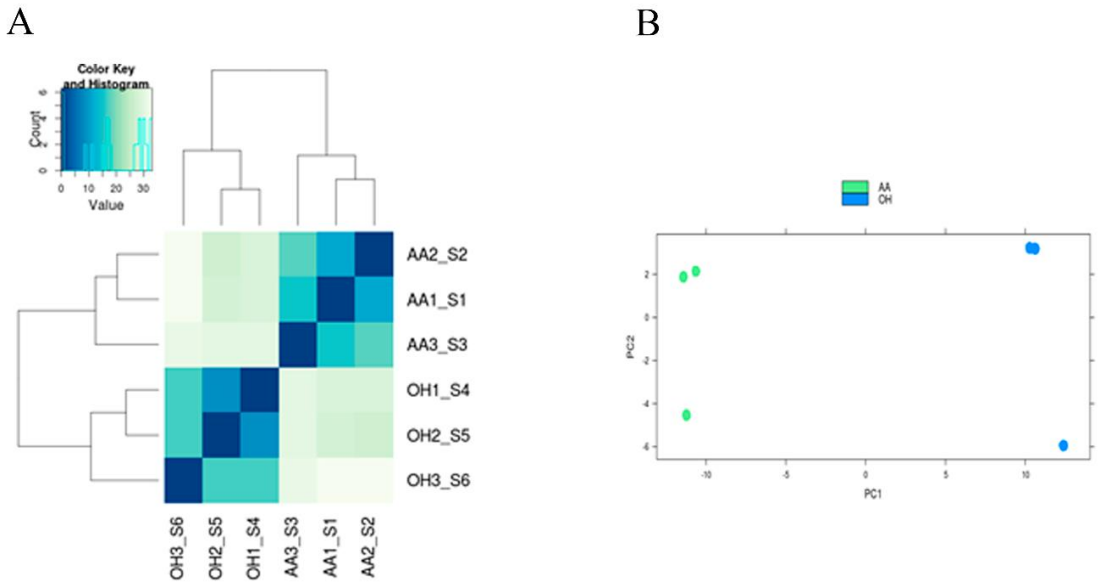

Fig 12: Hierarchical clustering and principal component analysis of the RNA-Seq data

Data Quality was evaluated via both hierarchical clustering (A) and Principal Component Analysis (B). Hierarchical clustering (hclust model in R) was used to illustrate the relation between the samples (S1, S2, S3, etc.) with a clear clustering of the replicates against the conditions, showing that the primary effect influencing the data was the exposure, not biological noise. Principal component analysis (prcomp model in R) was used to examine

the primary variance of the samples. For both the hierarchical clustering and Principal Component Analysis, the analysis shows that the change between arachidonic acid (AA) treatment and samples without pretreatment [ethanol only, zero amount Arachidonic Acid versus background exposure increase (OH)] caused the primary variance.

Functional categorization of the genes by Gene Ontology (GO) term analysis using the candida genome database [120] showed that 14% of the genes involved in lipid metabolic processes (GO:0006629) are upregulated (Fig 13A). The heat map indicates all of the upregulated ORFs in the induced condition (Fig 13B). Detailed GO term annotations of the upregulated genes can be found in supplementary table S3. For further analyses, we selected six upregulated genes with known lipid metabolic process regulatory homologous in *C. albicans*, (Table 2) and further validated the RNA sequencing data results by performing qRT-PCR analysis (Table 3). qRT-PCR confirmed that the six genes were upregulated following arachidonic acid pretreatment in both *C. parapsilosis* GA1 as well as in a second strain, CLIB 214. As five out of six genes showed higher expression levels in the CLIB 214 type strain, we subsequently used this strain for further analyses.

Table 2. Six up-regulated genes from the transcriptomic data analysis, their homologues in *C. albicans* and their fold change expression values in *C. parapsilosis*

CPAR2 GeneID	***Candida albicans* homologue**	**Fold Change**
CPAR2_807710	*POX1-3(2)*	2.48
CPAR2_205500	*ECI1*	2.48
CPAR2_102550	*FAA21*	2.19
CPAR2_800020	*POT1*	2.10
CPAR2_807700	*POX1-3(1)*	1.80
CPAR2_603600	*FET3*	1.63

Table 3. Confirmation of the RNA sequencing data: fold change values of the 6 selected genes in both *C. parapsilosis* strains (CLIB and GA1) determined by qRT-PCR analysis.

CPAR GeneID	CLIB	GA1
CPAR2_807710	20.96	4.70
CPAR2_205500	7.27	2.41
CPAR2_102550	11.81	3.14
CPAR2_800020	3.63	2.17
CPAR2_807700	7.48	1.08
CPAR2_603600	0.67	3.21

In order to determine the role of the identified genes in eicosanoid biosynthesis, we generated homozygous deletion mutant strains for each candidate gene by applying a gene disruption method previously introduced by Holland *et al.*,2014 [66].

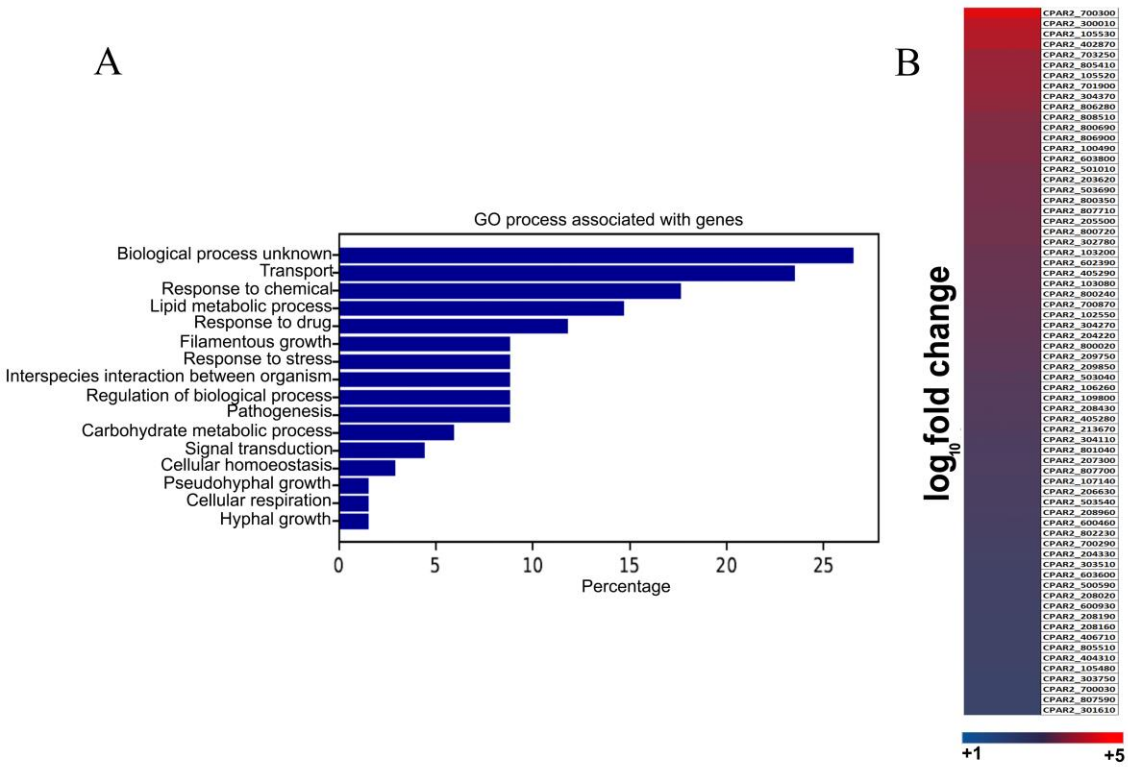

Fig 13: RNA sequencing and data analysis
(A) Global gene expression analysis was performed on the wild type *C. parapsilosis* strain after 3 hours of growth in presence of arachidonic acid. Functional analysis of genome wide expression data suggests that lipid metabolism and transport related pathways are significantly altered in the presence of arachidonic acid. (B) Heat map shows all the *C. parapsilosis* genes upregulated in presence of arachidonic acid. For further information see supplementary table S3.

4.2 Homozygous deletion mutants of CPAR2_603600, CPAR2_800020 and CPAR2_807710 genes showed a significant reduction in extracellular lipid mediator production

Using liquid chromatography-mass spectrometry (LC/MS), we analyzed all of the null mutant strains for their ability to produce eicosanoids. This approach has previously demonstrated that the storage of AA results in the production of auto-oxidation products [129,130]. Therefore, we also incubated 100 µM AA in 1xPBS at 30 °C for 24 hours to measure the amount of spontaneously produced eicosanoids without the presence of fungal cells. The LC/MS data for the secretory eicosanoid analysis revealed that the deletion mutant strains of *CPAR2_603600*, *CPAR2_800020* and *CPAR2_807710* produced less prostaglandin D_2 (PGD_2), prostaglandin E_2 (PGE_2) and 15-keto-prostaglandin E_2 (15-keto-

PGE_2) compared to the CLIB 214 wild type strain (Fig 14). These reductions were significant for PGD_2 and PGE_2 in *603600*Δ/Δ; PGD_2 and PGE_2 in *800020*Δ/Δ*;* PGE_2 and 15-keto-PGE_2 in *807710*Δ/Δ and 5D2-isoP in *800020Δ/Δ*.

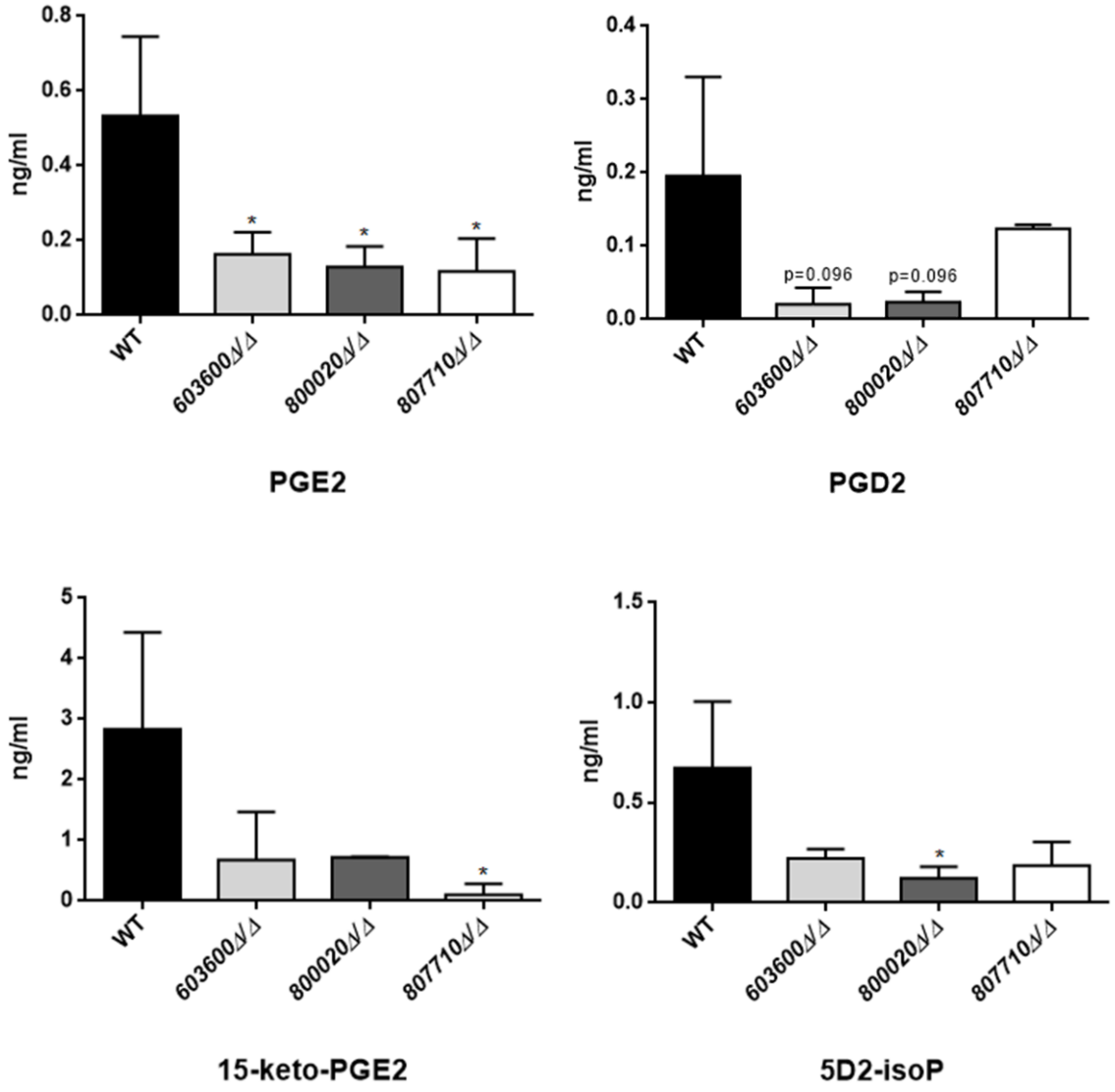

Fig 14: Reduced eicosanoid production by *C. parapsilosis* mutant strains
C. parapsilosis CLIB 214 wild type strain and three null mutant strains *603600Δ/Δ*, *800020Δ/Δ* and *807710Δ/Δ* were grown for 24 hours at 30 °C in the presence of 100 µM arachidonic acid in 1xPBS. PBS with only arachidonic acid served as control. After sterile infiltration, 100 µl of cell-free samples were analyzed with LC/MS. Among the examined eicosanoids, the three null mutants showed significant reductions in PGE_2 (*CPAR2_603600Δ/Δ, CPAR2_800020Δ/Δ* and *CPAR2_807710Δ/Δ*) and one strain in 15-keto-PGE_2 (*807710*Δ/Δ*)* production and one strain in 5D2-isoP production (*CPAR2_800020Δ/Δ)*. Strains *603600*Δ/Δand *800020*Δ/Δ had a strong trend toward a lower

production of PGD_2 compared to the wild type strain. Unpaired t-tests were used to determine differences between groups. *$P < 0.05$.

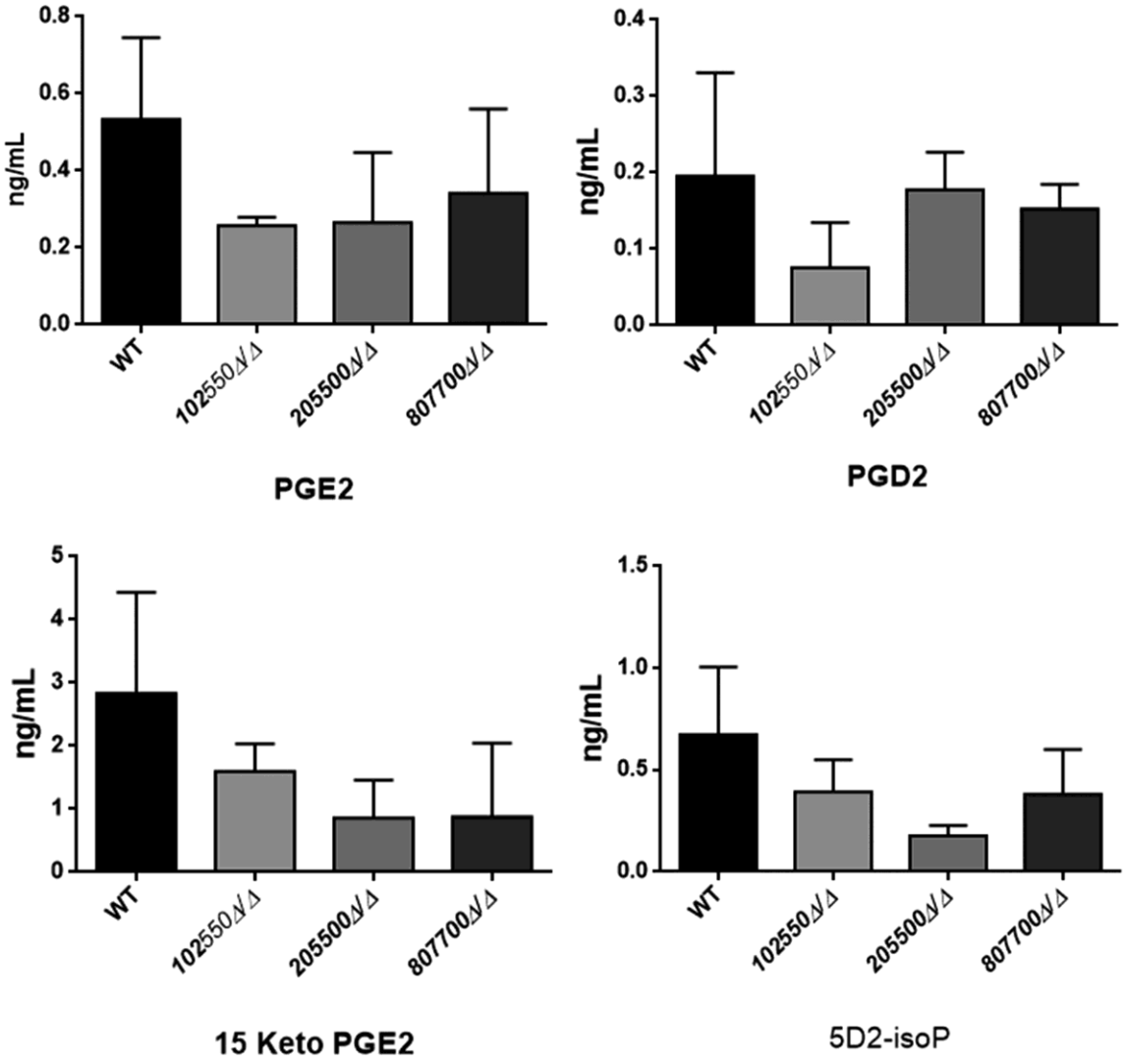

Fig 15: Secreted eicosanoid profile of the *102550*Δ/Δ, *205500*Δ/Δ, *807700*Δ/Δ deletion mutants.

C. parapsilosis CLIB 214 wild type strain and the three null mutant strains of *CPAR2_102550*, *CPAR2_205500* and *CPAR2_807700* were grown for 24hours at 30 °C in the presence of 100 μM arachidonic acid in 1xPBS. The eicosanoid profiles were determined as described. These did not show any significant change in the amount of PGD_2, PGE_2, 15-keto-PGE_2 and 5D2-isoP. Unpaired t-tests were used to determine differences between groups.

CPAR2_102550Δ/Δ, CPAR2_205500Δ/Δ and *CPAR2_807700Δ/Δ* did not show any difference in PGD_2, PGE_2 or 15-keto-PGE_2 production (Fig 15).

4.3 Internal eicosanoid analysis of the mutants

We also analyzed the amount of internal eicosanoids after AA induction. In this case, *603600*Δ/Δ showed a significant decrease in 5-HETE, while *800020*Δ/Δ had an increase in 18-HEPE and a decrease in 6-trans-LTB_4 production in comparison with the reference strain. Furthermore, *807710*Δ/Δ produced a significantly lower amount of 5-HETE, 12-epi-LTB_4 and 6-trans-LTB_4 compared to the wild type strain (Fig 16). We did not find any difference in the production of other internal eicosanoids.

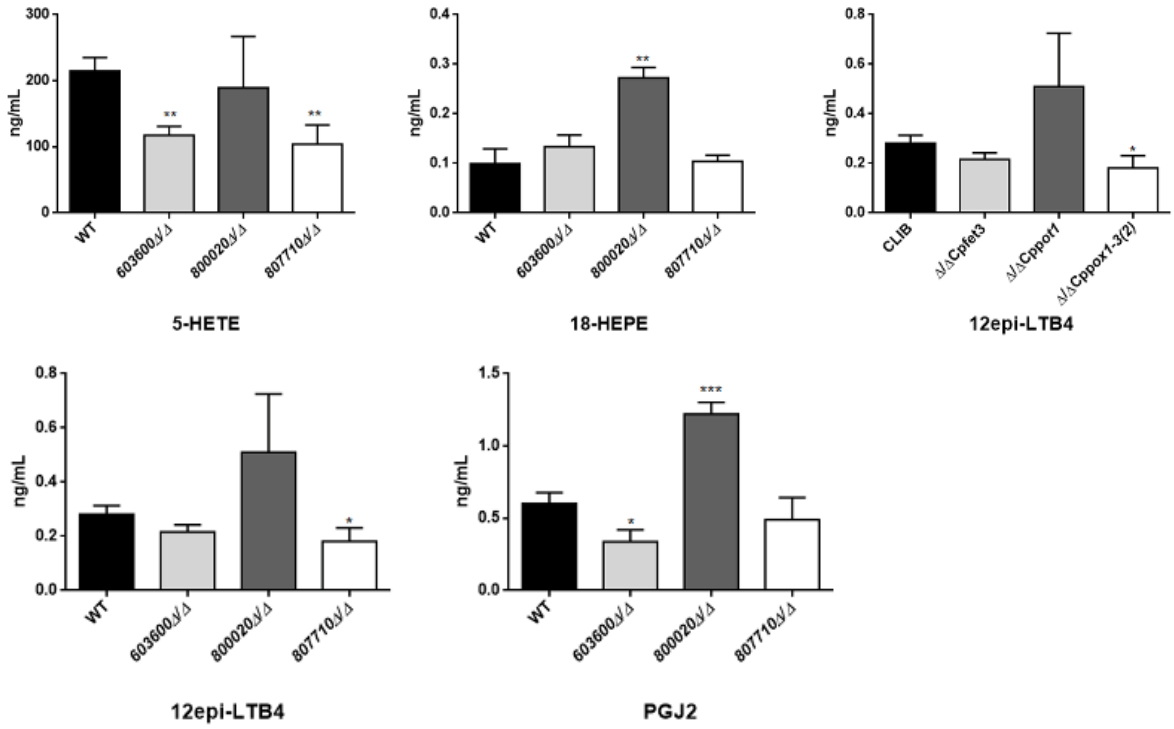

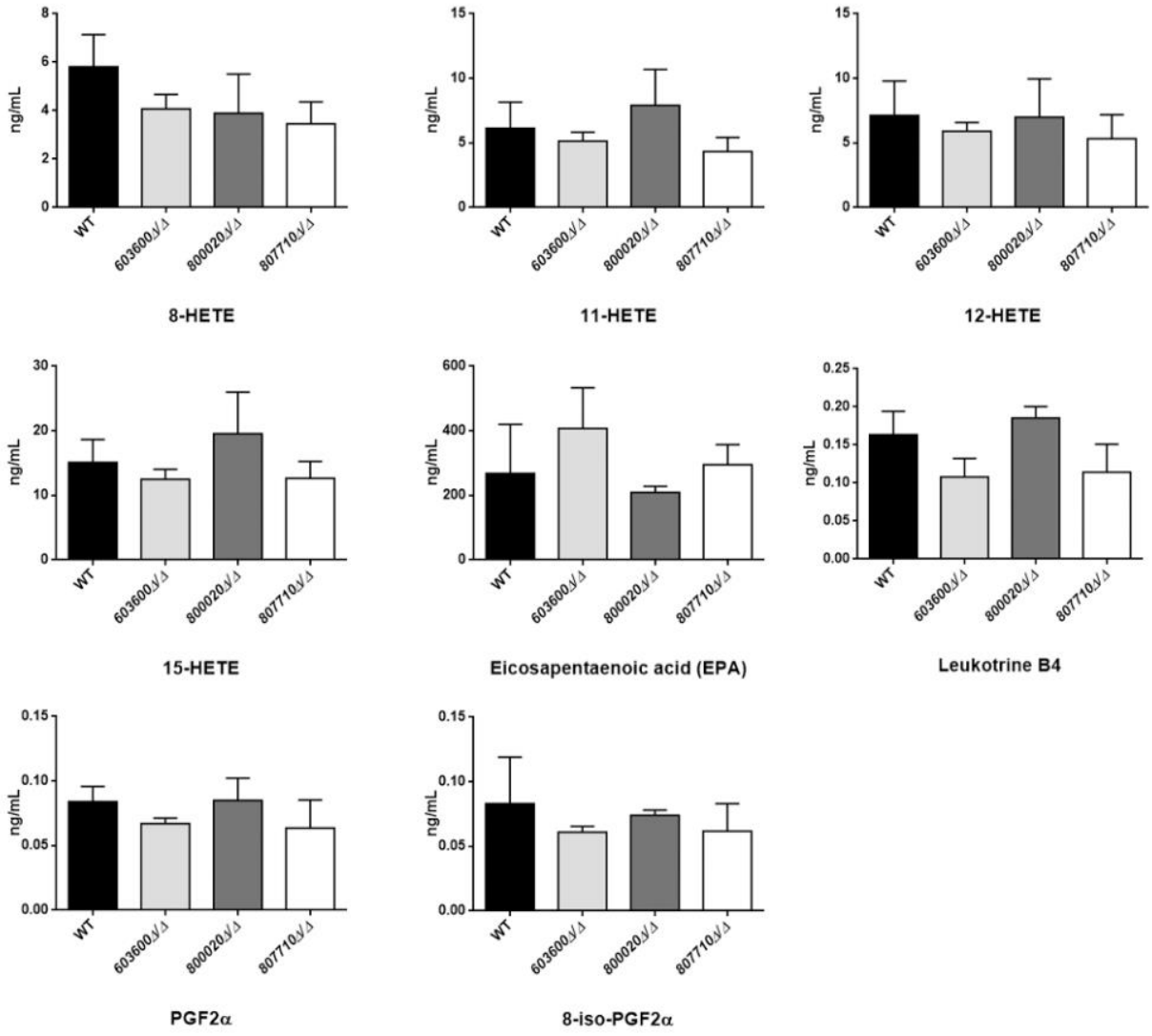

Fig 16: Intracellular eicosanoid analysis

C. parapsilosis strains were grown in the presence of 100 µM arachidonic acid for 24 hours at 30 °C. Internal eicosanoids were obtained and analyzed after disrupting of the cells with methanolic NaOH. The mutants showed significant reduction in the amount of 5-HETE (Δ/ΔCPAR2_603600, Δ/ΔCPAR2_807710), 12-epi-LTB4 (Δ/ΔCPAR2_807710 and 6-trans-LTB4 (Δ/ΔCPAR2_800020, Δ/Δ CPAR2_807710) and a significant increase in the amount of 18-HEPE and PGJ2 (Δ/ΔCPAR2_800020) production. Unpaired t-tests were used to determine differences between groups. **P* < 0.05, ***P* < 0.01, ****p*<0.002.

4.4 Phagocytosis and killing of *603600Δ/Δ*, *800020Δ/Δ* and *807710Δ/Δ* mutants by human macrophages

Human peripheral blood monocyte derived macrophages (PBMC-DM) were used to characterize the virulence properties of mutant strains with altered eicosanoid producing profiles. We first examined the phagocytic activity of PBMC-DM by fluorescence-activated cell sorting (FACS). *Candida* yeast cells were labeled with the fluorescent dye Alexa Fluor 488 (a succimidyl ester) and then co-incubated with PBMC-DMs for 2 hours.

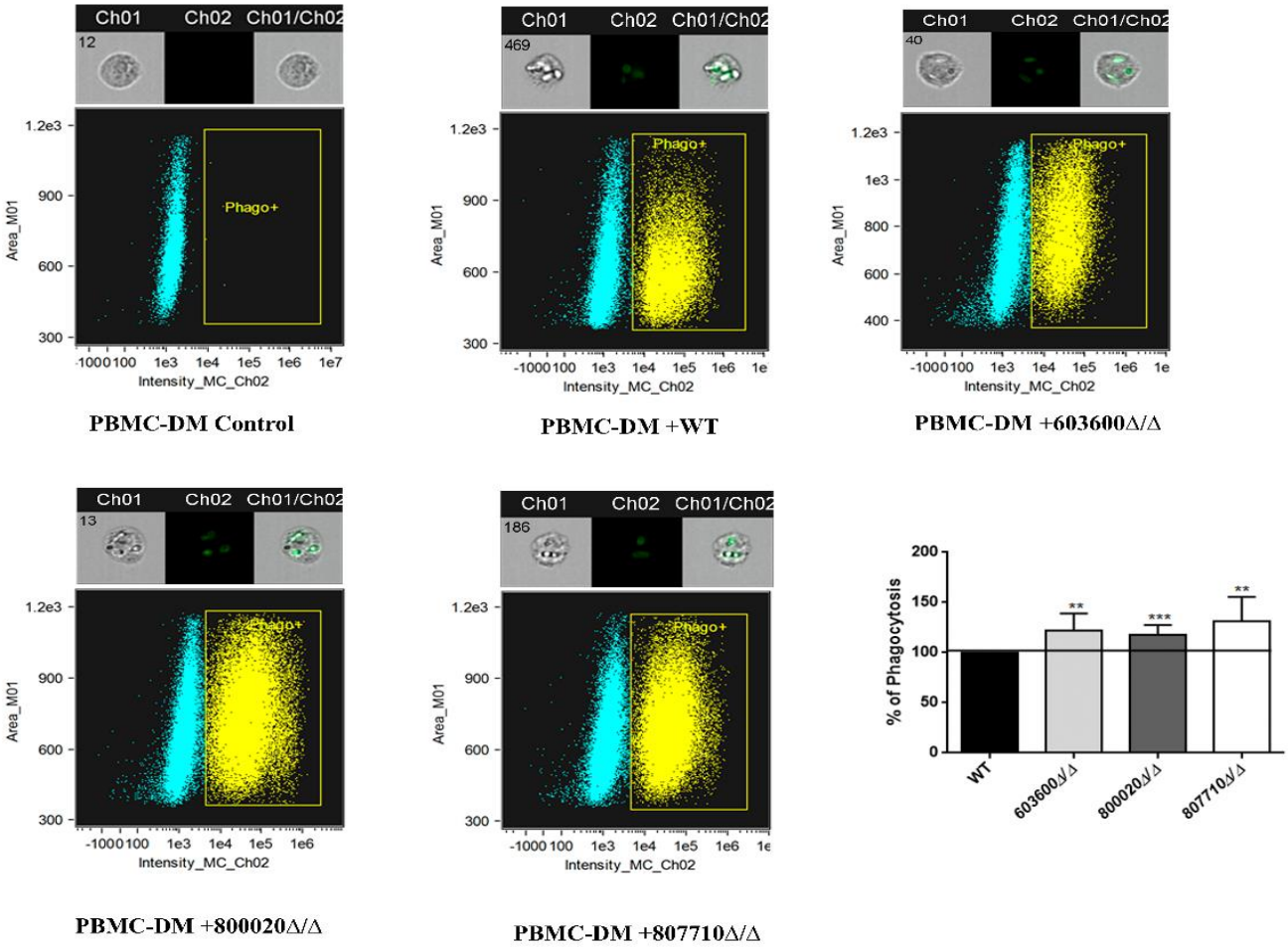

Fig 17: Phagocytosis of *C. parapsilosis* strains by human macrophages using flow cytometry

Yeast cells were co-incubated with macrophages for 2 hours. Representative dot plots and summarized data of the flow cytometric analysis are shown. **P* < 0.05, ***P* < 0.01, ****p*<0.002.

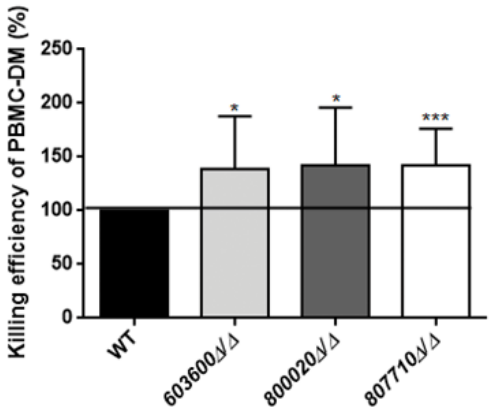

Fig 18: Killing of *C. parapsilosis* strains by human PBMC-DMs
The efficiency of killing by human macrophages was analyzed by CFU determination. Experiments were performed in triplicates. The obtained data represents the killing efficiency of macrophages gained from 5 healthy donors. Unpaired t-tests were used to determine differences between groups. *$P < 0.05$, **$P < 0.01$, ***$p<0.002$.

Our results indicated that PBMC-DMs ingested each of the mutant strains more efficiently compared to the wild type strain (Fig 17). We also examined the yeast cell killing efficiency of PBMC-DMs by comparing the recovered fungal CFUs. Our data showed that each of the mutant strains were killed more effectively by PBMC-DMs in comparison to the wild type strain (Fig 18).

4.5 Host cell damage is decreased upon infection with *603600*Δ/Δ, *800020*Δ/Δ and *807710*Δ/Δ strains

We next examined the mutant strains' abilities to cause host cell damage by measuring the amount of LDH released by human PBMC-DMs following infection. As shown in fig 19, we found that the PBMC-DMs showed significantly lower LDH release when infected with the mutants compared to the wild type. Our results indicated that *603600*Δ/Δ, *800020*Δ/Δ *and 807710*Δ/Δ mutant strains show a lower host cell damaging capacity than wild type cells (Fig 19).

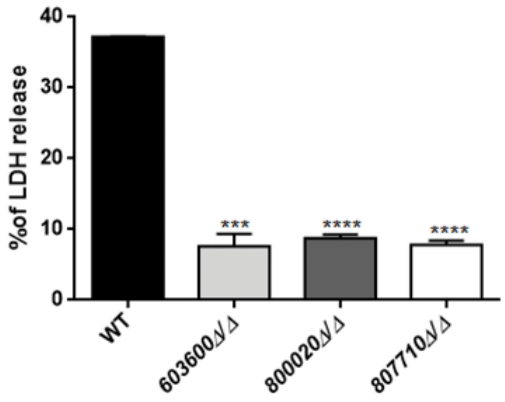

Fig 19: Host cell damage by LDH release
Human PBMC-DMs were infected with wild type and *C. parapsilosis* eicosanoid mutants for 24 hours and LDH release was measured. LDH release is expressed as % of positive control. Unpaired t-tests were used to determine differences between groups *$P < 0.05$, **$P < 0.01$, ***$p<0.002$, ****$p < 0.0001$.

4.6 Influence on phagosome-lysosome fusion

Next, we addressed whether the lack of the examined lipid mediators had any effect on phagosome-lysosome fusion in human PBMC-DMs. We analyzed the phagosome-lysosome co-localization after co-incubating pHrodo stained *Candida* cells with PBMC-DMs for 2 hours. Although, all three mutants are phagocytosed and killed more efficiently by PBMC-DMs, only the *603600*Δ/Δ strain induced a higher rate of phagosome-lysosome fusion, suggesting the corresponding gene's influence on phagosome maturation (Fig 20).

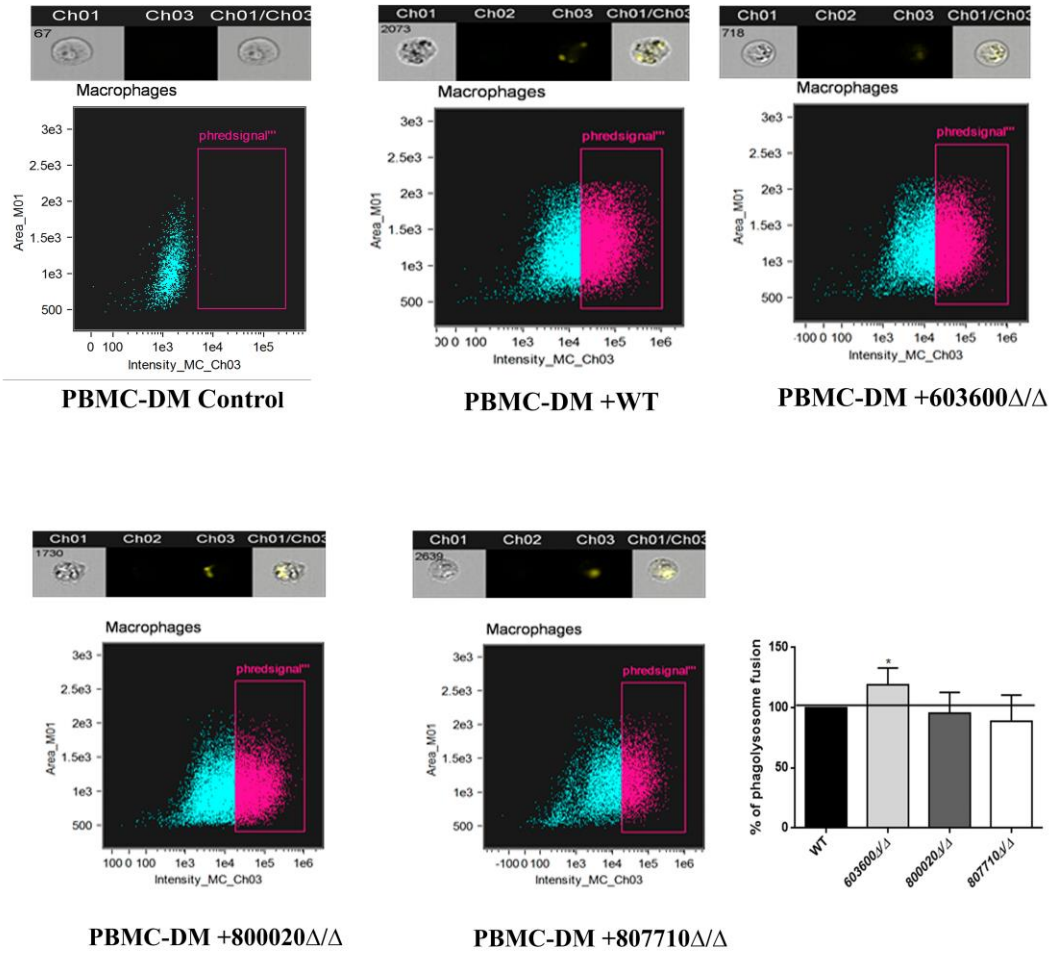

Fig 20: Phagosome-lysosome fusion in response to wild type and eicosanoid mutants
Phago-lysosome co-localization in human PBMC-DMs following the phagocytosis of pHrodo labeled *Candida* cells. Unpaired t-tests were used to determine differences between groups. **P* < 0.05.

4.7 Macrophages favor the uptake of *603600*Δ/Δ, 800020Δ/Δ and 807710Δ/Δ strains over the wild type

We tested the uptake efficiency of the mutants by human PBMC-DMs using a competition assay and compared them to the wild type strain. During the assay, we used differently labeled *Candida* strains: a GFP tagged wild type strain and mCherry labeled mutant strains. PBMC-DMs were infected with 2 types of fungal cells mixed in a ratio of 1:1 and co-incubated for 2 hours. Interactions were monitored via fluorescent imaging.

A

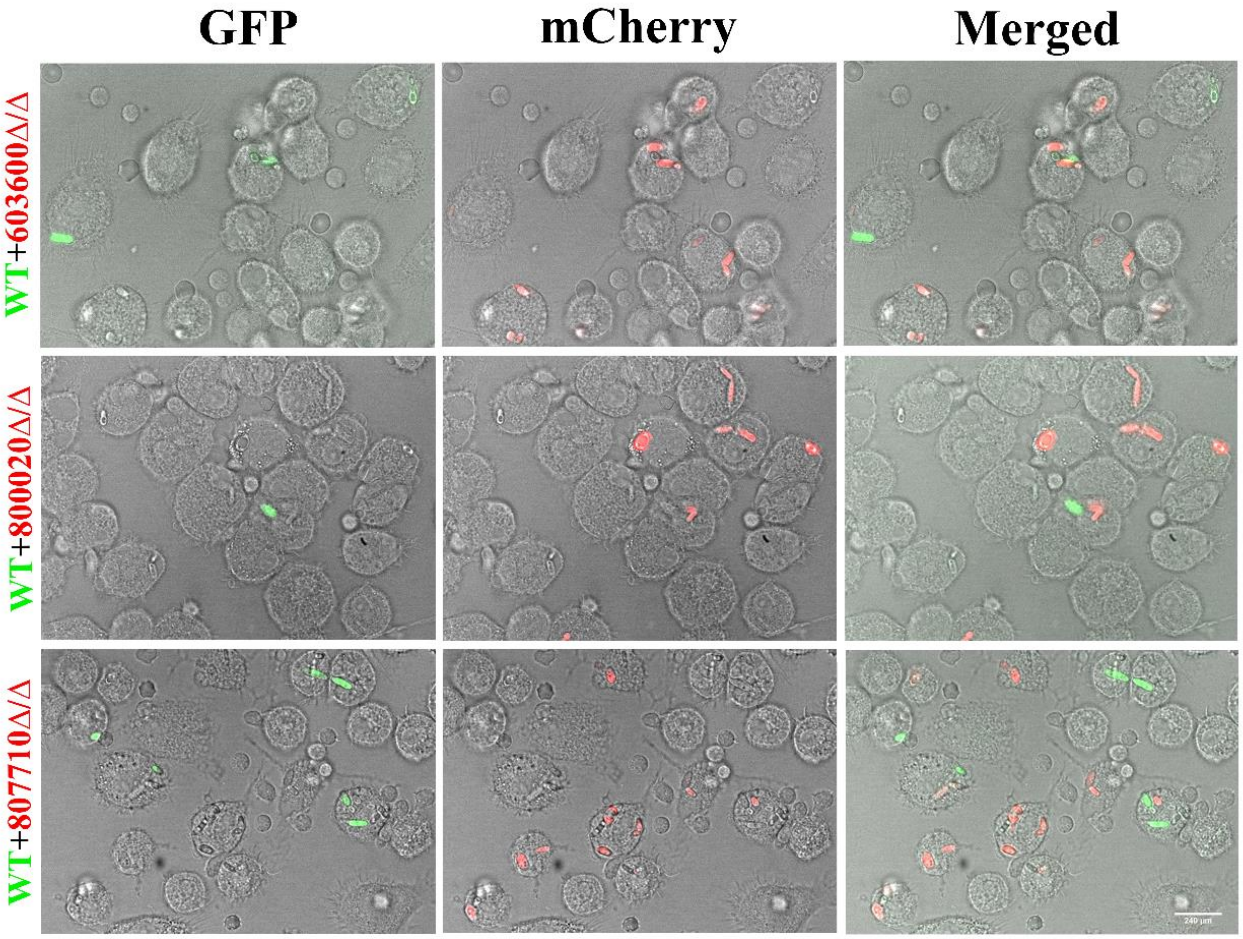
GFP
mCherry
Merged
WT+603600Δ/Δ
WT+800020Δ/Δ
WT+807710Δ/Δ

B

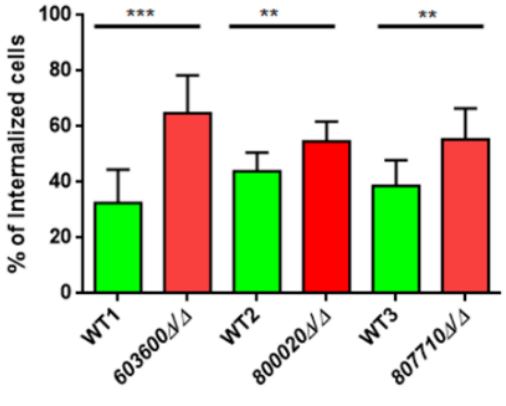
% of Internalized cells
100
80
60
40
20
0
***
**
**
WT1
603600Δ/Δ
WT2
800020Δ/Δ
WT3
807710Δ/Δ

C

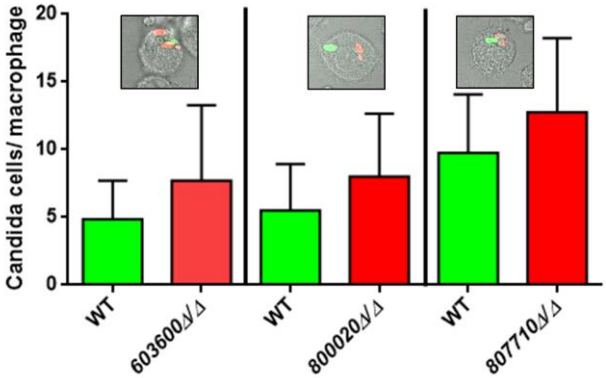
Candida cells/ macrophage
20
15
10
5
0
WT
603600Δ/Δ
WT
800020Δ/Δ
WT
807710Δ/Δ

Fig 21: Phagocytic competition assay

The competition assays were performed using combinations of GFP tagged wild type *C. parapsilosis* and mCherry tagged eicosanoid mutant strains. Equal numbers of yeast cells expressing GFP or mCherry were mixed together and added to human PBMC-DMs at the MOI of 1:2. (A) Representative image of macrophages with GFP and mCherry labeled *Candida* cells. (B) Macrophages phagocytosed significantly higher number of mutant cells compared to the wild type strain in case of all the three mutants. (C) Graph comparing percentage of phagocytosed candida cells in single macrophages with both type of cells. Unpaired t-tests were used to determine differences between groups. *$P < 0.05$, **$P < 0.01$, ***$p<0.002$.

The percentage of internalized cells was calculated for each strain, and the values for the mutants were compared to those of the wild type's (Fig 21A). We calculated the percentage of phagocytosis by counting the total number of PBMC-DMs (Fig 21B). The number of green and red cells inside a single PBMC-DM which phagocytosed both type of cells was also analyzed. Overall our results revealed that, PBMC-DMs significantly preferred the uptake of *603600*Δ/Δ, *800020*Δ/Δ and *807710*Δ/Δ cells over the wild type. However, when the PBMC-DMs phagocytosed both type of cells we did not find any significant preference for the mutant cells (Fig 21C).

4.8 Reduction in prostaglandin production alters the cytokine response

Eicosanoid derived lipid mediators effectively regulate inflammatory responses. Multiple functions, dependent on concentration, location and timing have been described for the prostaglandins (e.g.PGD_2 and PGE_2), while particularly anti-inflammatory and pro-resolving properties are assigned to LXA_4 functions [4]. In order to examine the immunological responses triggered by the *603600*Δ/Δ, *800020*Δ/Δ and *807710*Δ/Δ, we stimulated human PBMC-DMs for 24 hours with each strain and determined the amount of cytokine and chemokine production. During the experiments we measured pro-IL-1β, TNFα, Interleukin-1 receptor antagonist (IL-1ra), interleukin-6 (IL-6), interleukin-8 (IL-8) and interleukin-10 (IL-10) levels.

PBMC-DMs infected with *603600*Δ/Δ or *800020*Δ/Δ produced significantly higher Pro-IL-1β, IL-1ra, Il-6 and TNFα levels compared to the wild type strain. Whereas PBMC-DMs stimulated with *807710*Δ/Δ showed a higher amount of Pro-IL-1β, TNFα and IL-8

production, but no significant difference was observed in the IL-1ra and IL-10 levels compared with the reference strain. Notably, all mutant strains induced significantly higher amounts of IL-6 secretion (Fig 22A).

We analyzed the cytokine production of human primary PBMCs following fungal stimuli. PBMCs infected with *807710*Δ/Δ produced higher amounts of IL-1β and TNFα (Fig 22B), although there was no difference with the other mutant strains. These data suggest that fungal eicosanoids may also influence the host cytokine response.

A

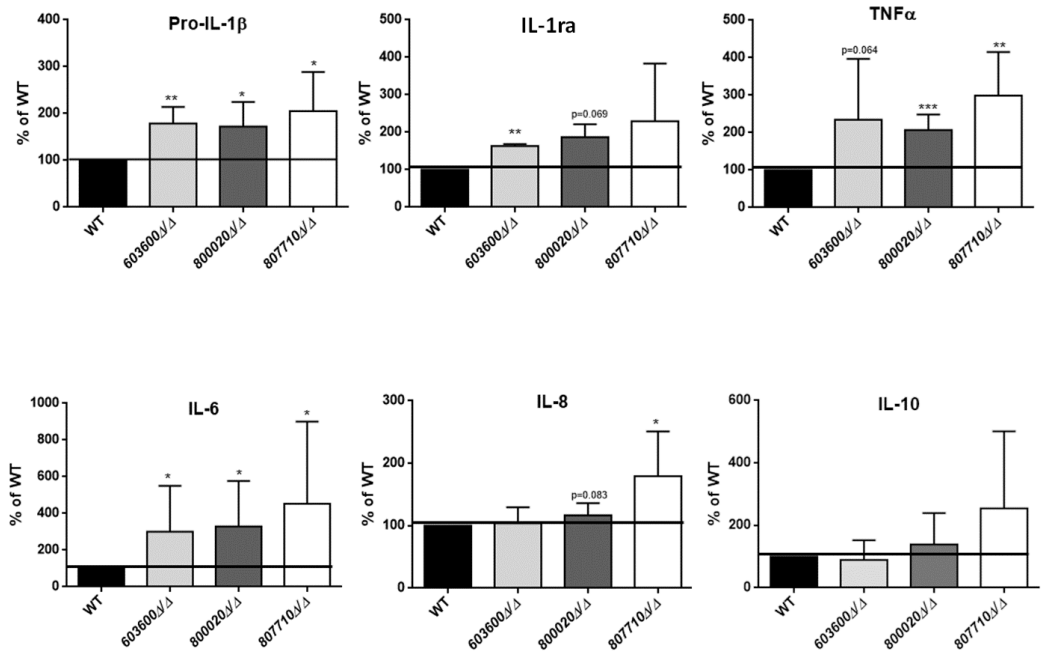

B

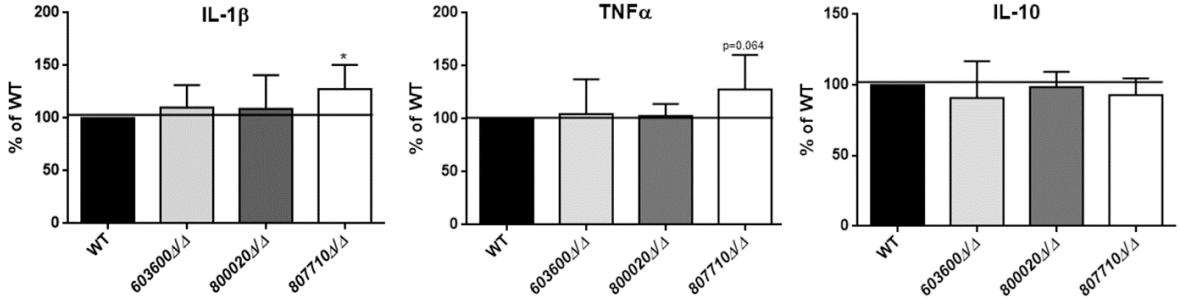

Fig 22: Cytokine secretion of human macrophages in response to wild type and eicosanoid mutants

(A)Pro IL-1β, secreted IL-1ra, TNFα, IL-6, IL-8, and IL-10 levels were measured by ELISA after stimulation of PBMC-DMs with wild type or eicosanoid mutant strains for 24 hours. Data were normalized for each donor to cytokine levels induced by the wild type strain (100 %) to minimize donor to-donor variability. (B) IL-1β, TNFα and IL-10 were also measured after infection of human PBMCs with the same strains. Data represent % cytokine production ± SEM for 6 donors. Unpaired t-tests were used to determine differences between groups. **P* < 0.05, ***P* < 0.01, ****p*<0.002.

4.9 *603600*Δ/Δ, *800020*Δ/Δ and *807710*Δ/Δ strains show attenuated virulence *in vivo*

Following *in vitro* studies, we also aimed to examine the virulence of the *603600*Δ/Δ, *800020*Δ/Δ and *807710*Δ/Δ *in vivo* using a mouse model of disseminated candidiasis. Following the intravenous infection of BALB/c mice, the fungal burdens of different organs were determined three days after the infection. After CFU recovery, we found that mice infected with *603600*Δ/Δ showed significantly reduced fungal burdens in the liver and kidneys, while *800020*Δ/Δ inoculated mice also revealed lower fungal burdens in the liver and kidneys. Finally, CFUs recovered following *807710*Δ/Δ injection were significantly less in the spleen and kidneys compared to those recovered from wild type-infected mice (Fig 23). These results indicate that these eicosanoid biosynthesis gene play a role in *C. parapsilosis* virulence.

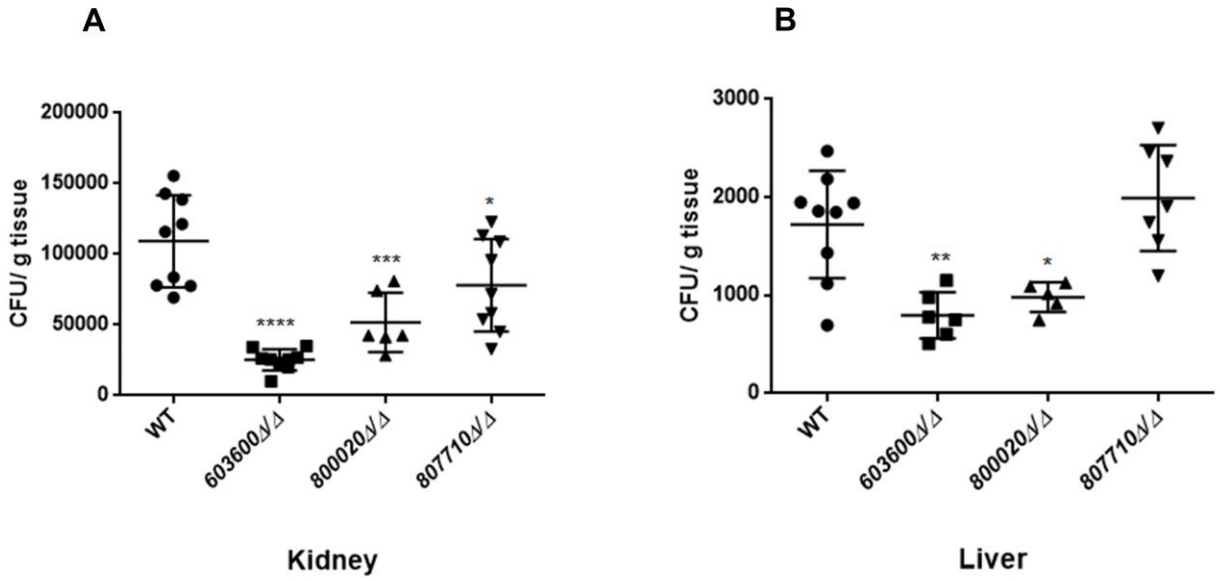

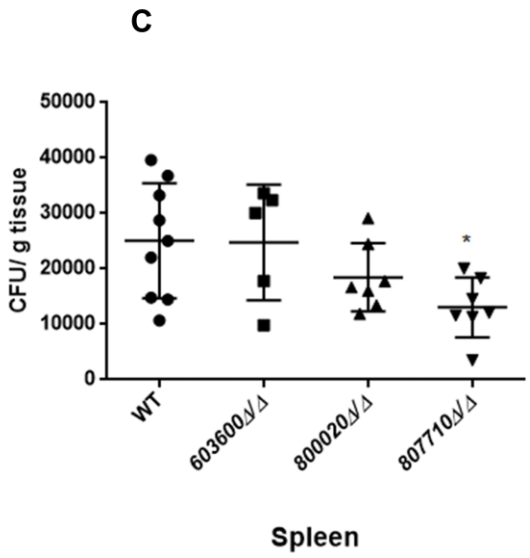

Fig 23: Fungal burden in organs after intravenous infection
Five mice were infected intravenously with 2×10^7 /µl of *C. parapsilosis* cells wild type or eicosanoid mutant cells. CFUs recovered from kidney (A), liver (B), and spleen (C) after 3 days of the infection. The results are pooled data from two independent experiments. One-way ANOVA with Dunnett's Post-Hoc test was used to determine the differences between groups. *P < 0.05, **P < 0.01, ***p<0.002, ****p < 0.0001.

4.10 Identification of three multicopper oxidase genes in *C. parapsilosis* by *in silico* analysis

To reveal the possible number of multi copper oxidase encoding genes present in the *C. parapsilosis* genome, a BLAST search performed in the Candida Genome Database (www.candidagenome.org) [120] using *Saccharomyces cerevisiae* Fet3p (YMR058W) as the query sequence. We found three multi copper oxidase family of gene having >40% identity with *S. cerevisiae FET3* gene (Fig S1) which are CPAR2_603600, CPAR2_304050 and CPAR2_303590. Whereas, the closely related species *C. albicans* have five different genes namely *FET3*, *FET31*, *FET33*, *FET34* and *FET99* [99]. To examine the role of CPAR2_603600 in *C. parapsilosis*, we generated two independent deletion mutants using the same gene disruption method as mentioned above.

4.11 Iron dependent growth of the Δ/Δ*CPAR2_603600* mutant strain

To investigate the role of *CPAR2_603600* in iron homeostasis regulation in *C. parapsilosis*, we examined the growth of the two independent homozygous deletion mutants in the presence of iron. Both mutants grew similarly to the wild type strain on YPD agar plates, indicating that *CPAR2_603600* is not essential for viability in complex media. Next, the growth of the mutants was examined in the presence of an iron chelator, BPS (Bathophenanthrolinedisulfonic acid) chelating ferrous iron(II). Under iron-limited conditions, both mutants trains showed a growth deficiency compared to the wild type strain (Fig 24). These results suggest that CPAR2_603600 is required for growth in low iron condition in *C. parapsilosis*.

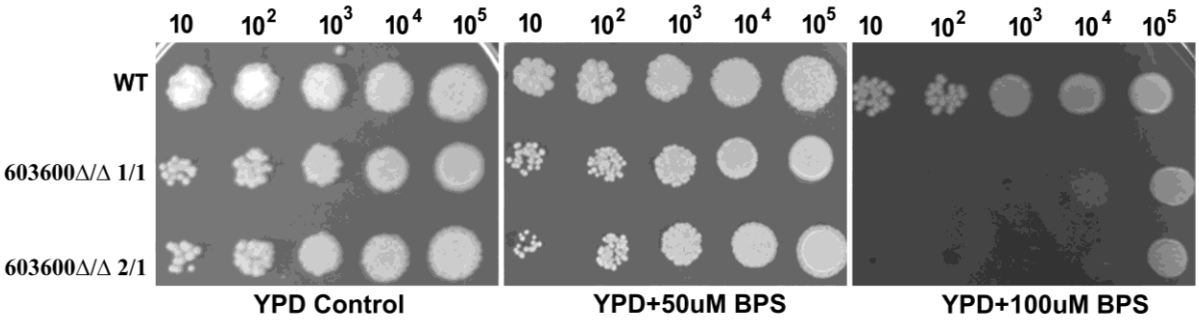

Fig 24: Growth of *CPAR2_603600* deletion mutants in iron restricted conditions (BPS supplemented YPD media).
Indicated cells numbers were used for the spotting experiment. Three days post-incubation the plates were scanned.

4.12 Phenotypic characterization of the Δ/Δ*CPAR2_603600* mutant

Phenotypic characterization was performed under 18 various growth conditions, including different temperatures, pHs, the presence of supplements such as cell wall, cell membrane, osmotic, oxidative and heavy metal stressors. YPD plate was used as an untreated control (Fig 25-26). Growth was scored using a color-coded scoring system where -4 indicates lack of growth, 0 similar growth to the wild type strain, and +1 indicating advanced growth compared to the reference strain. The mutants grew slowly at lower temperatures and under alkaline conditions. They were highly sensitive to the cell wall stressor Congo red, to the

cell membrane stressor SDS as well as to the presence of the metal ion chelator EDTA, and the oxidative stress inducer menadione and cadmium ($CdSO_4$). In contrast, the mutants were less sensitive to the presence of copper. There was no difference in growth on sorbitol or NaCl supplemented media.

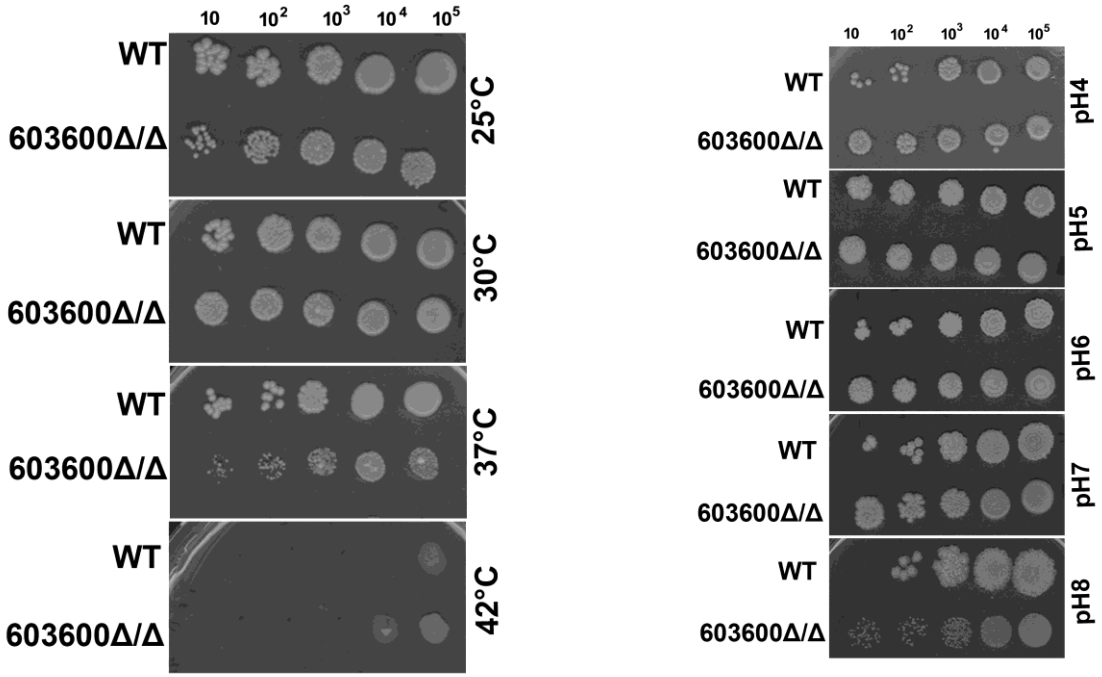

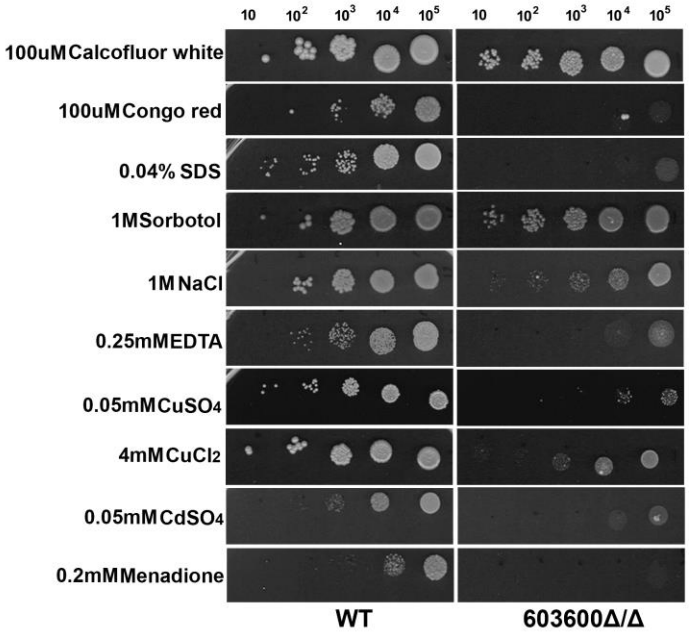

Fig 25: Phenotypic characterization of the *603600Δ/Δ* mutant under different growth conditions

Growth conditions include different temperatures, pHs, presence of osmotic, cell wall, cell membrane, oxidative and metal ion stressors.

	CLIB	Δ/Δ *fet3*
Temperature		
YPD 25 °C		
YPD 30 °C		
YPD 37 °C		
YPD 40 °C		
pH		
pH4		
pH5		
pH6		
pH7		
pH8		
Stress source		
CW(100uM)		
Congo Red(100uM)		
SDS(0.04%)		
NaCL(1M)		
CdSO4(0.05mM)		
$CuCl_2$(4mM)		
$CuSO_4$(4mM)		
1M Sorbitol		
EDTA(0.25mM)		
Menadione (0.2mM)		

Fig 26: Heat map indicating phenotypic defects of *603600Δ/Δ* mutant

Heat map showing the phenotypic difference of *603600Δ/Δ* mutant compared to the wild type strain.

4.13 Significant reduction in yeast to pseudohypha production in case of the *603600Δ/Δ* mutant

One of the most important virulence traits of *C. parapsilosis* is its ability to change morphology. Previously, it has been shown that *TUP1* in *C. albicans* is required for filamentous growth and is also involved in iron transport regulation. Therefore, we examined whether the deletion of CPAR2_603600 has any effect on pseudohypha formation in *C. parapsilosis*. Interestingly, the homozygous deletion mutant showed a significant reduction in pseudohypha formation in both solid and liquid media. Fig 27A shows

differences in colony morphology between the wild type and the mutant strains both on spider and YPS agar plates. Specifically, the mutant strains showed a smooth colony morphology rather than a wrinkled phenotype observed in case of the wild type. Consistent with the above-mentioned results, *603600Δ/Δ* mutant displayed well-defined colony edges on the spider media plate and no filamentous structures were visible by light microscopy (Fig 27B). Percentage of pseudohypha was calculated from the bright field microscopic images which revealed a significantly lesser amount of pseudohyphae present in the mutant strains in serum supplemented YPD, spider, YPS and in Lee's media (Fig 27C). When comparing the single colonies of the corresponding strains, differences in morphology were also clearly visible (Fig 28). We also quantified the amount of pseudohypha production in the examined strains in hypoxic condition (5 % CO_2) by flow cytometry after cell wall staining. The mutant strain showed lesser percentage of pseudohypha compared to the wild type strain (Fig 29).

A **B**

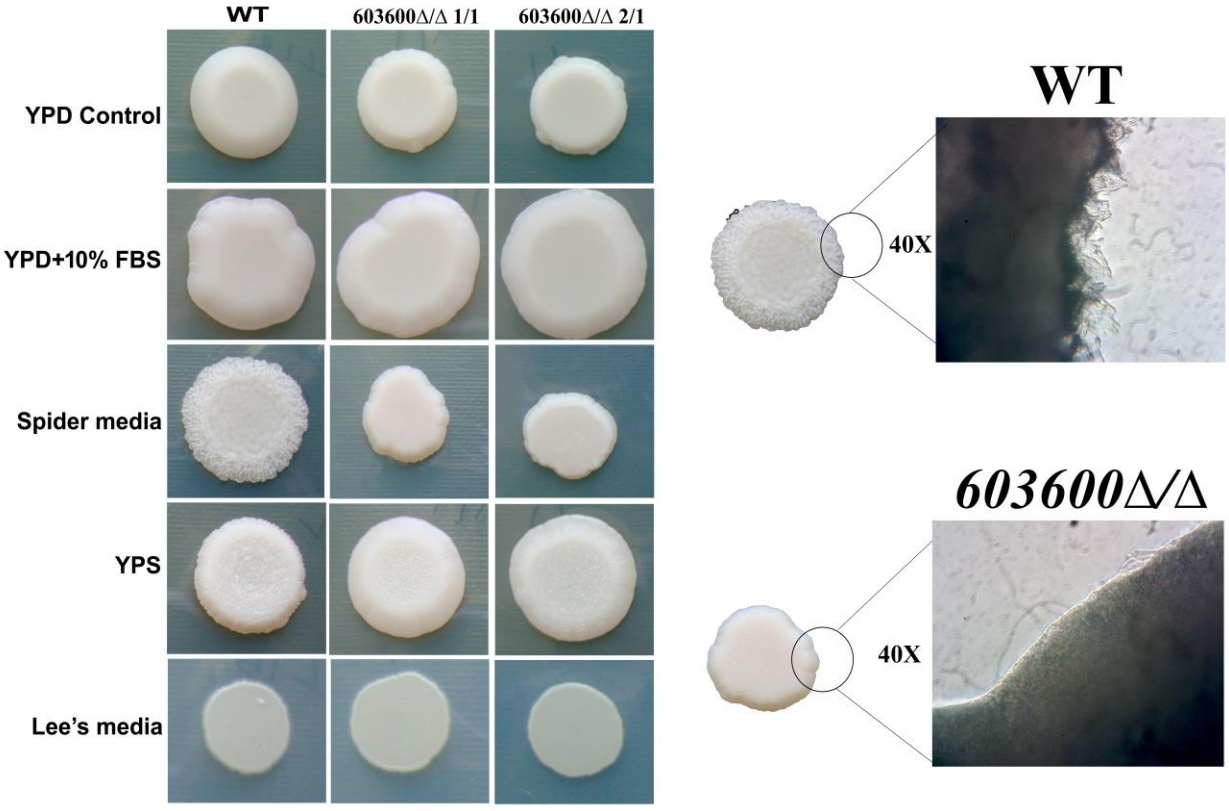

C

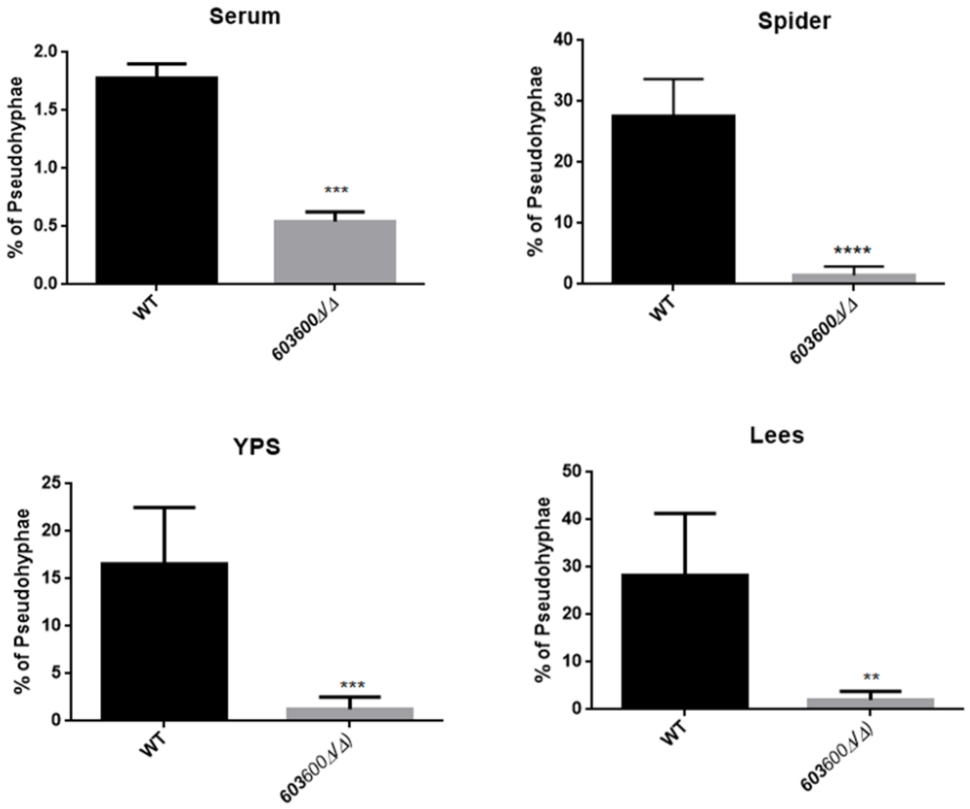

Fig 27: Pseudohypha formation defect of the *603600Δ/Δ* strain

(A) Colony morphology of the deletion mutants compared to the wild type strain under the shown conditions. Colony wrinkling is visible in Wild type strain in case of spider and YPS media but not in the mutants, whereas the other two media did not show any difference. Growth on YPD was used as a control. (B) Microscopic picture of the colony on spider media of both wild type and mutant strain (C) Pseudohypha formation was also examined in liquid media by bright field microscopy. Graph showing significant reduction in percentage of pseudohypha formation in the deletion mutant in both in different media compared to the parental strain. Unpaired t-tests were used to determine differences between groups. *P < 0.05, **P < 0.01, ***p<0.002, ****p<0.001.

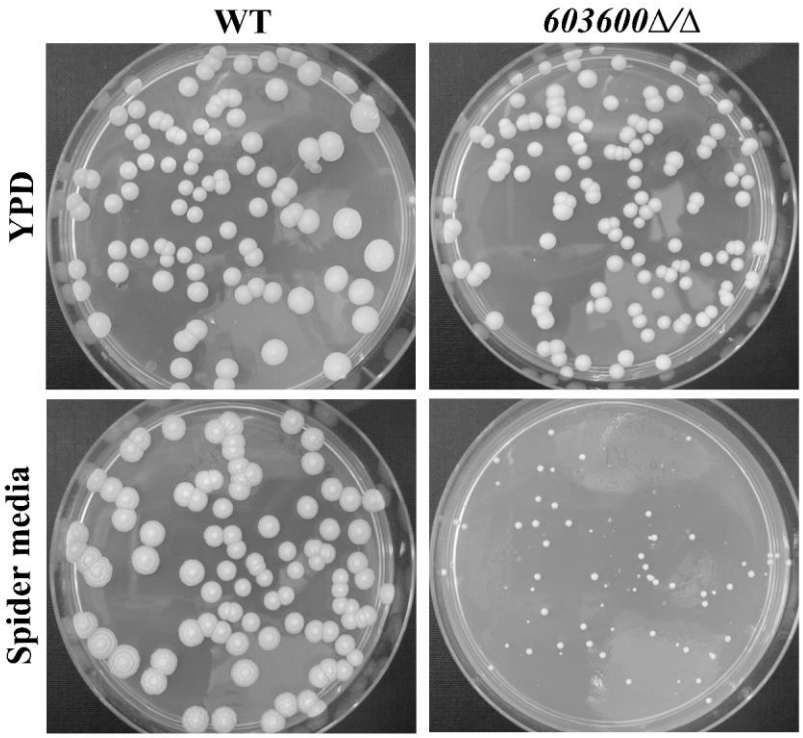

Fig 28: Single colony morphology on spider media
Single colonies of the mutant strain grow very slowly on spider media plate compared to the wild type without any visible colony wrinkling.

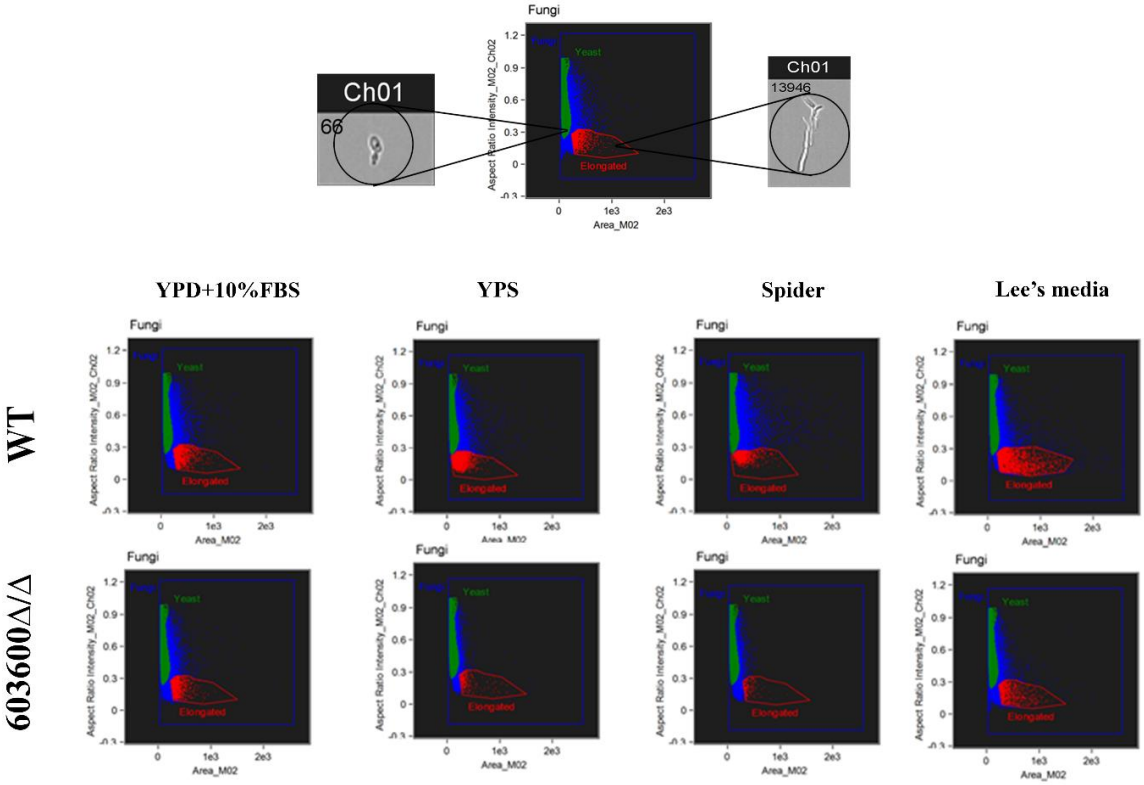

	CLIB	*603600Δ/Δ*
YPD	2.79%	2.5%
YPD+10% FBS	3.63%	3.03%
YPS	4.62%	0.35%
Spider	17.7%	0.67%
Lee's media	8.34%	2.7%

Fig 29: Comparison of the amount of pseudohypha by FACS analysis in hypoxic conditions
Percentage of pseudohypha formation was determined by FACS analysis after growing the cells in pseudohypha inducing media in presence of 5% CO_2.

4.14 The *Δ/ΔCPAR2_603600* mutant strain is defective of biofilm formation

The other major factor that is associated with *C. parapsilosis* pathogenicity is its ability to form biofilm on abiotic surfaces like medical implants. Biofilms produced by this fungus are composed of both yeast cells and pseudohyphae. Thus, the mutant's defect in pseudohypha formation inspired us to examine whether this alteration affected the strain's biofilm forming ability. To investigate the possible differences between the wild type and the mutant strains in terms of biofilm formation, all strains were plated into flat bottom 96 well tissue culture plates in spider media and kept at 37 °C for 48 hours. Cell free media was used as negative control. Biofilm forming abilities were quantified by using a metabolic assay (XTT reduction assay) and also by crystal violet staining (specific staining for biomass measurement). As a result, the deletion mutants showed a significant reduction in their biofilm forming ability compared to the wild type strain (Fig 30).

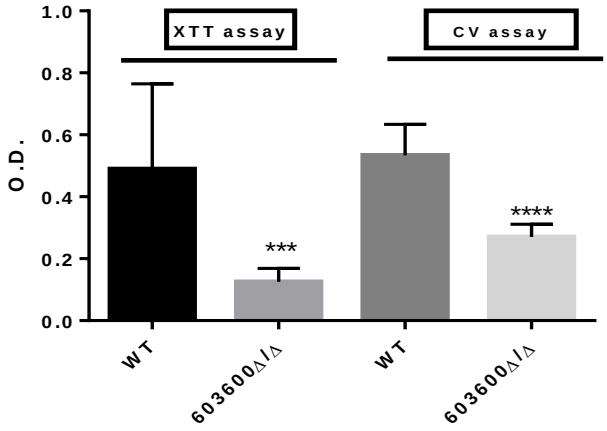

Fig 30: Loss of *CPAR2_603600* gene effects *C. parapsilosis* biofilm formation
Differences in biofilm formation on abiotic surfaces were determined by the XTT reduction assay (XTT assay) and also by crystal violet (CV) staining. The mutant strain showed a significant reduction in biofilm formation compared to the wild type *C. parapsilosis* strain. Unpaired t-tests were used to determine differences between groups. ****p*<0.002, ****p<0.001.

4.15 Iron supplemented media restored pseudohyphae formation and biofilm formation

To check if the defects in pseudohyphae and biofilm formation in the mutant depends on iron availability, all mutant strains were grown on YPD with additional 2 mM $FeCl_3$ (as the preculture media) for overnight at 30 °C. Next day, overnight culture was washed with 1xPBS and checked for the pseudophyphae and biofilm forming abilities. We found that both the wild type and the two-homozygous deletion mutant strains showed similar colony morphology on different pseudohyphae induction media. Percentage of pseudohyphae was also calculated from bright field microscopic images. The graph showed that the pseudohyphae formation was partially rescued in the mutant (Fig 31).

We also analyzed whether the addition of extra iron in the preculture can recover the biofilm forming defect of the mutant by previously mentioned XTT assay (Fig 32A) and crystal violet assay (Fig 32B). Our results clearly indicated that addition of iron also partially rescued the biofilm forming defects of mutant strain.

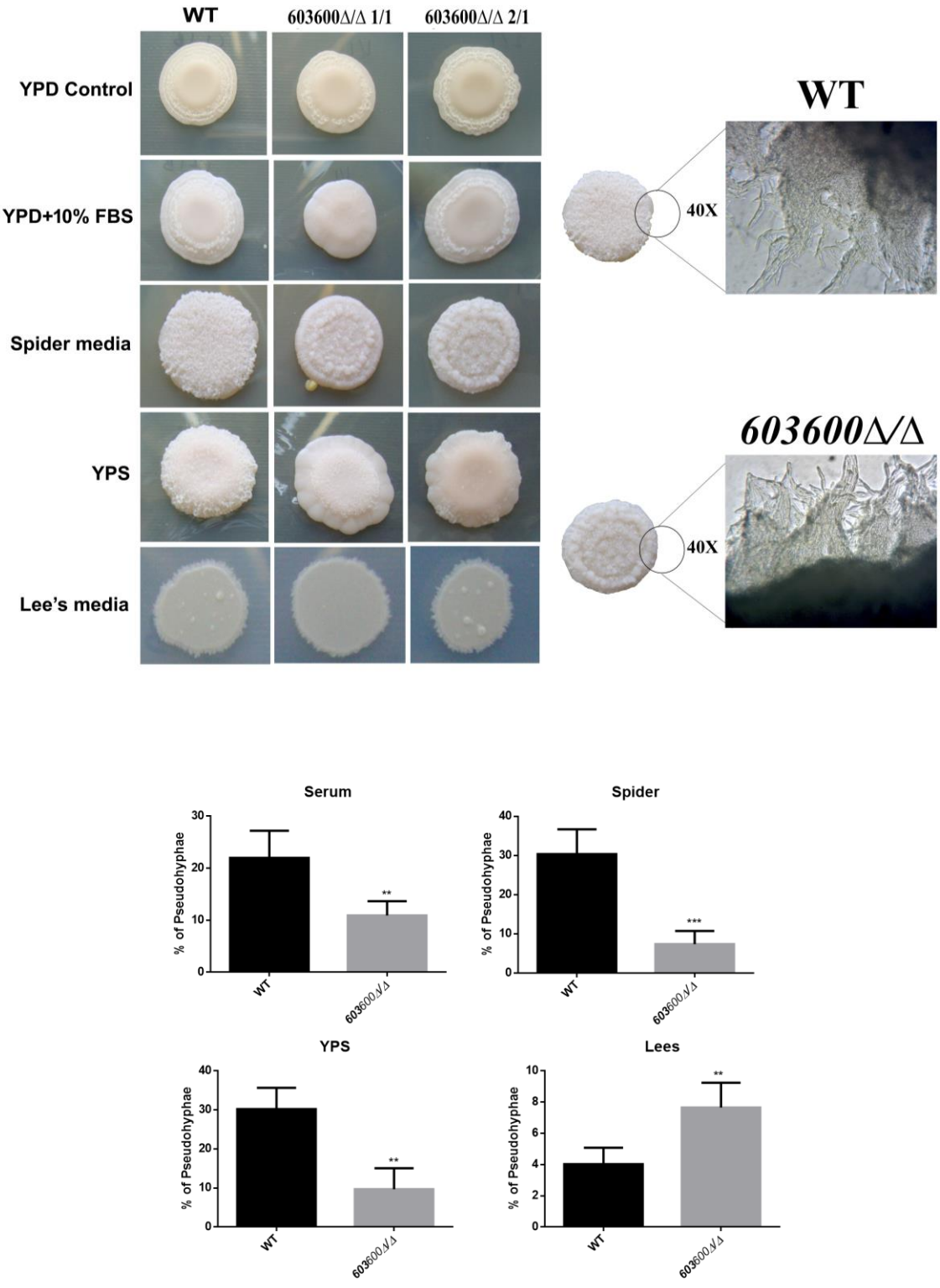

Fig 31: Growth defect rescued by addition of accessible iron to the preculture media
Pseudohypha and biofilm production was analyzed after growing the strains in the presence of 2mM $FeCl_3$ in the preculture media for overnight at 30 °C. Addition of excess iron to the media rescued the pseudohypha forming defect both in solid and liquid media. $^{**}P < 0.01$, $^{***}p<0.002$.

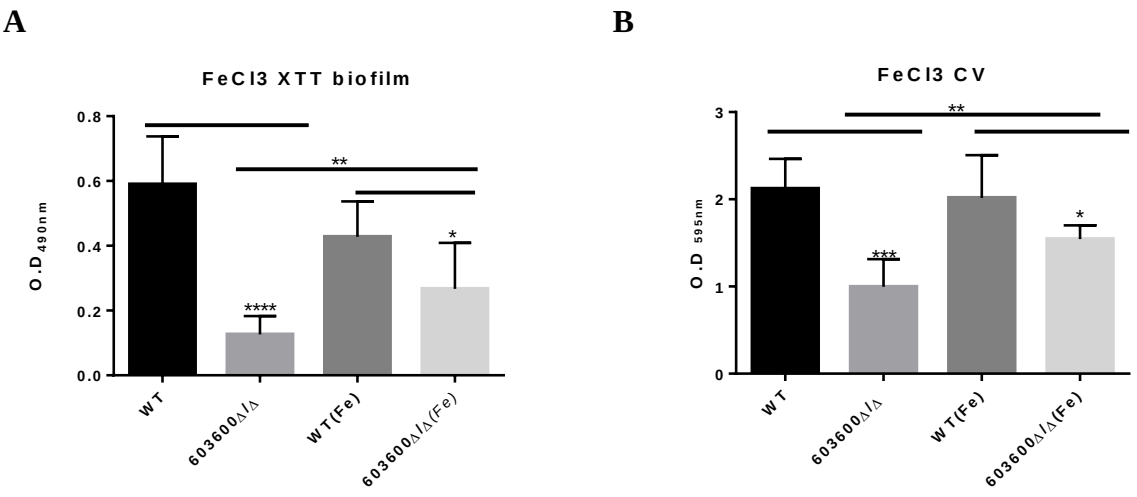

Fig 32: Biofilm formation after the growth in the presence of excess iron
Addition of extra iron in the preculture media partially rescued the biofilm forming defect in the mutant strain. *$P < 0.05$, **$P < 0.01$, ***$p<0.002$.

4.16 Overexpression of genes related to iron metabolism in the *603600Δ/Δ* strain

We also checked, if the lack of this multicopper oxidase gene alters the expression of other genes related to iron uptake and metabolism. We selected 15 genes (Table S4) by GO term analysis from the candida genome database, whose homologue play an important role in iron homoeostasis in *S. cerevisiae* or in *C. albicans*. By qRT-PCR analysis we found that the genes *CFL5*, *HEM15*, *FTH1* and *FTR1* were highly overexpressed (fold change >5), while *CCC2*, *SEF1*, *HMX1*, *RBT5* and *HAP43* were slightly overexpressed (fold change >2) (Fig 33). This indicates that in absence of the *CPAR2_603600* gene, orthologous genes of ferric reductase, ferrous iron transport and ferrous iron permease which play role in iron transport and metabolism was upregulated in *C. parapsilosis*.

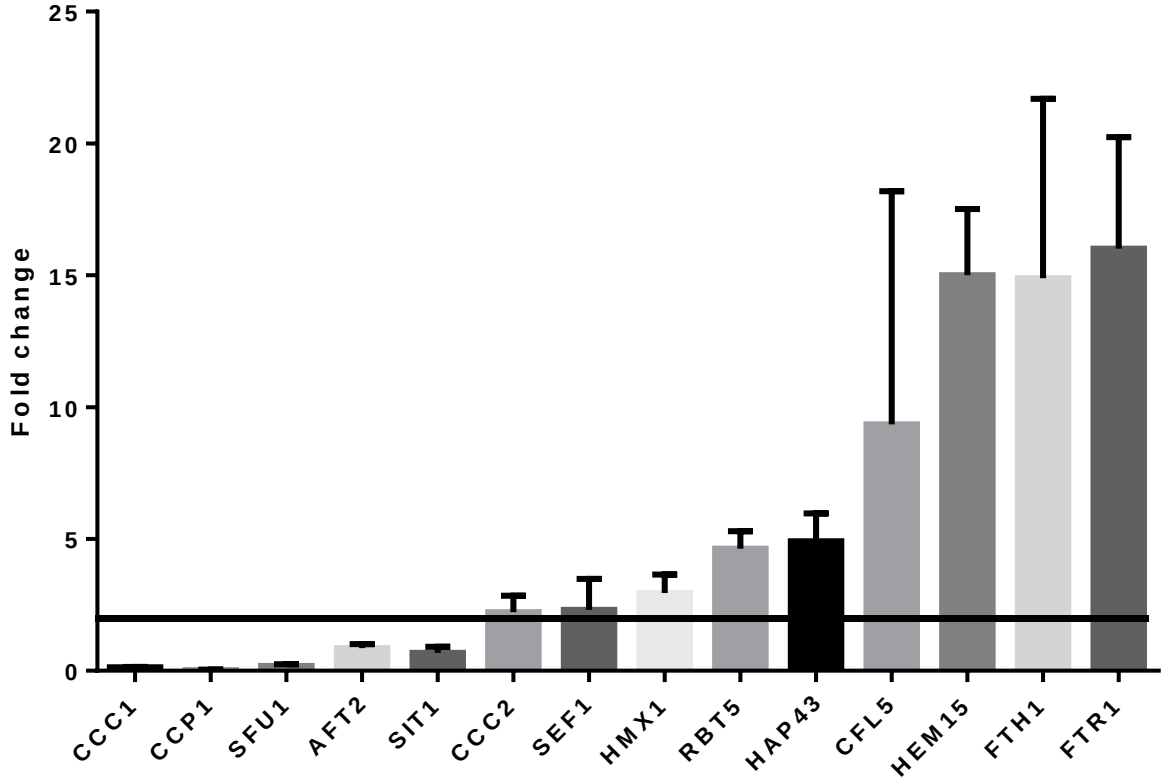

Fig 33: Expression level of genes involved in iron metabolism (ortholog of *C. albicans*) in the CPAR2_603600 deletion mutant

Fold change expression analysis of genes related to iron metabolism (GO term analysis) was performed using quantitative real time PCR in the mutants and compared to the wild type strain.

5 Discussion

Eicosanoids, a group of bioactive mediators, are signaling molecules with diverse physiological and pathological functions known to modulate inflammatory responses. Prostaglandins, leukotrienes and lipoxins are groups of eicosanoids involved in pro-, and/or anti-inflammatory responses. During vasodilation prostaglandins and leukotrienes induce increased permeability of post capillary venules and also recruit complement components and leukocytes to the site of inflammation [4]. In contrast, lipoxins act as pro-resolving lipid mediators, as for example, LXA_4 inhibits the recruitment of neutrophil and eosinophil granulocytes in post capillary venules [131]. Previously, it has been hypothesized that during fungal infection the invading fungi induce host prostaglandin biosynthesis that causes a local anti-inflammatory response, which in turn could contribute to fungal invasion [132].

In recent years, several studies have revealed that human pathogenic fungi are able to produce lipid mediators, specifically prostaglandins that might as well contribute to their virulence. This group of pathogens includes species such as *A. nidulans*, *A. fumigatus*, *Cr. neoformans*, *C. albicans* and *C. parapsilosis*.

Investigations have revealed several biosynthetic pathways used by some of these pathogens. As an example, *A. nidulans* and *A. fumigatus* have three dioxygenase-encoding genes, namely *ppoA*, *ppoB* and *ppoC* with high sequence similarity to mammalian cyclooxygenases [27]. Besides regulating sexual and asexual sporulation, all three *ppo* genes contribute to prostaglandin biosynthesis, possibly via oxygenating arachidonic acid, thereby generating the prostaglandin precursor PGH_2 [27].

Other studies have revealed that certain pathogenic fungi, such as *C. albicans* and *Cr. neoformans*, do not possess COX-like enzymes, thus they must have evolved prostaglandin biosynthetic pathways different from those of mammals (Erb-Downward and Huffnagle, 2006, Fischer and Keller, 2016). In *Cr. neoformans*, a member of the multicopper oxidase family, the Lac1 laccase regulates PGE_2 biosynthesis, possibly by converting the prostaglandin precursor PGG_2 to PGE_2 and 15-keto-PGE_2 [28].

In *C. albicans* however, the fatty acid desaturase *OLE2* and a multicopper oxidase *FET3* play a role in prostaglandin production via novel pathways using exogenous arachidonic

acid as precursor [30]. *CaFET3,* a laccase homolog (and also a member of the Fet family of multicopper oxidases) is suggested to regulate PGE_2 biosynthesis through a mechanism similar to that of *LAC1* in *Cr. neoformans*. On the other hand, Ole2, a putative delta9 desaturase also containing a cytochrome B domain, is hypothesized to regulate PGE_2 production via the oxidation of exogenous arachidonic acids [30].

Notably, in these species, the identified genes are pleiotropic regulators as they also participate in mechanisms such as sporulation (*ppo* genes), cell wall homeostasis (*LAC1*) or iron uptake (*FET3*), and thus contribute to virulence in a complex manner. Nevertheless, the role of fungal prostaglandins in virulence is evident as, in all examined fungal species, their production has been associated with markedly altered immune responses [27]. To expand our knowledge about the role of fungal eicosanoids in pathogenesis, we examined lipid mediator production in another important human fungal pathogen, *C. parapsilosis*. As the incidence of this species has increased over the past two decades and the patient group at risk includes immunosuppressed children and adults as well as neonates, understanding the pathogenesis of *C. parapsilosis* has gained increased attention [135,136]. Preliminary studies have started to elucidate the prostaglandin profile of this species, however, the involved biosynthetic pathways and the presence or role of other fungal eicosanoids remained elusive. Previously, we have shown that in the presence of exogenous arachidonic acid, *C. parapsilosis* is capable of producing fungal prostaglandins, although *OLE2* is not involved in the synthetic mechanisms, leaving the corresponding biosynthetic processes unexplored [89] .

Therefore, in the current study, we aimed to reveal regulators involved in eicosanoid biosynthetic mechanisms and to investigate their roles in the virulence of this species. Following arachidonic acid induction, we identified three genes that significantly influence the biosynthesis of fungal prostaglandins. Our results indicate, that *CPAR2_603600,* a homologous gene of *CaFET3* is involved in PGE_2 and PGD_2 production, *CPAR2_807710*, a homologue of the acyl-coenzyme A oxidase *ScPOX1-3,* regulates PGE_2 and 15-keto-PGE_2 synthesis, and *CPAR2_800020*, a homologue of 3-ketoacyl-CoA thiolase *ScPOT1*, influences PGE_2 biosynthesis. Using LC/MS analysis, we observed that the disruption of each gene led to the decrease in the corresponding eicosanoids' production.

While *CaFET3* is known to interfere with fungal prostaglandin production [30], no such role has been associated with *CaPOX1-3*, and *CaPOT1* in *C. albicans*, suggesting a novel function of the corresponding homologues in *C. parapsilosis*.

Since fungal prostaglandins can hijack host inflammatory responses [132], we also examined if the identified regulators could impact this phenomenon by examining the genes' contribution to *C. parapsilosis* pathogenicity. According to our results, *CPAR2_603600*, *CPAR2_807710* and *CPAR2_800020* all contribute to the virulence of *C. parapsilosis in vitro*, as deletion mutants of the corresponding genes were phagocytosed and killed more efficiently by human PBMC-DMs. The three null mutant strains also induced less damage to PBMC-DMs compared to the wild type strain. Following Balb/c mice infection two of the deletion mutants showed reduced virulence when compared to the reference strain.

The roles of *CaFET3* and *CaPOT1* in *C. albicans'* virulence have been investigated. Deletion of *CaFET3* resulted in reduced adhesiveness to fibroblasts, although no significant differences were observed between the virulence of the wild type and the *Δ/Δfet3* strain in a mouse model of systemic candidiasis [114]. In contrast, *CaPOT1*, a 3-ketoacyl-CoA thiolase, involved in fatty acid utilization, is not required for virulence in an embryonated chicken egg infection model [137]. Unfortunately, to date, we lack information about the role of the hypothetical acyl-coenzyme A oxidase (*CaPOX1-3*) in *C. albicans* pathogenesis. The examined literature and our obtained data suggest, that in contrast to *C. albicans*, the homologous genes of *FET3*, *POT1* and *POX1-3* in *C. parapsilosis* indeed contribute to fungal virulence, although the corresponding mechanisms still need to be elucidated.

Interestingly, *CPAR2_603600* might be involved in delaying phagosome-lysosome fusion, although additional studies are needed to confirm this hypothetical mechanism.

Fungal prostaglandins produced by *C. albicans* and *Cr. neoformans* alter host cytokine responses by down-regulating chemokine (IL-8) and pro-inflammatory cytokine (e.g. TNFα) production while concomitantly up-regulating anti-inflammatory responses via promoting IL-10 release [132]. Our results suggest a similar effect with *C. parapsilosis* eicosanoids, as mutant strains defective in prostaglandin production induced higher pro-inflammatory cytokine responses, as shown by the increased levels of Pro-IL-1β, IL-1ra, IL-6 and TNFα released by human PBMC-DMs. Although, stimulation of human PBMCs with only one of

the mutant strain (*CPAR2_807710 Δ/Δ*) resulted in an increased IL-1β and TNF-α release. These data suggest that *CPAR2_807710, CPAR2_800020* and *CPAR2_603600* contribute unequally to the alteration of host immune responses.

We have identified three *C. parapsilosis* eicosanoid biosynthesis regulatory genes, namely *CPAR2_807710*, *CPAR2_800020* and *CPAR2_603600*, that are involved in the production of fungal prostaglandins. Virulence studies performed with the corresponding null mutant strains suggests that these regulatory genes also influence the fungal virulence. Although, further investigation is needed to thoroughly understand the importance of fungal eicosanoids, our results can contribute to a better understanding of host pathogen interactions during candidiasis.

The role of metal homoeostasis in the virulence of human pathogenic fungi such as *C. albicans*, *Cr. neoformans* and *A. fumigatus* has been well studied throughout the years [95]. Among all the trace elements, iron plays the most important role in fungal pathogenesis. The availability of free iron in the blood is tightly restricted by the host as part of the nutritional immunity. *Candida* spp., as commensal pathogens, evolved different iron uptake mechanisms to survive within different host niches [99]. *C. albicans* can utilize iron from different sources within the host. These sources include hemoglobin, transferrin, lactoferrin, ferritin and also siderophores produced by other microorganisms. The main enzymes or proteins involved in iron homoeostasis in *C. albicans* include surface ferric reductases (*CFL1*/*FRE1*) [138] (*CFL95*/*FRE10*/*RBT2*) [105,139], multicopper oxidases (*FET3, FET99*) [140,141] and finally high affinity iron permeases (*FTR1*) [106]. Among the five multicopper oxidase genes present in *C. albicans*, deletion of the *FET3* gene resulted in a growth defect in low iron conditions and reduced prostaglandin production [30] but the deletion mutant remained as virulent as the wild type strain. Deletion of *FET34* had a slight iron dependent growth defect, a reduction in hypha formation and resulted in a hypo virulence in a mouse model of systemic infection. Removal of *FET33* had no such defect [142,143]. In case of *C. parapsilosis*, the mechanism of iron homoeostasis is largely unknown.

In the present study, we identified three orthologs of the *FET3* multicopper oxidase gene in *C. parapsilosis* by *in silico* analysis. We generated a homozygous deletion mutant strain of the gene *CPAR2_603600*, which had 79% identity with *CaFET3* and 54% identity with

ScFET3 at amino acid level. We found that deletion of the corresponding homologue in *C. parapsilosis* resulted in a severe growth defect on iron limiting media (BPS). It has been reported that there is a correlation between iron availability and filamentous growth and the presence of BPS induces the expression of hypha specific gene (*EFG1*) in *C. albicans* [144]. The deletion of *FET34* also reduced hypha formation in this pathogenic fungus. All these data inspired us to check whether the effect is the same in *C. parapsilosis* or not. We observed that the *603600Δ/Δ* mutant in *C. parapsilosis* showed a visible reduction in pseudohypha formation on solid spider and YPS plate. The microscopic picture of the colony on the spider media plate also showed that the wild type colony has the capacity to form more pseudohypha. Analysis of the number of pseudohyphae grown in liquid pseudohypha inducing media also showed a significant reduction in pseudohypha production. The mutant also showed a significant reduction in biofilm formation on abiotic surfaces that we quantified by both crystal violet staining and the XTT metabolic reduction assay. However, growth in the presence of excess iron in the media the pseudohypha formation activity was restored. All the above observations suggest that *CPAR2_603600* has a role in iron dependent growth and morphology regulation in *C. parapsilosis*. Similarly to *C. albicans*, we also found that the deletion strain had a significant reduction in prostaglandin production. Although in contrast to *C. albicans*, the *603600Δ/Δ* mutant is less virulent in a mouse model of systemic infection. We found that in absence of the *FET3* ortholog in *C. parapsilosis*, expression of several other putative iron metabolism regulatory genes elevated that can be a compensatory effect in response to iron toxicity. Altogether our results provide a novel insight into the role of the ortholog of multicopper oxidase *CaFET3* gene CPAR2_603600 in iron homoeostasis and morphology regulation in *C. parapsilosis.* However, further investigation is needed to understand the complete mechanism of iron metabolism in this species.

6 Summary

Candida parapsilosis is one of the major human fungal pathogens in terms of invasive candidiasis, primarily causing invasive infections among low birth weight infants. Despite its increasing prevalence very little is known about the mechanisms involved in its interaction with the human host. The eicosanoids are 20 carbon long chain fatty acid molecules that are mainly derived from arachidonic acids. They are the oxygenated metabolites of arachidonic acid produced mostly by the enzymatic action of COX and LOX enzymes. There are different eicosanoids produced in the mammalian host belonging to different subfamilies. These include prostaglandins, thromboxanes, leukotrienes, lipoxins, resolvins and HETEs (Hydroperooxy-eicosatraenoic acid). These eicosanoids are the bioactive signaling lipid molecules that play a major role not only in infection and inflammation but also in the resolution of inflammation. Although fungi lack the homologue of Cox/Lox enzymes, they are able to produce prostaglandins from exogenous arachidonic acid. In recent years it has been shown by different groups that human pathogenic fungi like *C. albicans*, *C. parasilosis*, *Cr. neoformans*, *P. brasiliensis* and *A. fumigatus* also produce prostaglandin molecules that are similar to mammalian prostaglandins. In case of *C. albicans*, it has been shown that two genes namely *OLE2* (Fatty acid desaturase homologue) and *FET3* (Multicopper oxidase homologue) are involved in the production of prostaglandinE_2 (PGE_2). However, it has been shown previously that, unlike in *C. albicans*, *OLE2* (fatty acid desaturase gene) is not involved in the biosynthesis of prostaglandin in *C. parapsilosis*. In our current work we identified novel genes involved in the production of different eicosanoids in *C. parapsilosis* and we have shown how these fungal lipid mediators are involved in the fungus' virulence.

To identify genes for eicosanoid biosynthesis in *C. parapsilosis*, we performed RNA-seq analysis after growing the cells in the presence of arachidonic acid, the main precursor for eicosanoid production. The sequence analysis showed that a total of 68 genes were upregulated and 83 genes were downregulated. From the upregulated genes we found that 14.5% are involved in lipid metabolism. Six probable candidate genes were selected by gene ontology term analyses that were supposedly involved in the lipid metabolism process. Homozygous deletion mutants for these genes were generated using the fusion PCR technique. The six mutants were then analyzed in terms of eicosanoid production. Cell free

supernatants were analyzed after growth in the presence of 100 µM arachidonic acid. The eicosanoid analysis performed by LC/MS revealed that out of the six mutants three - a multi copper oxidase (CPAR2_603600), an Acyl-CoA thiolase (CPAR2_80020) and an Acyl-CoA oxidase (CPAR2_807710) - showed a significant reduction in prostaglandins production compared to the wild type.

Homozygous deletion mutants of these genes were more efficiently phagocytosed and killed by human macrophages. They also induced higher levels of pro-inflammatory cytokine production by macrophages and were less virulent *in vivo*. Taken together, all the above observation indicate that these fungal lipid mediators modulate host immune system and play an important role in host pathogen interaction during *C. parapsilosis* infection.

Among all the essential micronutrients, iron plays an important role in mammalian biology. It is also extremely important for pathogens infecting the mammalian host such as bacteria, fungi and protozoans. As free iron is limited in mammalian host, human fungal pathogens like *C. albicans, Cr. neoformans, C. glabrata* and *A. fumigatus* evolved various routes to acquire iron from the host. Whereas, in case of *C. parapsilosis* this mechanism is largely unknown. In the current study, we showed that the ortholog of a multicopper oxidase gene *FET3* in *C. parapsilosis (CPAR2_603600)* is essential for growth in low iron condition. Homozygous deletion of CPAR2_603600 resulted in a growth defect under low iron conditions and also sensitivity to various stress conditions. We also found that the mutants were less capable of pseudohypha and biofilm formation, although reintroduction of accessible iron to the pre-culturing media rescued these defects. The expression of additional putative iron metabolism related genes also increased in the mutant compared to the wild type strain, suggesting a compensatory effect under iron limited conditions. In summary our study revealed the critical role of *CPAR2_603600* in iron homoeostasis and morphological switch regulation in this species.

7 ÖSSZEFOGLALÁS

A *Candida parapsilosis* egy humán patogén gomba, amely elsősorban a kis születési súlyú csecsemőknél okoz fertőzést. A növekvő gyakorisága ellenére keveset tudunk a gazdával történő kölcsönhatás során történő molekuláris mechanizmusokról. Az eicosanoidok 20 szénatomból álló zsírsav molekulák, amelyek főleg arachidonsavból származnak, annak oxidált metabolitjai, amelyek főleg a COX és LOX enzimek segítségével keletkeznek. Emlősökben az eicosanoidok különböző alcsaládokba sorolhatóak, mint például prosztaglandinok, tromboxánok, leukotriének, lipoxinok, resolvinok és HETE-k (hidropero-oxi-eikozatrénsav). Ezek az eicosanoidok bioaktív lipidek, amelyek főszerepet játszanak nem csak a fertőzésben és a gyulladásban, hanem a gyulladás csökkentésében is. Habár, a gombákban nincsenek jelen a COX/LOX enzimek megfelelői, ennek ellenére képesek prosztaglandinokat termelni exogén arachidonsavakból. Az utóbbi időben több kutatócsoport is igazolta, hogy a humán patogén gombák, úgy, mint a *C. albicans*, *C. parasilosis*, *Cryptococcus neoformans*, *Paracoccidioides brasiliensis* és *Aspergillus fumigatus* is képesek prosztaglandinokat termelni, amelyek hasonlóak az emlősök által termelt prosztaglandinokhoz. *C. albicans* esetében két gén, az *OLE2* (zsírsav-deszaturáz) és *FET3* (multicopper oxidáz) vesznek részt a prosztaglandin E2 (PGE_2) termelésben. Korábbi tanulmányok megerősítették, hogy a *C. albicans-tól* eltérően, az *OLE2* (zsírsav desztauráz) gén nem vesz részt a prosztaglandin bioszintézisében *C. parapsilosis* esetében. Jelen munkánkban új géneket mutattunk be, amelyek a *C. parapsilosis* eicosanoid bioszintézisében játszanak szerepet és megvizsáltuk, hogy ezen lipid mediátorok hogyan befolyásolják a gomba virulenciáját. A *C. parapsilosis* eicosanoid bioszintézisében résztvevő gének beazonosításához RNS-szekvenálást végeztünk arachidonsavas indukciót követően. A szekvencia analízis alapján, összesen 68 gén túltermelődését és 83 gén csökkent expresszióját figyeltük meg. Megállapítottuk, hogy a túltermelődött gének közül feltételezhetően 14.5% vesz részt lipid metabolizmus szabályozásban. A „Gene ontology term" analízis során hat gént választolttunk ki, amelyek részt vehetnek a lipid anyagcsere szabályozásában. A hat génre nézve fúziós PCR technikával homozigóta deléciós mutánsokat állítottunk elő. Ezután, a hat mutáns törzs eicosanoid termelését elemeztük. Az eicosanoidokat LC/MS módszerrel mértük. A hat kiválasztott gén közül háromra, a multicopper oxidáz (CPAR2_603600), az Acyl-CoA tioláz (CPAR2_800020) és az Acyl-

CoA oxidáz (CPAR2_807710) kódoló génekre nézve deléciós törzsek esetében jelentősen csökkent a vizsgált prosztaglandinok termelődése a vad típussal szemben. Ezeket a törzseket hatékonyabban fagocitálták és ölték humán makrofágok. Továbbá nagyobb mennyiségű gyulladást elősegítő citokin termelést indukáltak makrofágokban, és kevésbé virulensek *in vivo*. Összegzésképpen, a fent említett megfigyeléseink alapján, a gomba lipid mediátorai részt vesznek a gazda immunválaszának módosításában így fontos szerepet töltenek be a gazda - patogén kölcsönhatásban *C. parapsilosis* fertőzés esetén. A nélkülözhetetlen mikrotápanyagok közül a vas kiemelt szerepet játszik az élő organizmusok biológiájában. Rendkívül fontos a kórokozók számára is fertőzések során.. Mivel a felhasználható vas ionok ritkán elérhetőek és felvehetőek a gazda szervezetben, sok humán kórokozó gomba, úgy, mint a *C. albicans, Cr. neoformans, C. glabrata* és *A. fumigatus* különböző módszereket fejlesztettek ki annak érdekében, hogy a kötött formában jelen lévő vas nyomelemekhez hozzáférhessenek. Bár ezen stratégiák és a mögöttük álló molekuláris mechanizmusok jól jellemzettek az említett gomba fajoknál, keveset tudunk ugyanezen folyamatokról *C. parapsilosis* esetében. Munkánk során ismertettük, hogy ezen fajban a multicopper oxidáz *FET3 (CPAR2_603600)* ortológja *C. parapsilosis*-ban szerepet játszik a vas felvételében és anyagcseréjében. A homozigóta deléciós törzsn (CPAR2_603600) alacsony vas tartalom mellett növekedési defektet mutatott, valamint érzékenyekebbnek bizonyult számos stresszor jelenlétére. Megállapítottuk továbbá, hogy a null mutáns törzs nem képes hatékonyan pseudohifa képzésre és kevésbé hatékony biofilm képzést mutatott. , Továbbá, a vas anyagcserét befolyásoló egyéb gének expressziója is megelemekedett ugyanezen törzsben a vad típusú törzshöz képest.

Összefoglalva, a munkánk során bizonyítottuk, hogy a *CPAR2_603600* gén *C. parapsilosis*-ban kritikus szerepet tölt be a vas homeosztázis szabályozásában és befolyással bír a gomba morfológia szabályozása felett.

8 Financial support

This work was supported by GINOP-2.3.2-15-2016-00035 and by GINOP-2.3.3-15-2016-00006.

9 Acknowledgement

I take this opportunity to thank all the people who have made this experience of doing PhD worthwhile.

My first acknowledgement must go to my supervisor Dr. Attila Gácser, for giving me the opportunity to work on this very exciting project, for sparing his time for discussions even during busy times, for giving useful scientific input, who, above and over his role as a Principal Investigator (P.I), has been a true mentor for me. I would like to express my sincere gratitude to him for his continuous support during my PhD. His guidance helped me in all the tough times of writing the thesis. He not only helped me in developing my academic skills but also supported me during the tough times of my life during my stay in Szeged.

I am greatly thankful to Prof. Csaba Vágvölgyi, our Head of the Department as well as the Head of the PhD school of Biology for giving me the opportunity to work in Department of Microbiology, University of Szeged. I was always inspired by his personality and leadership, and grateful for the support that he has extended over the years for all the students, including me. Similarly, I am grateful to be part of this department as I have had the opportunity to interact, through the coursework, seminars or just plain conversations with such a diverse group of distinguished scientists.

I am deeply indebted to Prof. Karl Kuchler for giving me the opportunity to be part of the "ImResFun" consortium.

I am Especially thankful to our collaborator Prof. Toni Gabaldon from CRG Barcelona, Spain, for the RNA sequencing data analysis, Prof. Martin Giera from LUMC, Leiden, The Netherlands, for the lipid analysis experiment and László Bodai, Department of Biochemistry and Molecular Biology, Szeged, Hungary, for the RNA sequencing.

I would also like to extend my special thank you to Prof. Kaustuv Sanyal, JNCASR, India for giving me the opportunity to start my research career in the field of Candida biology.

On this occasion, I want to express my gratitude to my inspirational teacher, Dr. Bhaskar Bhadra who taught me the preliminary concept of genetics and molecular biology and ignite self-belief to take research as a career.

I am also thankful to Prof. Bernerd Hube for his suggestion on my project as a thesis committee member.

I would like to thank Dr. Ernst Thuer as well for the RNA sequencing data analysis and Marieke Heijink for lipid analysis with LC/MS experiment respectively.

I am also grateful to Prof. Christophe D'Enfert for sharing the plasmids for the Gateway system, Prof. Judith Berman for providing us with the GFP and mCherry plasmids and Prof. Geraldin Butler for sharing the Candida parapsilosis strains which are helpful resources for my research work.

I thank Dr. Ferenc Jankovics for helping with the confocal images. Similarly, I am grateful to Dr. Marton Annamária for helping with the mouse experiment and Kotogány Edit for helping with the FACS in the beginning part of my project.

I am humbled to be a part of ImResFun consortium and I would like to thank all the PIs: Prof. Karl Kuchler, Prof. Steffen Rupp, Prof. Per Ljungdahl, Prof.Uwe Gross, Prof. Julian Naglik, Prof. Hana Sychrová, Prof. Renate Spohn, Prof. Concha Gil, Prof. Toni Gabaldón, Prof. Thomas Lion, Prof. Leif Schauser for their critical comments during the presentations and course works.

I am thankful to our administrative staff and academic staff for their excellent support that had provided so many useful facilities.

I am grateful to the MARIE SKŁODOWSKA-CURIE ACTIONS as Initial Training Network of European Commission for granting me the PhD scholarship.

On a more personal note –

I am very happy to have been part of the Candida Laboratory (302). As a first full time international student, it would have been very difficult to complete this whole process without the help of all my lab members. I always enjoyed my stimulating conversations with Dr. Tibor Németh and appreciate him for sharing many plasmids and strains with me that he had developed in the lab. I am very thankful to Dr. Renáta Tóth for teaching me many molecular biology techniques, critically reviewing and correcting my manuscript. I greatly appreciate Katalin Csonka and Erik Zajta for teaching and helping me with the theory and practical knowledge of cell culture work and mouse experiment. I would like to thank Csaba Papp for assisting me with the confocal microscopy, teaching me the technique of PBMC isolation, helping with the FACS and always bringing me the blood for PBMC isolation whenever I asked him. I am very grateful to Judit Szenzenstein for teaching me some molecular biology techniques in the beginning and who has been invaluable in the smooth running of our experiments by keeping track of all the finance and ordering of the chemicals and reagents. I also enjoyed the company of our two new lab members Sára Pál and Máté Vadovics. I am also thankful to our previous lab members: Dr. Zsuzsanna Grózer, who initiated the prostaglandin project and helped me in the beginning to understand the basics of the project; Dr. Adél Tóth who established and standardized many immunological techniques in the lab and Dr. Péter Horváth for helping me initially to be accustomed in the lab. I would also like to thank Dr. Zsuzsanna Grózer for helping me in the first few weeks with many administrative works in immigration office and student office. Finally, I appreciate all of them for helping me with the difficulties that I faced with the Hungarian language during my stay in Szeged.

As a foreigner I always missed speaking in my own language in the lab during 1st couple of years. But after Dhirendra joined in our lab as a PhD student, not only he helped me with many small things during my experiments, I could finally speak with somebody in the lab in my own language. We had lot of fun times during many Indian parties and gatherings.

I also had a very nice time working with Regina E Bernátsky and help her with her MS dissertation in the lab.

We have a great and talented group of BS and MS students: Flóra Bohner, Gergő Molnár, Katica Kocsis, Tamás Takács, Gergó Drabbant, Zsolt Tasi, Emese Halmos, Máté Csikós, Márton Horváth, Mónika Homolya and Benedikta Balla who have all enriched the lab atmosphere with their beautiful personalities in the lab.

I am grateful that, as a part of the ImResFun family, where I have had the opportunity to interact, through the coursework, seminars or just plain conversations with such a diverse group of students, Dr. Andreas Kühbacher, Dr. Nathalie Uwamahoro, Dr. Nitesh Kumar Singh, Dr. Ernst Thür, Dr. Mariana Blagojevic, Dr. Vicent Llopis-Torregrosa, Catarina Oliveira Vaz, Emilia Gomez Molero, Clàudia Roca Aunós, Leonel Pereira, Fitz Gerald Silao and Raju Shivarathri from all around the world. I will always cherish the memory and fun time I spent with all of them.

I am very happy to have been part of the Molecular Mycology Laboratory (MML), JNCASR, India, where I started my research career. I have had the opportunity to work with some exceptional seniors Dr. Uttara Chakraborty, Dr. Jitendra Thakur, Dr. Babhrubahan Roy, Dr. Arti Baban Dumbre Patil, Dr. Shudhanshu Yadav, Dr. Sreyoshi Mitra and specially Dr.Abhishek Baghela, Dr. Laxmi Shanker Rai and Dr. Gautam Chatterjee who have taught me the initial experimental skills in the lab. I am very thankful to many other colleagues from the lab, Dr. Neha Varshney, Dr. Vikas Yadav, Lakshmi, Asif, Vaijayanthi, Shreyas, Sundar, Krishnendu and Rima.

I have been blessed with few good friends throughout my stay in Szeged. Dr. Ricky Sahni is one of them, with whom I had innumerable good and fun times and being my roommate for last 3 years, he helped me to deal with many personal crises. As a doctor he was also a great support during my sickness. I cherish the friendship of Zsófia Kovács and Máté Tombácz with whom I really had great times in many different occasions. I also had chance to spent some great times with István Ferencsik, Andrea Kokavecz and her family.

Also I had the pleasure of spending some good times with my friends Dr. Soujanya Kuntam, Mariam, Arghya, Arijit, Payel, Dilip and Kabi here in Szeged.

I would also like to say a big thank you to Pawan and Madan paji from the Indian Restaurant, Taj Mahal, here in Szeged who provided me with good Indian food whenever I have had craving for some home food. I also get to know the owner of the restaurant Amarjit Paji, Aman Bhabhi, Jaspreetji and their three beautiful daughters Simi, Ekam and Nimrit who always made me feel like a part of their family.

Finally,

At this journey's end, I must thank my roots, my family, who taught me the values of life. I sincerely acknowledge the help and support of my two sisters Diti, Dipi and my nephew Sayan during good as well as bad times of my life. I thank the Almighty for his/her ever-loving presence.

Last but not the least, I would like to dedicate my thesis to my loving parents, Ma & Baba, for being supportive with my career choices, being so strong to let me stay so far away from them for so many years and to my beautiful and dearest niece Diya for her presence in my life.

10 References

1. Funk CD. Prostaglandins and leukotrienes:advances in eicosanoid biology. Science (80-). 2001;294: 1871–1875.
2. Chandrasekharan JA, Marginean A, Sharma-Walia N. An insight into the role of arachidonic acid derived lipid mediators in virus associated pathogenesis and malignancies. Prostaglandins Other Lipid Mediat. Elsevier Inc.; 2016;126: 46–54. doi:10.1016/j.prostaglandins.2016.07.009.
3. Buczynski MW, Dumlao DS, Dennis EA. *Thematic Review Series: Proteomics.* An integrated omics analysis of eicosanoid biology,. J Lipid Res. United States; 2009;50: 1015–1038. doi:10.1194/jlr.R900004-JLR200.
4. Dennis EA, Norris PC. Eicosanoid storm in infection and inflammation. Nat Rev Immunol. Nature Publishing Group; 2015;15: 511–523. doi:10.1038/nri3859.
5. Smith WL, DeWitt DL, Garavito RM. Cyclooxygenases: structural, cellular, and molecular biology. Annu Rev Biochem. United States; 2000;69: 145–182. doi:10.1146/annurev.biochem.69.1.145.
6. Peters-Golden M, Brock TG. Intracellular compartmentalization of leukotriene synthesis: unexpected nuclear secrets. FEBS Lett. England; 2001;487: 323–326.
7. Narumiya S, FitzGerald GA. Genetic and pharmacological analysis of prostanoid receptor function. J Clin Invest. United States; 2001;108: 25–30. doi:10.1172/JCI13455.
8. Hirai H, Tanaka K, Yoshie O, Ogawa K, Kenmotsu K, Takamori Y, et al. Prostaglandin D2 selectively induces chemotaxis in T helper type 2 cells, eosinophils, and basophils via seven-transmembrane receptor CRTH2. J Exp Med. United States; 2001;193: 255–261.
9. von Moltke J, Trinidad NJ, Moayeri M, Kintzer AF, Wang SB, van Rooijen N, et al. Rapid induction of inflammatory lipid mediators by the inflammasome in vivo. Nature. England: Nature Publishing Group; 2012;490: 107–111. doi:10.1038/nature11351.
10. Samuelsson B. Leukotrienes: mediators of immediate hypersensitivity reactions and inflammation. Science. United States; 1983;220: 568–575.
11. Ricciotti E, Fitzgerald GA. Prostaglandins and inflammation. Arterioscler Thromb Vasc Biol. 2011;31: 986–1000. doi:10.1161/ATVBAHA.110.207449.

12. Lammermann T, Afonso P V, Angermann BR, Wang JM, Kastenmuller W, Parent CA, et al. Neutrophil swarms require LTB4 and integrins at sites of cell death in vivo. Nature. England; 2013;498: 371–375. doi:10.1038/nature12175.
13. Shinomiya S, Naraba H, Ueno A, Utsunomiya I, Maruyama T, Ohuchida S, et al. Regulation of TNFalpha and interleukin-10 production by prostaglandins I(2) and E(2): studies with prostaglandin receptor-deficient mice and prostaglandin E-receptor subtype-selective synthetic agonists. Biochem Pharmacol. England; 2001;61: 1153–1160.
14. Murakami K, Ide T, Suzuki M, Mochizuki T, Kadowaki T. Evidence for direct binding of fatty acids and eicosanoids to human peroxisome proliferators-activated receptor alpha. Biochem Biophys Res Commun. United States; 1999;260: 609–613. doi:10.1006/bbrc.1999.0951.
15. Serhan CN, Savill J. Resolution of inflammation: The beginning programs the end. Nat Immunol. 2005;6: 1191–1197. doi:10.1038/ni1276.
16. Soyombo O, Spur BW, Lee TH. Effects of lipoxin A4 on chemotaxis and degranulation of human eosinophils stimulated by platelet-activating factor and N-formyl-L-methionyl-L-leucyl-L-phenylalanine. Allergy. Denmark; 1994;49: 230–234.
17. Godson C, Mitchell S, Harvey K, Petasis NA, Hogg N, Brady HR. Cutting edge: lipoxins rapidly stimulate nonphlogistic phagocytosis of apoptotic neutrophils by monocyte-derived macrophages. J Immunol. United States; 2000;164: 1663–1667.
18. Si Q, Zhao M-L, Morgan ACA, Brosnan CF, Lee SC. 15-deoxy-Delta12,14-prostaglandin J2 inhibits IFN-inducible protein 10/CXC chemokine ligand 10 expression in human microglia: mechanisms and implications. J Immunol. United States; 2004;173: 3504–3513.
19. Castrillo A, Díaz-Guerra MJM, Hortelano S, Martín-Sanz P, Boscá L. Inhibition of IκB Kinase and IκB Phosphorylation by 15-Deoxy-Δ(12,14)-Prostaglandin J(2) in Activated Murine Macrophages. Molecular and Cellular Biology. 2000. pp. 1692–1698.
20. Fierro IM, Serhan CN. Mechanisms in anti-inflammation and resolution: the role of lipoxins and aspirin-triggered lipoxins. Brazilian J Med Biol Res = Rev Bras Pesqui medicas e Biol. Brazil; 2001;34: 555–566.
21. Suram S, Brown GD, Ghosh M, Gordon S, Loper R, Taylor PR, et al. Regulation of

Cytosolic Phospholipase A 2 Activation and Cyclooxygenase 2 Expression in Macrophages by the β-Glucan Receptor. J Biol Chem. 2006;281: 5506–5514. doi:10.1074/jbc.M509824200.

22. Suram S, Gangelhoff T a, Taylor PR, Rosas M, Brown GD, Bonventre J V, et al. Pathways regulating cytosolic phospholipase A2 activation and eicosanoid production in macrophages by *Candida albicans*. J Biol Chem. 2010;285: 30676–85. doi:10.1074/jbc.M110.143800.
23. Gagliardi MC, Teloni R, Mariotti S, Bromuro C, Chiani P, Romagnoli G, et al. Endogenous PGE2 promotes the induction of human Th17 responses by fungal -glucan. J Leukoc Biol. 2010;88: 947–954. doi:10.1189/jlb.0310139.
24. Smeekens SP, van de Veerdonk FL, van der Meer JWM, Kullberg BJ, Joosten LAB, Netea MG. The *Candida* Th17 response is dependent on mannanand β-glucan-induced prostaglandin E2. Int Immunol. 2010;22: 889–895. doi:10.1093/intimm/dxq442.
25. Noverr MC, Toews GB, Huffnagle GB. Production of prostaglandins and leukotrienes by pathogenic fungi. Infect Immun. 2002;70: 400–402. doi:10.1128/IAI.70.1.400-402.2002.
26. Noverr MC, Erb-Downward JR, Huffnagle GB. Production of eicosanoids and other oxylipins by pathogenic eukaryotic microbes. Clin Microbiol Rev. 2003;16: 517–533. doi:10.1128/CMR.16.3.517-533.2003.
27. Tsitsigiannis DI, Bok J, Andes D, Nielsen KF, Frisvad JC, Keller NP. Aspergillus Cyclooxygenase-Like Enzymes Are Associated with Prostaglandin Production and Virulence. Infection Immunity. 2005;73: 4548–4559. doi:10.1128/IAI.73.8.4548.
28. Erb-Downward JR, Huffnagle GB. *Cryptococcus neoformans* produces authentic prostaglandin E2 without a cyclooxygenase. Eukaryot Cell. 2007;6: 346–350. doi:10.1128/EC.00336-06.
29. Biondo GA, Dias-Melicio LA, Bordon-Graciani AP, Acorci-Valerio MJ, Soares AMVC. *Paracoccidioides brasiliensis* uses endogenous and exogenous arachidonic acid for PGE x production. Mycopathologia. Netherlands; 2010;170: 123–130. doi:10.1007/s11046-010-9301.
30. Erb-Downward JR, Noverr MC. Characterization of prostaglandin E2 production by *Candida albicans*. Infect Immun. United States; 2007;75: 3498–3505. doi:10.1128/IAI.00232-07.

31. Erb-Downward JR, Noggle RM, Williamson PR, Huffnagle GB. The role of laccase in prostaglandin production by *Cryptococcus neoformans*. Mol Microbiol. England; 2008;68: 1428–1437. doi:10.1111/j.1365-2958.2008.06245.
32. Bordon-Graciani AP, Dias-Melicio LA, Acorci-Valerio MJ, Araujo JPJ, de Campos Soares AMV. Inhibitory effect of PGE(2) on the killing of *Paracoccidioides brasiliensis* by human monocytes can be reversed by cellular activation with cytokines. Med Mycol. England; 2012;50: 726–734. doi:10.3109/13693786.2012.676740.
33. Tsitsigiannis DI, Keller NP. Oxylipins as developmental and host-fungal communication signals. Trends Microbiol. 2007;15: 109–118. doi:10.1016/j.tim.2007.01.005.
34. Noverr MC, Huffnagle GB. Regulation of Candida albicans Morphogenesis by Fatty Acid Metabolites Regulation of *Candida albicans* Morphogenesis by Fatty Acid Metabolites. Infect Immun. 2004;72: 6206–6210. doi:10.1128/IAI.72.11.6206.
35. Levitin A, Whiteway M. The effect of prostaglandin E2 on transcriptional responses of *Candida albicans*. Microbiol Res. 2007;162: 201–210. doi:10.1016/j.micres.2007.02.001.
36. Alem M a S, Douglas LJ. Prostaglandin production during growth of *Candida albicans* biofilms. J Med Microbiol. 2005;54: 1001–1005. doi:10.1099/jmm.0.46172-0.
37. Salas SD, Bennett JE, Kwon-Chung KJ, Perfect JR, Williamson PR. Effect of the laccase gene CNLAC1, on virulence of *Cryptococcus neoformans*. J Exp Med. 1996;184: 377–386. doi:10.1084/jem.184.2.377.
38. Noverr MC, Williamson PR, Fajardo RS, Huffnagle GB. CNLAC1 is required for extrapulmonary dissemination of *Cryptococcus neoformans* but not pulmonary persistence. Infect Immun. United States; 2004;72: 1693–1699.
39. Noverr MC, Phare SM, Toews GB, Coffey MJ, Huffnagle GB. Pathogenic yeasts *Cryptococcus neoformans* and *Candida albicans* produce immunomodulatory prostaglandins. Infect Immun. United States; 2001;69: 2957–2963. doi:10.1128/IAI.69.5.2957-2963.2001.
40. Nickerson KW, Atkin AL, Hornby JM. Quorum sensing in dimorphic fungi: farnesol and beyond. Appl Environ Microbiol. United States; 2006;72: 3805–3813. doi:10.1128/AEM.02765-05.
41. Davidson RC, Moore TD, Odom AR, Heitman J. Characterization of the MFalpha

pheromone of the human fungal pathogen *Cryptococcus neoformans*. Mol Microbiol. England; 2000;38: 1017–1026.

42. Valdez PA, Vithayathil PJ, Janelsins BM, Shaffer AL, Williamson PR, Datta SK. Prostaglandin E2 Suppresses Antifungal Immunity by Inhibiting Interferon Regulatory Factor 4 Function and Interleukin-17 Expression in T Cells. Immunity. Elsevier Inc.; 2012;36: 668–679. doi:10.1016/j.immuni.2012.02.013.
43. Lepak A, Andes D. Fungal sepsis: optimizing antifungal therapy in the critical care setting. Crit Care Clin. United States; 2011;27: 123–147. doi:10.1016/j.ccc.2010.11.001.
44. Guinea J. Global trends in the distribution of *Candida* species causing candidemia. Clin Microbiol Infect. England; 2014;20 Suppl 6: 5–10. doi:10.1111/1469-0691.12539.
45. Pfaller MA, Diekema DJ. Epidemiology of invasive candidiasis: a persistent public health problem. Clin Microbiol Rev. United States; 2007;20: 133–163. doi:10.1128/CMR.00029-06.
46. Quindos G. Epidemiology of candidaemia and invasive candidiasis. A changing face. Rev Iberoam Micol. Spain; 2014;31: 42–48. doi:10.1016/j.riam.2013.10.001.
47. el-Mohandes AE, Johnson-Robbins L, Keiser JF, Simmens SJ, Aure M V. Incidence of *Candida parapsilosis* colonization in an intensive care nursery population and its association with invasive fungal disease. Pediatr Infect Dis J. United States; 1994;13: 520–524.
48. Pammi M, Holland L, Butler G, Gacser A, Bliss JM. *Candida parapsilosis* is a significant neonatal pathogen: a systematic review and meta-analysis. Pediatr Infect Dis J. United States; 2013;32: e206-16. doi:10.1097/INF.0b013e3182863a1c.
49. Trofa D, Gacser A, Nosanchuk JD. *Candida parapsilosis*, an emerging fungal pathogen. Clin Microbiol Rev. United States; 2008;21: 606–625. doi:10.1128/CMR.00013-08.
50. Lupetti A, Tavanti A, Davini P, Ghelardi E, Corsini V, Merusi I, et al. Horizontal transmission of *Candida parapsilosis* candidemia in a neonatal intensive care unit. J Clin Microbiol. United States; 2002;40: 2363–2369.
51. Bonassoli LA, Bertoli M, Svidzinski TIE. High frequency of *Candida parapsilosis* on the hands of healthy hosts. J Hosp Infect. England; 2005;59: 159–162. doi:10.1016/j.jhin.2004.06.033.

52. Clerihew L, Lamagni TL, Brocklehurst P, McGuire W. *Candida parapsilosis* infection in very low birthweight infants. Arch Dis Child Fetal Neonatal Ed. England; 2007;92: F127-9. doi:10.1136/fnn.2006.097758.

53. Laffey SF, Butler G. Phenotype switching affects biofilm formation by *Candida parapsilosis*. Microbiology. England; 2005;151: 1073–1081. doi:10.1099/mic.0.27739-0.

54. Santos MA, Tuite MF. The CUG codon is decoded in vivo as serine and not leucine in *Candida albicans*. Nucleic Acids Res. 1995;23. doi:10.1093/nar/23.9.1481.

55. Fitzpatrick DA, Logue ME, Stajich JE, Butler G. A fungal phylogeny based on 42 complete genomes derived from supertree and combined gene analysis. BMC Evol Biol. 2006;6: 99. doi:10.1186/1471-2148-6-99.

56. Massey SE, Moura G, Beltrao P, Almeida R, Garey JR, Tuite MF, et al. Comparative evolutionary genomics unveils the molecular mechanism of reassignment of the CTG codon in *Candida* spp. Genome Res. 2003;13. doi:10.1101/gr.811003.

57. Miranda I, Rocha R, Santos MC, Mateus DD, Moura GR, Carreto L, et al. A genetic code alteration is a phenotype diversity generator in the human pathogen *Candida albicans*. PLoS One. United States; 2007;2: e996. doi:10.1371/journal.pone.0000996.

58. Papon N, Courdavault V, Clastre M, Bennett RJ. Emerging and Emerged Pathogenic *Candida* Species: Beyond the *Candida albicans* Paradigm. PLOS Pathog. Public Library of Science; 2013;9: e1003550. doi:10.1371/journal.ppat.1003550.

59. Kim S-K, El Bissati K, Ben Mamoun C. Amino acids mediate colony and cell differentiation in the fungal pathogen *Candida parapsilosis*. Microbiology. England; 2006;152: 2885–2894. doi:10.1099/mic.0.29180-0.

60. Toth R, Cabral V, Thuer E, Bohner F, Nemeth T, Papp C, et al. Investigation of *Candida parapsilosis* virulence regulatory factors during host-pathogen interaction. Sci Rep. England; 2018;8: 1346. doi:10.1038/s41598-018-19453-4.

61. Connolly LA, Riccombeni A, Grozer Z, Holland LM, Lynch DB, Andes DR, et al. The APSES transcription factor Efg1 is a global regulator that controls morphogenesis and biofilm formation in *Candida parapsilosis*. Mol Microbiol. England; 2013;90: 36–53. doi:10.1111/mmi.12345.

62. Ramage G, Martinez JP, Lopez-Ribot JL. *Candida* biofilms on implanted biomaterials: a clinically significant problem. FEMS Yeast Res. England; 2006;6: 979–986.

doi:10.1111/j.1567-1364.2006.00117.

63. Katragkou A, Chatzimoschou A, Simitsopoulou M, Dalakiouridou M, Diza-Mataftsi E, Tsantali C, et al. Differential activities of newer antifungal agents against *Candida albicans* and *Candida parapsilosis* biofilms. Antimicrob Agents Chemother. United States; 2008;52: 357–360. doi:10.1128/AAC.00856-07.

64. Nobile CJ, Fox EP, Nett JE, Sorrells TR, Mitrovich QM, Hernday AD, et al. A recently evolved transcriptional network controls biofilm development in *Candida albicans*. Cell. Elsevier Inc.; 2012;148: 126–138. doi:10.1016/j.cell.2011.10.048.

65. Pannanusorn S, Ramirez-Zavala B, Lunsdorf H, Agerberth B, Morschhauser J, Romling U. Characterization of biofilm formation and the role of BCR1 in clinical isolates of *Candida parapsilosis*. Eukaryot Cell. United States; 2014;13: 438–451. doi:10.1128/EC.00181-13.

66. Holland LM, Schröder MS, Turner SA, Taff H, Andes D, Grózer Z, et al. Comparative Phenotypic Analysis of the Major Fungal Pathogens *Candida parapsilosis* and *Candida albicans*. PLoS Pathog. 2014;10. doi:10.1371/journal.ppat.1004365.

67. Modrzewska B, Kurnatowski P. Adherence of *Candida* sp. to host tissues and cells as one of its pathogenicity features. Ann Parasitol. Poland; 2015;61: 3–9.

68. Cota E, Hoyer LL. The *Candida albicans* agglutinin-like sequence family of adhesins: functional insights gained from structural analysis. Future Microbiol. England; 2015;10: 1548–1635. doi:10.2217/fmb.15.79.

69. Hoyer LL, Green CB, Oh S-H, Zhao X. Discovering the secrets of the *Candida albicans* agglutinin-like sequence (ALS) gene family--a sticky pursuit. Med Mycol. England; 2008;46: 1–15. doi:10.1080/13693780701435317.

70. Pryszcz LP, Nemeth T, Gacser A, Gabaldon T. Unexpected genomic variability in clinical and environmental strains of the pathogenic yeast *Candida parapsilosis*. Genome Biol Evol. England; 2013;5: 2382–2392. doi:10.1093/gbe/evt185.

71. Bertini A, Zoppo M, Lombardi L, Rizzato C, De Carolis E, Vella A, et al. Targeted gene disruption in *Candida parapsilosis* demonstrates a role for CPAR2_404800 in adhesion to a biotic surface and in a murine model of ascending urinary tract infection. Virulence. United States; 2016;7: 85–97. doi:10.1080/21505594.2015.1112491.

72. Gacser A. Adhesins in *Candida parapsilosis*: Understudied players in virulence. Virulence. United States; 2016. pp. 65–67. doi:10.1080/21505594.2015.1135288.

73. Monod M, Borg-von ZM. Secreted aspartic proteases as virulence factors of *Candida* species. Biol Chem. Germany; 2002;383: 1087–1093. doi:10.1515/BC.2002.117.

74. Hube B, Naglik J. *Candida albicans* proteinases: resolving the mystery of a gene family. Microbiology. England; 2001;147: 1997–2005. doi:10.1099/00221287-147-8-1997.

75. Merkerova M, Dostal J, Hradilek M, Pichova I, Hruskova-Heidingsfeldova O. Cloning and characterization of Sapp2p, the second aspartic proteinase isoenzyme from *Candida parapsilosis*. FEMS Yeast Res. England; 2006;6: 1018–1026. doi:10.1111/j.1567-1364.2006.00142.

76. Odds FC. *Candida* infections: an overview. Crit Rev Microbiol. England; 1987;15: 1–5. doi:10.3109/10408418709104444.

77. De Bernardis F, Lorenzini R, Verticchio R, Agatensi L, Cassone A. Isolation, acid proteinase secretion, and experimental pathogenicity of *Candida parapsilosis* from outpatients with vaginitis. J Clin Microbiol. United States; 1989;27: 2598–2603.

78. Horvath P, Nosanchuk JD, Hamari Z, Vagvolgyi C, Gacser A. The identification of gene duplication and the role of secreted aspartyl proteinase 1 in *Candida parapsilosis* virulence. J Infect Dis. United States; 2012;205: 923–933. doi:10.1093/infdis/jir873.

79. Ruchel R, de Bernardis F, Ray TL, Sullivan PA, Cole GT. *Candida* acid proteinases. J Med Vet Mycol. England; 1992;30 Suppl 1: 123–132.

80. Pichova I, Pavlickova L, Dostal J, Dolejsi E, Hruskova-Heidingsfeldova O, Weber J, et al. Secreted aspartic proteases of *Candida albicans*, *Candida tropicalis*, *Candida parapsilosis* and *Candida lusitaniae*. Inhibition with peptidomimetic inhibitors. Eur J Biochem. England; 2001;268: 2669–2677.

81. Brockerhoff H. Model of interaction of polar lipids, cholesterol, and proteins in biological membranes. Lipids. Germany; 1974;9: 645–650.

82. Schaller M, Borelli C, Korting HC, Hube B. Hydrolytic enzymes as virulence factors of *Candida albicans*. Mycoses. Germany; 2005;48: 365–377. doi:10.1111/j.1439-0507.2005.01165.

83. Hube B, Stehr F, Bossenz M, Mazur A, Kretschmar M, Schafer W. Secreted lipases of *Candida albicans*: cloning, characterisation and expression analysis of a new gene family with at least ten members. Arch Microbiol. Germany; 2000;174: 362–374.

84. Gacser A, Stehr F, Kroger C, Kredics L, Schafer W, Nosanchuk JD. Lipase 8 affects

the pathogenesis of *Candida albicans*. Infect Immun. United States; 2007;75: 4710–4718. doi:10.1128/IAI.00372-07.

85. Neugnot V, Moulin G, Dubreucq E, Bigey F. The lipase/acyltransferase from *Candida parapsilosis*: molecular cloning and characterization of purified recombinant enzymes. Eur J Biochem. England; 2002;269: 1734–1745.
86. Gacser A, Trofa D, Schafer W, Nosanchuk JD. Targeted gene deletion in *Candida parapsilosis* demonstrates the role of secreted lipase in virulence. J Clin Invest. United States; 2007;117: 3049–3058. doi:10.1172/JCI32294.
87. Toth A, Nemeth T, Csonka K, Horvath P, Vagvolgyi C, Vizler C, et al. Secreted *Candida parapsilosis* lipase modulates the immune response of primary human macrophages. Virulence. United States; 2014;5: 555–562. doi:10.4161/viru.28509.
88. Toth R, Toth A, Vagvolgyi C, Gacser A. *Candida parapsilosis* Secreted Lipase as an Important Virulence Factor. Curr Protein Pept Sci. Netherlands; 2017;18: 1043–1049. doi:10.2174/1389203717666160813163054.
89. Grozer Z, Toth A, Toth R, Kecskemeti A, Vagvolgyi C, Nosanchuk JD, et al. *Candida parapsilosis* produces prostaglandins from exogenous arachidonic acid and OLE2 is not required for their synthesis. Virulence. United States; 2015;6: 85–92. doi:10.4161/21505594.2014.988097.
90. Netea MG, Joosten LAB, van der Meer JWM, Kullberg B-J, van de Veerdonk FL. Immune defence against *Candida* fungal infections. Nat Rev Immunol. England; 2015;15: 630–642. doi:10.1038/nri3897.
91. Netea MG, Brown GD, Kullberg BJ, Gow NAR. An integrated model of the recognition of *Candida albicans* by the innate immune system. Nat Rev Microbiol. England; 2008;6: 67–78. doi:10.1038/nrmicro1815.
92. Tóth A, Csonka K, Jacobs C, Vágvölgyi C, Nosanchuk JD, Netea MG, et al. *Candida albicans* and *Candida parapsilosis* induce different T-cell responses in human peripheral blood mononuclear cells. J Infect Dis. 2013;208: 690–8. doi:10.1093/infdis/jit188.
93. Tóth A, Zajta E, Csonka K, Vágvölgyi C, Netea MG, Gácser A. Specific pathways mediating inflammasome activation by *Candida parapsilosis*. Sci Rep. Nature Publishing Group; 2017;7: 1–12. doi:10.1038/srep43129.
94. Hood MI, Skaar EP. Nutritional immunity: transition metals at the pathogen-host

interface. Nat Rev Microbiol. England; 2012;10: 525–537. doi:10.1038/nrmicro2836.

95. Gerwien F, Skrahina V, Kasper L, Hube B, Brunke S. Metals in fungal virulence. FEMS Microbiol Rev. England; 2018;42. doi:10.1093/femsre/fux050.

96. Andreini C, Banci L, Bertini I, Rosato A. Counting the zinc-proteins encoded in the human genome. J Proteome Res. United States; 2006;5: 196–201. doi:10.1021/pr050361j.

97. Andreini C, Banci L, Bertini I, Rosato A. Zinc through the three domains of life. J Proteome Res. United States; 2006;5: 3173–3178. doi:10.1021/pr0603699.

98. North M, Steffen J, Loguinov A V, Zimmerman GR, Vulpe CD, Eide DJ. Genome-wide functional profiling identifies genes and processes important for zinc-limited growth of *Saccharomyces cerevisiae*. PLoS Genet. United States; 2012;8: e1002699. doi:10.1371/journal.pgen.1002699.

99. Almeida RS, Wilson D, Hube B. *Candida albicans* iron acquisition within the host. FEMS Yeast Res. 2009;9: 1000–1012. doi:10.1111/j.1567-1364.2009.00570.

100. Almeida RS, Wilson D, Hube B. *Candida albicans* iron acquisition within the host. FEMS Yeast Res. England; 2009;9: 1000–1012. doi:10.1111/j.1567-1364.2009.00570.

101. Weissman Z, Shemer R, Conibear E, Kornitzer D. An endocytic mechanism for haemoglobin-iron acquisition in *Candida albicans*. Mol Microbiol. England; 2008;69: 201–217. doi:10.1111/j.1365-2958.2008.06277.

102. Weissman Z, Kornitzer D. A family of *Candida* cell surface haem-binding proteins involved in haemin and haemoglobin-iron utilization. Mol Microbiol. England; 2004;53: 1209–1220. doi:10.1111/j.1365-2958.2004.04199.

103. Heymann P, Gerads M, Schaller M, Dromer F, Winkelmann G, Ernst JF. The siderophore iron transporter of *Candida albicans* (Sit1p/Arn1p) mediates uptake of ferrichrome-type siderophores and is required for epithelial invasion. Infect Immun. United States; 2002;70: 5246–5255.

104. Almeida RS, Brunke S, Albrecht A, Thewes S, Laue M, Edwards JE, et al. The hyphal-associated adhesin and invasin Als3 of *Candida albicans* mediates iron acquisition from host ferritin. PLoS Pathog. United States; 2008;4: 1–17. doi:10.1371/journal.ppat.1000217.

105. Knight SAB, Vilaire G, Lesuisse E, Dancis A. Iron acquisition from transferrin by *Candida albicans* depends on the reductive pathway. Infect Immun. United States;

2005;73: 5482–5492. doi:10.1128/IAI.73.9.5482-5492.2005.

106. Ramanan N, Wang Y. A high-affinity iron permease essential for *Candida albicans* virulence. Science. United States; 2000;288: 1062–1064.

107. Miret S, Simpson RJ, McKie AT. Physiology and molecular biology of dietary iron absorption. Annu Rev Nutr. United States; 2003;23: 283–301. doi:10.1146/annurev.nutr.23.011702.073139.

108. Pierre JL, Fontecave M, Crichton RR. Chemistry for an essential biological process: the reduction of ferric iron. Biometals. Netherlands; 2002;15: 341–346.

109. Chen C, Pande K, French SD, Tuch BB, Noble SM. An iron homeostasis regulatory circuit with reciprocal roles in *Candida albicans* commensalism and pathogenesis. Cell Host Microbe. United States; 2011;10: 118–135. doi:10.1016/j.chom.2011.07.005.

110. Hsu P-C, Yang C-Y, Lan C-Y. *Candida albicans* Hap43 is a repressor induced under low-iron conditions and is essential for iron-responsive transcriptional regulation and virulence. Eukaryot Cell. United States; 2011;10: 207–225. doi:10.1128/EC.00158-10.

111. Singh RP, Prasad HK, Sinha I, Agarwal N, Natarajan K. Cap2-HAP complex is a critical transcriptional regulator that has dual but contrasting roles in regulation of iron homeostasis in *Candida albicans*. J Biol Chem. United States; 2011;286: 25154–25170. doi:10.1074/jbc.M111.233569.

112. Noble SM. *Candida albicans* specializations for iron homeostasis: From commensalism to virulence. Curr Opin Microbiol. England: Elsevier Ltd; 2013;16: 708–715. doi:10.1016/j.mib.2013.09.006.

113. Chen C, Noble SM. Post-transcriptional regulation of the Sef1 transcription factor controls the virulence of *Candida albicans* in its mammalian host. PLoS Pathog. United States; 2012;8: e1002956. doi:10.1371/journal.ppat.1002956.

114. Eck R, Hundt S, Hartl A, Roemer E, Kunkel W. A multicopper oxidase gene from *Candida albicans*: cloning, characterization and disruption. Microbiology. England; 1999;145 (Pt 9: 2415–2422. doi:10.1099/00221287-145-9-2415.

115. Bolger AM, Lohse M, Usadel B. Trimmomatic: a flexible trimmer for Illumina sequence data. Bioinformatics. England; 2014;30: 2114–2120. doi:10.1093/bioinformatics/btu170.

116. Kim D, Pertea G, Trapnell C, Pimentel H, Kelley R, Salzberg SL. TopHat2: accurate alignment of transcriptomes in the presence of insertions, deletions and gene fusions.

Genome Biol. England; 2013;14: R36. doi:10.1186/gb-2013-14-4-r36.

117. Langmead B, Salzberg SL. Fast gapped-read alignment with Bowtie 2. Nat Methods. United States; 2012;9: 357–359. doi:10.1038/nmeth.1923.

118. Montgomery SB, Sammeth M, Gutierrez-Arcelus M, Lach RP, Ingle C, Nisbett J, et al. Transcriptome genetics using second generation sequencing in a Caucasian population. Nature. England; 2010;464: 773–777. doi:10.1038/nature08903.

119. Love MI, Huber W, Anders S. Moderated estimation of fold change and dispersion for RNA-seq data with DESeq2. Genome Biol. England; 2014;15: 550. doi:10.1186/s13059-014-0550-8.

120. Skrzypek MS, Binkley J, Binkley G, Miyasato SR, Simison M, Sherlock G. The Candida Genome Database (CGD): incorporation of Assembly 22, systematic identifiers and visualization of high throughput sequencing data. Nucleic Acids Res. England; 2017;45: D592–D596. doi:10.1093/nar/gkw924.

121. Noble SM, French S, Kohn LA, Chen V, Johnson AD. Systematic screens of a *Candida albicans* homozygous deletion library decouple morphogenetic switching and pathogenicity. Nature genetics. 2010. pp. 590–598. doi:10.1038/ng.605.

122. Liu H, Kohler J, Fink GR. Suppression of hyphal formation in *Candida albicans* by mutation of a STE12 homolog. Science. United States; 1994;266: 1723–1726.

123. Lee KL, Buckley HR, Campbell CC. An amino acid liquid synthetic medium for the development of mycelial and yeast forms of *Candida Albicans*. Sabouraudia. England; 1975;13: 148–153.

124. Schlenke P, Kluter H, Muller-Steinhardt M, Hammers HJ, Borchert K, Bein G. Evaluation of a novel mononuclear cell isolation procedure for serological HLA typing. Clin Diagn Lab Immunol. United States; 1998;5: 808–813.

125. Gross O, Poeck H, Bscheider M, Dostert C, Hannesschlager N, Endres S, et al. Syk kinase signalling couples to the Nlrp3 inflammasome for anti-fungal host defence. Nature. England; 2009;459: 433–436. doi:10.1038/nature07965.

126. Jonasdottir HS, Brouwers H, Kwekkeboom JC, van der Linden HMJ, Huizinga T, Kloppenburg M, et al. Targeted lipidomics reveals activation of resolution pathways in knee osteoarthritis in humans. Osteoarthr Cartil. England; 2017;25: 1150–1160. doi:10.1016/j.joca.2017.01.018.

127. Keppler-Ross S, Douglas L, Konopka JB, Dean N. Recognition of yeast by murine

macrophages requires mannan but not glucan. Eukaryot Cell. United States; 2010;9: 1776–1787. doi:10.1128/EC.00156-10.

128. Ifrim DC, Bain JM, Reid DM, Oosting M, Verschueren I, Gow NAR, et al. Role of Dectin-2 for host defense against systemic infection with *Candida glabrata*. Infect Immun. United States; 2014;82: 1064–1073. doi:10.1128/IAI.01189-13.

129. Brose SA, Thuen BT, Golovko MY. LC/MS/MS method for analysis of E $_2$ series prostaglandins and isoprostanes. J Lipid Res. 2011;52: 850–859. doi:10.1194/jlr.D013441.

130. Galano J-M, Lee YY, Oger C, Vigor C, Vercauteren J, Durand T, et al. Isoprostanes, neuroprostanes and phytoprostanes: An overview of 25years of research in chemistry and biology. Prog Lipid Res. England; 2017;68: 83–108. doi:10.1016/j.plipres.2017.09.004.

131. Lawrence T, Willoughby DA, Gilroy DW. Anti-inflammatory lipid mediators and insights into the resolution of inflammation. Nat Rev Immunol. 2002;2: 787–795. doi:10.1038/nri915.

132. Noverr M, Phare SM, Toews GB, Coffey MJ, Huffnagle GB. Pathogenic yeasts *Cryptococcus neoformans* and *Candida albicans* produce immunomodulatory prostaglandins. Infect Immun. 2001;69: 2957–2963. doi:10.1128/IAI.69.5.2957.

133. Erb-Downward JR, Huffnagle GB. Role of oxylipins and other lipid mediators in fungal pathogenesis. Future Microbiol. 2006;1: 219–227. doi: 10.2217/17460913.1.2.219.

134. Fischer GJ, Keller NP. Production of cross-kingdom oxylipins by pathogenic fungi: An update on their role in development and pathogenicity. J Microbiol. 2016;54: 254–264. doi:10.1007/s12275-016-5620.

135. van Asbeck EC, Clemons K V, Stevens DA. *Candida parapsilosis*: a review of its epidemiology, pathogenesis, clinical aspects, typing and antimicrobial susceptibility. Crit Rev Microbiol. England; 2009;35: 283–309. doi:10.3109/10408410903213393.

136. Chow BDW, Linden JR, Bliss JM. *Candida parapsilosis* and the neonate: Epidemiology, virulence and host defense in a unique patient setting. Expert Rev Anti Infect Ther. 2012;10: 935–946. doi:10.1586/eri.12.74.

137. Otzen C, Bardl B, Jacobsen ID, Nett M, Brock M. *Candida albicans* utilizes a modified beta-oxidation pathway for the degradation of toxic propionyl-CoA. J Biol Chem.

United States; 2014;289: 8151–8169. doi:10.1074/jbc.M113.517672.

138. Hammacott JE, Williams PH, Cashmore AM. *Candida albicans* CFL1 encodes a functional ferric reductase activity that can rescue a *Saccharomyces cerevisiae* fre1 mutant. Microbiology. England; 2000;146 (Pt 4: 869–876. doi:10.1099/00221287-146-4-869.

139. Knight SAB, Dancis A. Reduction of 2,3-bis(2-methoxy-4-nitro-5-sulfophenyl)-2H-tetrazolium-5-carboxanilide inner salt (XTT) is dependent on CaFRE10 ferric reductase for *Candida albicans* grown in unbuffered media. Microbiology. England; 2006;152: 2301–2308. doi:10.1099/mic.0.28843.

140. Eck R, Hundt S, Härtl A, Roemer E, Künkel W, Hartl A, et al. A multicopper oxidase gene from *Candida albicans*: Cloning, characterization and disruption. Microbiology. England; 1999;145: 2415–2422. doi:10.1099/00221287-145-9-2415.

141. Knight SAB, Lesuisse E, Stearman R, Klausner RD, Dancis A. Reductive iron uptake by *Candida albicans*: role of copper , iron and the TUP1 regulator. 2016; 29–40. Microbiol (United Kingdom). England; 2002; DOI: 10.1099/00221287-148-1-29.

142. Cheng X, Xu N, Yu Q, Ding X, Qian K, Zhao Q, et al. Novel insight into the expression and function of the multicopper oxidases in *Candida albicans*. Microbiol (United Kingdom). England; 2013;159: 1044–1055. doi:10.1099/mic.0.065268-0.

143. Mamouei Z, Zeng G, Wang YY-MM, Wang YY-MM. *Candida albicans* possess a highly versatile and dynamic high-affinity iron transport system important for its commensal-pathogenic lifestyle. Mol Microbiol. England; 2017;106: 986–998. doi:10.1111/mmi.13864.

144. Hameed S, Prasad T, Banerjee D, Chandra A, Mukhopadhyay CK, Goswami SK, et al. Iron deprivation induces EFG1-mediated hyphal development in *Candida albicans* without affecting biofilm formation. FEMS Yeast Res. England; 2008;8: 744–755. doi:10.1111/j.1567-1364.2008.00394.

11 Supplementary information

Table S1: *C. parapsilosis* strains used in the study

Strain Name	Parent	CPAR GeneID	Genotype	Reference
GA1				Type Strain
CLIB214				Type Strain
CPL2H1			*leu2::FRT/leu2::FRT, his1::FRT/his1::FRT*	Holland et al,2014
102550Δ/Δ	CPL2H1	CPAR2_102550	*leu2::FRT/leu2::FRT, his1::FRT/his1::FRT, cpar2_102550::LEU2/cpar2_102550::HIS1*	This study
205500Δ/Δ	CPL2H1	CPAR2_205500	*leu2::FRT/leu2::FRT, his1::FRT/his1::FRT, cpar2_205500::LEU2/cpar2_205500::HIS1*	This study
603600Δ/Δ	CPL2H1	CPAR2_603600	*leu2::FRT/leu2::FRT, his1::FRT/his1::FRT, cpar2_603600::LEU2/cpar2_603600::HIS1*	This study
800020Δ/Δ	CPL2H1	CPAR2_800020	*leu2::FRT/leu2::FRT, his1::FRT/his1::FRT, cpar2_800020::LEU2/cpar2_800020::HIS1*	This study
807700Δ/Δ	CPL2H1	CPAR2_807700	*leu2::FRT/leu2::FRT, his1::FRT/his1::FRT, cpar2_807700::LEU2/cpar2_807700::HIS1*	This study
807710Δ/Δ	CPL2H1	CPAR2_807710	*leu2::FRT/leu2::FRT, his1::FRT/his1::FRT, cpar2_807710::LEU2/cpar2_807710::HIS1*	This study
CPL2H1-GFP	CPL2H1		*leu2::FRT/leu2::FRT, his1::FRT/his1::FRT, CpNEUT5L/Cpneut5l : : GFP-LEU2*	This study

603600Δ/Δ-mCherry			*leu2::FRT/leu2::FRT, his1::FRT/his1::FRT, cpar2_603600::LEU2/cpar2_603600::HIS1,CpNEUT5L/Cpneut5l: : mCHERRY-NAT1*	This study
800020Δ/Δ-mCherry			*leu2::FRT/leu2::FRT, his1::FRT/his1::FRT, cpar2_800020::LEU2/cpar2_800020::HIS1,CpNEUT5L/Cpneut5l: : mCHERRY-NAT1*	This study
807710Δ/Δ-mCherry			*leu2::FRT/leu2::FRT, his1::FRT/his1::FRT, cpar2_807710::LEU2/cpar2_807710::HIS1,CpNEUT5L/Cpneut5l: : mCHERRY-NAT1*	This study

Table S2: Primers used in the study

Primer Name	Sequence (5' to 3')
102550 RTF	ACAGGTGCAAATCCAAAAGG
102550 RTR	CGGCATCTTGCTTTGGTAAT
205500 RTF	TTGGAAGAGACCCAGTCGTT
205500 RTR	ACTGGCCAATTCAGCAAATC
603600 RTF	AGTAGGTGTGCCATGGGAAG
603600 RTR	GTGAATCCAGTGGGCAATCT
800020 RTF	AACGTTCATTTGCCGAAAAG
800020 RTR	GCTGGACCAACACCCATAAT
807700 RTF	TTGATTGTCGATGGCAAAGA
807700 RTR	CAATGTCACCAACGGAAACA
807710 RTF	ACGGTACTGCCGATCAAATC
807710 RTR	ATCCGTGAGCCAACTCAGTC
qTub4F	GAACACTTATGCCGAGGACAAC
qTub4R	ACTCTCACCACTGACTCCTTGC
102550 Pri1	GTCATCGATATTTGCCATCCTAG
102550 Pri3	cacggcgcgcctagcagcggGGTGCCATGATAACCGGAG
102550Pri5	gcagggatgcggccgctgacAGTGCTACTCTGACCTACTTagctcggatccactagtaacg
102550 Pri4	gtcagcggccgcatccctgcGTTGATGTTGAGCCCTTATCGG
102550 Pri6	CGAAGCGATTCGAACATCTTC
205500 Pri1	CCGAAGGTGAAGCAATCGTTAC
205500 Pri3	cacggcgcgcctagcagcggGGCGCATTTACCTTTAACTTCG
205500Pri5	gcagggatgcggccgctgacAGGCACTTGCTCCAGGACTTagctcggatccactagtaacg
205500 Pri4	gtcagcggccgcatccctgcGCCAAAGAGGCGTAACTAGA
205500 Pri6	GGTTAAGGCTCATATGGCGG
603600 Pri1	GCTTTCCAATGTCGTAGTTTACC
603600 Pri3	cacggcgcgcctagcagcggCGAGTGCCAATATAGTGAGG
603600Pri5	cagggatgcggccgctgacACGAGGTCTTGCATCTACTTagctcggatccactagtaacg
603600 Pri4	gtcagcggccgcatccctgcGCCAGAGACTTGGATGTTG
603600 Pri6	GCGAAATAGCACTCCCATTATC

800020 Pri1	CGTTGGTAGCTCGGATGTAA
800020 Pri3	cacggcgcgcctagcagcggGTTGTTGAGTGATTCCATGGTG
800020Pri5	gcagggatgcggccgctgacATGGCCGTGTCAGCCTACTTagctcggatccactagtaacg
800020 Pri4	gtcagcggccgcatccctgcCGGTGGTGCTATTGCATTAGG
800020 Pri6	CAAATCCTCGATGGTGGGTGTC
807700 Pri1	AGCGGTATACTCCACCTGG
807700 Pri3	cacggcgcgcctagcagcggGGCCCTTGCTTAAACTGACAG
807700Pri5	gcagggatgcggccgctgacACGCGCTGCTTAGATTACTTagctcggatccactagtaacg
807700 Pri4	gtcagcggccgcatccctgcGCTATT GGTAAATACGACGGTG
807700 Pri6	CGTGTGTTTGTGTTGCTCTAT
807710 Pri1	AGAATTGGCGATCGAAAACAACG
807710 Pri3	cacggcgcgcctagcagcggGCTGTGAATGGAACCGACAT
807710Pri5	gcagggatgcggccgctgacAAGCTGACCTTCTTGCACTTagctcggatccactagtaacg
807710 Pri4	gtcagcggccgcatccctgcGTCCAAGTAAACCCGACTTCTTG
807710 Pri6	GGGGGTACTTGTTATCAGGTGA
Univ_Primer_2	ccgctgctaggcgcgccgtgACCAGTGTGATGGATATCTGC
HIS Chk1	AAAATCAATGGGCATTCTCG
HIS Chk2	TGGGAAGCAGACATTCAACA
LEU2 Chk1	GAAGTTGGTGACGCGATTGT
LEU2Chk2	TTCCCCTTCAATGTATGCAA
102550 attb2FP(5′Chk)	GGGGACCACTTTGTACAAGAAAGCTGGGTGATGAGGTGCTTGACTACGG
102550 attb1RP(3′Chk)	GGGGACAAGTTTGTACAAAAAAGCAGGCTGCTTTTAAAGTGCAACGCATGG
205500 attb2FP(5′Chk)	GGGGACCACTTTGTACAAGAAAGCTGGGTGCGAACTGGGAATCGAACC
205500 attb1RP(3′Chk)	GGGGACAAGTTTGTACAAAAAAGCAGGCTCCATCGTGTTTCTCTCCATGG
603600 attb2FP(5′Chk)	GGGGACCACTTTGTACAAGAAAGCTGGGTGCACAAACGGCATTAAAAGTTTG
603600 attb1RP(3′Chk)	GGGGACAAGTTTGTACAAAAAAGCAGGCTAATCTGATTGGTGGGAGAAC
800020 attb2FP(5′Chk)	GGGGACCACTTTGTACAAGAAAGCTGGGTACGCCATGTCGTCAACAAC

800020 attb1RP(3′Chk)	GGGGACAAGTTTGTACAAAAAAGCAGGCTCTCTTGAGCCTGTGTGCG
807700 attb2FP(5′Chk)	GGGGACCACTTTGTACAAGAAAGCTGGGTTGAAAAGGGGAGGGGCAAAA
807700 attb1RP(3′Chk)	GGGGACAAGTTTGTACAAAAAAGCAGGCTATCGCCAATTCTCCCTCGG
807710 attb2FP(5′Chk)	GGGGACCACTTTGTACAAGAAAGCTGGGTCAATTTCCACTTTCAACGCTCTT
807710 attb1RP(3′Chk)	GGGGACAAGTTTGTACAAAAAAGCAGGCTAGTCTCTATTCTCAAGGGACTC

Table S3: GO term of upregulated genes from RNA sequencing analysis

CPAR GeneID	Fold Change	*Candida albicans* homologue	Predicted function
CPAR2_700300	4.47451615	*C1_14020W_A*	Has domain(s) with predicted Rho GDP-dissociation inhibitor activity and cytoplasm localization
CPAR2_300010	3.79312472	*CDR1*	Pseudogene
CPAR2_105530	3.67087524	*DUR3*	Ortholog(s) have putrescine transmembrane transporter activity, spermidine transmembrane transporter activity, urea transmembrane transporter activity and role in putrescine transport, spermidine transport, urea transport
CPAR2_402870	3.65542755	*MEP2*	Ortholog(s) have high-affinity secondary active ammonium transmembrane transporter activity, methylammonium transmembrane transporter activity
CPAR2_703250	3.20780930		Protein of unknown function; expression increased in fluconazole and voriconazole resistant strains
CPAR2_805410	3.17580505	*FAA2-3*	Has domain(s) with predicted catalytic activity and role in metabolic process
CPAR2_105520	3.13796806	*DUR1,2*	Ortholog(s) have allophanate hydrolase activity, urea carboxylase activity, role in cellular response to alkaline pH, nitrogen utilization, pathogenesis, urea catabolic process and cytoplasm localization
CPAR2_701900	3.12965309	*CR_07700W_A*	Has domain(s) with predicted protein serine/threonine kinase activity, transferase activity, transferring phosphorus-containing groups activity and role in protein phosphorylation
CPAR2_304370	3.04396652	*CDR1*	Has domain(s) with predicted ATP binding, ATPase activity, ATPase activity, coupled to transmembrane movement of substances, nucleoside-triphosphatase activity, nucleotide binding activity and role in drug export, transport
CPAR2_806280	2.99134972	*PHO13*	Has domain(s) with predicted hydrolase activity and role in metabolic process
CPAR2_808510	2.79452119	*C3_06730W_A*	Ortholog(s) have glyoxysome localization
CPAR2_800690	2.72903906	*CR_02570C_A*	Ortholog(s) have triglyceride lipase activity, role in triglyceride catabolic process and peroxisomal matrix localization

CPAR2_806900	2.71800712	*C3_03570C_A*	Has domain(s) with predicted oxidoreductase activity and role in oxidation-reduction process
CPAR2_100490	2.71306215	*GIT3*	Ortholog(s) have glycerophosphodiester transmembrane transporter activity and role in glycerophosphodiester transport
CPAR2_603800	2.71163940	*CDR1*	Has domain(s) with predicted ATP binding, ATPase activity, ATPase activity, coupled to transmembrane movement of substances, nucleoside-triphosphatase activity, nucleotide binding activity and role in drug export, transport
CPAR2_501010	2.58423681	*XUT1*	Ortholog(s) have purine nucleobase transmembrane transporter activity, role in purine nucleobase transport and fungal-type vacuole, plasma membrane localization
CPAR2_203620	2.57836162	*C1_11530C_A*	Ortholog(s) have sulfonate dioxygenase activity and role in sulfur compound catabolic process
CPAR2_503690	2.54904104	*FOX3*	Ortholog(s) have glyoxysome localization
CPAR2_800350	2.53962599	*C3_04350C_A*	Has domain(s) with predicted oxidoreductase activity and role in metabolic process
CPAR2_807710	2.483301215	*POX1-3*	Has domain(s) with predicted acyl-CoA dehydrogenase activity, acyl-CoA oxidase activity, flavin adenine dinucleotide binding, oxidoreductase activity, acting on the CH-CH group of donors' activity
CPAR2_205500	2.481248275	*ECI1*	Ortholog(s) have dodecenoyl-CoA delta-isomerase activity, role in fatty acid beta-oxidation, filamentous growth and peroxisome localization
CPAR2_800720	2.468074427	*OPT1*	Ortholog(s) have proton-dependent oligopeptide secondary active transmembrane transporter activity, tetrapeptide transmembrane transporter activity
CPAR2_302780	2.463534476	*C5_03690W_A*	
CPAR2_103200	2.342975463	*FUR4*	Pseudogene
CPAR2_602390	2.338988982	*C6_01420C_A*	Putative oxidoreductase; expression increased in fluconazole and voriconazole resistant strains
CPAR2_405290	2.29177377	*CDR1*	Ortholog(s) have ATP binding, drug binding, fluconazole transporter activity, phospholipid-translocating ATPase activity, xenobiotic-transporting ATPase activity
CPAR2_103080	2.287467581	*GLX3*	Ortholog(s) have glyoxalase III activity and role in cellular response to nutrient levels, cellular response to oxidative stress, methylglyoxal catabolic process to D-lactate via S-lactoyl-glutathione

CPAR2_800240	2.284063025	*OPT2*	Ortholog(s) have oligopeptide transmembrane transporter activity and role in nitrogen utilization, oligopeptide transmembrane transport
CPAR2_700870	2.244383043	*PGA6*	Putative GPI-anchored cell wall protein; ortholog of C. albicans orf19.4765/PGA6; expression increased in fluconazole and voriconazole resistant strains
CPAR2_102550	2.191941927	*FAA21*	Ortholog(s) have long-chain fatty acid-CoA ligase activity, medium-chain fatty acid-CoA ligase activity, very long-chain fatty acid-CoA ligase activity and role in long-chain fatty acid metabolic process
CPAR2_304270	2.190063355	*GRP2*	Similar to S. cerevisiae Gre2p (methylglyoxal reductase); expression increased in fluconazole and voriconazole resistant strains
CPAR2_204220	2.165445494	*ALK8*	Ortholog(s) have alkane 1-monooxygenase activity, oxygen binding activity and role in fatty acid omega-oxidation, lauric acid metabolic process
CPAR2_800020	2.107629768	*POT1*	Ortholog(s) have acetyl-CoA C-acyltransferase activity, mRNA binding activity, role in fatty acid beta-oxidation and mitochondrial intermembrane space, peroxisomal matrix localization
CPAR2_209750	2.094149889	*C2_05640W_A*	Ortholog(s) have role in filamentous growth
CPAR2_209850	2.07919037	*TES15*	Ortholog(s) have glyoxysome localization
CPAR2_503040	1.999850027	*FOX2*	Ortholog(s) have 3-hydroxyacyl-CoA dehydrogenase activity, 3-hydroxybutyryl-CoA epimerase activity, enoyl-CoA hydratase activity
CPAR2_106260	1.978403933	*C1_02270C_A*	Ortholog(s) have cytosol, nucleus localization
CPAR2_109800	1.961847171	*C1_01140C_A*	
CPAR2_208430	1.938195717	*COI1*	Ortholog(s) have cell surface, extracellular region localization
CPAR2_405280	1.917931809	*CDR1*	Ortholog(s) have role in fluconazole transport
CPAR2_213670	1.890075591	*PGA52*	Ortholog(s) have anchored component of plasma membrane, endoplasmic reticulum, fungal-type cell wall, mitochondrion localization
CPAR2_304110	1.846691183	*C5_00390C_A*	
CPAR2_801040	1.821295786	*CR_02570C_A*	Ortholog(s) have triglyceride lipase activity, role in triglyceride catabolic process and peroxisomal matrix localization
CPAR2_207300	1.814253043	*C1_10360C_A*	Protein of unknown function; expression increased in fluconazole and voriconazole resistant strains
CPAR2_807700	1.806876842	*POX1-3*	Ortholog(s) have role in fatty acid beta-oxidation and peroxisomal matrix localization

CPAR2_107140	1.800815294	*C1_04150C_A*	Has domain(s) with predicted hydrolase activity
CPAR2_206630	1.795626243	*C2_05130W_A*	Protein of unknown function; expression increased in fluconazole and voriconazole resistant strains
CPAR2_503540	1.780401329	*PTR22*	Ortholog(s) have dipeptide transmembrane transporter activity, tripeptide transporter activity and role in dipeptide transmembrane transport, tripeptide transport
CPAR2_208960	1.767915495	*C1_06920C_A*	
CPAR2_600460	1.742597811	*HGT10*	Has domain(s) with predicted substrate-specific transmembrane transporter activity, transmembrane transporter activity, role in transmembrane transport and integral component of membrane, membrane localization
CPAR2_802230	1.739837554	*CR_03540W_A*	Ortholog(s) have cytoplasm, lipid particle localization
CPAR2_700290	1.695825557	*C1_14020W_A*	Has domain(s) with predicted Rho GDP-dissociation inhibitor activity and cytoplasm localization
CPAR2_204330	1.660923151	*HSP104*	Ortholog(s) have ADP binding, ATP binding, ATPase activity, coupled, chaperone binding, misfolded protein binding, unfolded protein binding activity
CPAR2_303510	1.646877415	*TAC1*	Ortholog(s) have sequence-specific DNA binding, transcription coactivator activity, transcription factor activity, RNA polymerase II distal enhancer sequence-specific binding activity
CPAR2_603600	1.639560294	*FET31*	Ortholog(s) have role in cellular response to drug, ferrous iron import across plasma membrane and endoplasmic reticulum, plasma membrane localization, prostaglandin biosynthesis
CPAR2_500590	1.629695081	*GAT1*	Ortholog(s) have sequence-specific DNA binding, transcription factor activity, RNA polymerase II transcription factor binding and transcriptional activator activity
CPAR2_208020	1.628387873	*C1_07160C_A*	
CPAR2_600930	1.614743718	*C6_03370W_A*	
CPAR2_208190	1.606410269	*PHO84*	Ortholog(s) have phosphate:proton symporter activity
CPAR2_208160	1.605557038	*PHO84*	Ortholog(s) have inorganic phosphate transmembrane transporter activity, manganese ion transmembrane transporter activity, phosphate:proton symporter activity, selenite:proton symporter activity
CPAR2_406710	1.595465854	*ARE2*	Ortholog(s) have ergosterol O-acyltransferase activity, role in ergosterol metabolic process and endoplasmic reticulum localization

CPAR2_805510	1.593655443	*LEU2*	Ortholog(s) have 3-isopropylmalate dehydrogenase activity, role in glyoxylate cycle, leucine biosynthetic process, pathogenesis and biofilm matrix, cytosol localization
CPAR2_404310	1.592215777	*MDH1-3*	Ortholog(s) have L-malate dehydrogenase activity, mRNA binding activity, role in NADH regeneration, fatty acid beta-oxidation and peroxisomal importomer complex, peroxisomal matrix localization
CPAR2_105480	1.569347115	*C1_04460C_A*	Protein of unknown function; expression increased in fluconazole and voriconazole resistant strains
CPAR2_303750	1.535070361	*HMS1*	Ortholog(s) have transcription regulatory region DNA binding activity
CPAR2_700030	1.530620174	*CDR1*	Has domain(s) with predicted ATP binding, ATPase activity, ATPase activity, coupled to transmembrane movement of substances, nucleoside-triphosphatase activity, nucleotide binding activity and role in drug export, transport
CPAR2_807590	1.530311577	*C3_04730C_A*	
CPAR2_301610	1.510390828	*C7_00350C_A*	

Table S4: List of genes related to iron metabolism in *C. parapsilosis* with their corresponding orthologs in *C. albicans*

CPAR Gene ID	*Candida albicans* homologue	Function
CPAR2_210110	*CFL5*	Ferric reductase; induced in low iron; ciclopirox olamine, flucytosine induced; amphotericin B, Sfu1 repressed; Tbf1, Hap43 induced
CPAR2_700570	*FTR1*	High-affinity iron permease; required for mouse virulence, low-iron growth; iron, amphotericin B, caspofungin, ciclopirox, Hog1p, Sef1p, Sfu1p, and Hap43p regulated; complements S. cerevisiae ftr1 iron transport; Hap43p-repressed
CPAR2_303120	*CCC2*	Copper-transporting P-type ATPase of Golgi; required for wild-type iron assimilation (indirect effect via Fet3p); induced by iron starvation, ciclopirox olamine; caspofungin repressed; not required for virulence in mouse systemic infection
CPAR2_808120	*CFL5*	Ferric reductase; induced in low iron; ciclopirox olamine, flucytosine induced; amphotericin B, Sfu1 repressed; Tbf1, Hap43 induced
CPAR2_405240	*CCC1*	Manganese transporter; required for normal filamentous growth; mRNA binds She3, localized to hyphal tips; repressed by NO, alkaline pH; colony morphology-related regulation by Ssn6; regulated by Sef1, Sfu1, Hap43; Spider biofilm induced
CPAR2_402920	*RBT5*	GPI-linked cell wall protein; hemoglobin utilization; Rfg1, Rim101, Tbf1, Fe regulated; Sfu1, Hog1, Tup1, serum, alkaline pH, antifungal drugs, geldamycin repressed; Hap43 induced; required for RPMI biofilms; Spider biofilm induced
CPAR2_105690	*HMX1*	Heme oxygenase; utilization of hemin iron; transcript induced by heat, low iron, or hemin; repressed by Efg1; induced by low iron; upregulated by Rim101 at pH 8; Hap43-induced; Spider and flow model biofilm induced
CPAR2_700810	*SFU1*	GATA-type transcription factor; regulator of iron-responsive genes; represses iron utilization genes if iron is present; Hap43-repressed; promotes gastrointestinal commensalism in mice; Spider biofilm induce
CPAR2_209090	*HAP43*	CCAAT-binding factor-dependent transcription factor; repressor; also called CAP2; required for low iron response; similar to bZIP transcription factor AP-1; repressed by Sfu1; ciclopirox olamine induced; rat catheter, Spider biofilm induced
CPAR2_210100	*FTH1*	Protein similar to S. cerevisiae Fth1p, a high affinity iron transporter for intravacuolar stores of iron; repressed by Sfu1p, amphotericin B, caspofungin; induced by alkaline pH, ciclopirox olamine; regulated by Sef1p, Sfu1p, and Hap43p

CPAR2_801430	*SEF1*	Zn2-Cys6 transcription factor; regulates iron uptake; negatively regulated by Sfu1p, positively regulated by Tbf1; promotes virulence in mice; mutants display decreased colonization of mouse kidneys; Spider biofilm induced
CPAR2_406510	*AFT2*	Putative Aft domain transcription factor; role in regulation of iron metabolism, oxidative stress, adhesion, hyphal growth, colony morphology, virulence; complements S. cerevisiae aft1 mutation; Spider biofilm induced
CPAR2_407560	*SIT1*	Transporter of ferrichrome siderophores, not ferrioxamine B; required for human epithelial cell invasion in vitro, not for mouse systemic infection; regulated by iron, Sfu1, Rfg1, Tup1, Hap43; rat catheter and Spider biofilm induced
CPAR2_102830	*CCP1*	Cytochrome-c peroxidase N terminus; Rim101, alkaline pH repressed; induced in low iron or by macrophage interaction; oxygen-induced activity; regulated by Sef1, Sfu1, and Hap43; Spider biofilm induced; rat catheter biofilm repressed
CPAR2_406320	*HEM15*	Putative ferrochelatase involved in heme biosynthesis; transcript not regulated by iron levels and not affected by a yfh1 null mutation; Spider biofilm repressed

Table S5: MRM characteristics of the monitored eicosanoids

Name entry	Compound	Lipid Maps ID	Retention time (min)	m/z in Q1	m/z in Q3	Declustering potential [V]	Collision energy [V]	Collision cell exit potential [V]	Group	_2 method	_5 method
ALA_2	ALA	LMFA01030152	8.6	277	182.1	-55	-24	-7	Polyunsaturated fatty acids	0	1
GLA	GLA	LMFA01030141	8.6	277	179.1	-75	-20	-11	Polyunsaturated fatty acids	0	1
	13,14-dihydro-15-keto-PGE2	LMFA03010031	4.8	351.1	235	-45	-30	-13	Prostaglandins (PG)	1	1
19(20)EpDPA	19(20)-EpDPA	LMFA04000038	8.1	343.1	281.1	-70	-16	-11	Epoxydocosapentaenoic acids	0	1
	11(12)-EET	LMFA03080004	8.2	318.9	166.9	-90	-18	-19	Epoxyeicosatrienoic acids (EET)	1	1
	14(15)-EET	LMFA03080005	8.1	319	218.9	-5	-16	-55	Epoxyeicosatrienoic acids (EET)	1	1
	8(9)-EET	LMFA03080003	8.2	319	154.9	-60	-18	-13	Epoxyeicosatrienoic acids (EET)	1	1
	10-HDHA	LMFA04000027	7.9	343.1	153	-25	-20	-15	Hydroxydocosahexaenoic acids (HDHA)	1	1
14(S)-HDHA	14(S)-HDHA	LMFA04000058	8.0	343.1	204.9	-60	-18	-27	Hydroxydocosahexaenoic acids (HDHA)	0	1
	17-HDHA	LMFA04000072	7.9	343.1	245	-65	-16	-15	Hydroxydocosahexaenoic acids (HDHA)	1	1
4-HDHA	4-HDHA	LMFA04000058	8.2	343.1	101	-50	-18	-9	Hydroxydocosahexaenoic acids (HDHA)	0	1
	7-HDHA	LMFA04000025	8.0	343.1	141.1	-85	-18	-23	Hydroxydocosahexaenoic acids (HDHA)	1	1
	19,20-DiHDPA	LMFA04000043	7.4	361.1	273	-55	-22	-15	Hydroxydocosapentaenoic acids (HDPA)	1	1
	7,17-DiHDPA	N/A	7.0	361.1	198.9	-45	-26	-23	Hydroxydocosapentaenoic acids (HDPA)	1	1
12-HEPE	12-HEPE	LMFA03070031	7.6	317	179	-60	-18	-17	Hydroxyeicosapentaenoic acids (HEPE)	0	1

	15-HEPE	LMFA03070009	7.5	317.1	219	-65	-18	-19	Hydroxyeicosapentaenoic acids (HEPE)	1	1
	18-HEPE	LMFA03070038	7.4	317.1	259	-5	-16	-7	Hydroxyeicosapentaenoic acids (HEPE)	1	1
5-HEPE	5-HEPE	LMFA03070027	7.7	317	114.9	-55	-18	-11	Hydroxyeicosapentaenoic acids (HEPE)	0	1
	11-HETE	LMFA03060003	7.9	319.1	167	-70	-22	-15	Hydroxyeicosatetraenoic acids (HETE)	1	1
	12-HETE	LMFA03060007	7.9	319.1	179	-65	-20	-23	Hydroxyeicosatetraenoic acids (HETE)	1	1
	14,15-diHETE	LMFA03060077	7.0	335.1	207	-65	-24	-21	Hydroxyeicosatetraenoic acids (HETE)	1	1
	15-HETE	LMFA03060001	7.8	319.1	219.1	-55	-18	-9	Hydroxyeicosatetraenoic acids (HETE)	1	1
	17-OH-DH-HETE	N/A	8.2	347.1	247	-110	-22	-27	Hydroxyeicosatetraenoic acids (HETE)	1	1
20-HETE_2	20-HETE	LMFA03060009	7.7	319	289.1	-70	-24	-15	Hydroxyeicosatetraenoic acids (HETE)	0	1
	5,15-diHETE	LMFA03060010	6.8	335	173.1	-55	-20	-11	Hydroxyeicosatetraenoic acids (HETE)	1	1
	5-HETE	LMFA03060002	8.0	319.1	115	-65	-18	-11	Hydroxyeicosatetraenoic acids (HETE)	1	1
	8(S),15(S)-diHETE	LMFA03060050	6.7	335.1	207.9	-55	-22	-17	Hydroxyeicosatetraenoic acids (HETE)	1	1
	8-HETE	LMFA03060006	7.9	319.1	154.9	-70	-20	-19	Hydroxyeicosatetraenoic acids (HETE)	1	1
	13-HoDE	LMFA02000228	7.7	295	194.9	-110	-24	-21	Hydroxyoctadecadienoic acids (HoDE)	1	1
	9-HoDE	LMFA02000188	7.7	295	171	-130	-22	-7	Hydroxyoctadecadienoic acids (HoDE)	1	1
	13-HoTrE	LMFA02000051	7.4	293	195	-45	-24	-19	Hydroxyoctadecatrienoic acids (HoTrE)	1	1
	9-HoTrE	LMFA02000024	7.4	293	170.9	-75	-20	-15	Hydroxyoctadecatrienoic acids (HoTrE)	1	1
	15-HETE-d8	LMFA03060080	7.8	327.2	226	-85	-18	-11	Internal standards	1	1
	DHA-d5	LMFA01030762	8.8	332	288.1	-75	-16	-13	Internal standards	1	1
	LTB4-d4	LMFA03020030	6.9	339.1	196.9	-70	-22	-19	Internal standards	1	1

	PGE2-d4	LMFA03010008	4.9	355.1	193	-50	-26	-17	Internal standards	1	1
	17-F2t-dihomo-IsoP	LMFA03110167	6.1	381.1	318.9	-115	-32	-41	Isoprostanes (IsoP) and neuroprostanes (NeuroP)	1	1
	4-F4t-NeuroP	N/A	5.2	377.1	270.9	-15	-26	-13	Isoprostanes (IsoP) and neuroprostanes (NeuroP)	1	1
	5-F3t-IsoP	N/A	3.8	351	114.8	-95	-26	-13	Isoprostanes (IsoP) and neuroprostanes (NeuroP)	1	1
12-KETE	12-KETE	LMFA03060019	7.9	317	153	-60	-22	-9	Keto-eicosatetraenoic acids (KETE/OxoETE)	0	1
15-KETE	15-KETE	LMFA03060051	7.8	317	113	-10	-22	-5	Keto-eicosatetraenoic acids (KETE/OxoETE)	0	1
5-KETE	5-KETE	LMFA03060011	8.1	317	203.1	-70	-24	-11	Keto-eicosatetraenoic acids (KETE/OxoETE)	0	1
	20-OH-LTB4	LMFA03020018	4.0	351.1	195	-60	-24	-17	Leukotrienes (LT)	1	1
	6-trans-12-epi-LTB4	LMFA03020014	6.8	335.1	194.9	-80	-22	-25	Leukotrienes (LT)	1	1
	6-trans-LTB4	LMFA03020013	6.7	335.1	194.9	-105	-22	-11	Leukotrienes (LT)	1	1
	LTB4	LMFA03020001	6.9	335.1	195	-65	-22	-21	Leukotrienes (LT)	1	1
	LTD4	LMFA03020006	6.7	495.1	177	-70	-28	-19	Leukotrienes (LT)	1	1
	LTE4	LMFA03020002	7.0	438.1	333.1	-55	-26	-15	Leukotrienes (LT)	1	1
	AT-LXA4	LMFA03040003	5.6	351.1	114.9	-20	-22	-11	Lipoxins (LX)	1	1
	LXA4	LMFA03040001	5.5	351.1	114.8	-40	-20	-11	Lipoxins (LX)	1	1
	LXB4	LMFA03040002	5.1	351.1	220.9	-60	-22	-13	Lipoxins (LX)	1	1
	Mar1	LMFA04050001	7.0	359.2	250.2	-65	-20	-13	Maresins (MaR)	1	1
	7(S)-MaR1	N/A	6.6	359.1	249.9	-20	-20	-19	Maresins (MaR)	1	1
	AA	LMFA01030001	8.8	303	205.1	-155	-20	-11	Polyunsaturated fatty acids	1	1
	AdA	LMFA01030178	9.1	331.1	233	-130	-22	-11	Polyunsaturated fatty acids	1	1
	ALA (+ GLA)	LMFA01030152 (LMFA01030141)	8.6	277	233	-90	-22	-29	Polyunsaturated fatty acids	1	1
DGLA	DGLA	LMFA01030158	9.0	305.1	261.2	-85	-22	-13	Polyunsaturated fatty acids	0	1
	DHA	LMFA01030185	8.8	327.1	229.2	-115	-18	-11	Polyunsaturated fatty acids	1	1
	DPAn-3	LMFA04000044	8.9	329.1	231.1	-50	-20	-17	Polyunsaturated fatty acids	1	1
DPAn-6	DPAn-6	LMFA01030182							Polyunsaturated fatty acids	0	1
	EPA	LMFA01030759	8.6	301	202.9	-125	-18	-21	Polyunsaturated fatty acids	1	1

	LA	LMFA01030120	8.8	279	261	-115	-28	-13	Polyunsaturated fatty acids	1	1
	13,14-dihydro-15-keto-PGF2alpha	LMFA03010027	5.4	353.1	195	-110	-32	-11	Prostaglandins (PG)	1	1
	15-deoxy-PGJ2	LMFA03010021	7.3	315	203	-50	-28	-19	Prostaglandins (PG)	1	1
	15-keto-PGE2	LMFA03010030	4.5	349	234.9	-65	-20	-13	Prostaglandins (PG)	1	1
	8-iso-PGE2	LMFA03110003	4.6	351.1	271	-5	-24	-19	Prostaglandins (PG)	1	1
	8-iso-PGF2alpha	LMFA03110001	4.5	353.1	193	-135	-34	-11	Prostaglandins (PG)	1	1
	PGD2	LMFA03010004	5.0	351.1	233	-30	-16	-13	Prostaglandins (PG)	1	1
	PGE2	LMFA03010003	4.9	351.2	271.1	-50	-22	-21	Prostaglandins (PG)	1	1
	PGF2alpha	LMFA03010002	5.2	353.1	193	-80	-34	-11	Prostaglandins (PG)	1	1
	PGJ2	LMFA03010019	6.1	333	271	-30	-22	-17	Prostaglandins (PG)	1	1
	PD1	LMFA04040001	6.9	359.1	153	-70	-22	-9	Protectins (PD)	1	1
	PDX	LMFA04040003	6.8	359.1	153	-70	-22	-9	Protectins (PD)	1	1
	18R-RvE3	LMFA03140006	7.1	333.1	245	-55	-18	-23	Resolvins (Rv)	1	1
	18S-RvE3	LMFA03140007	6.7	333.1	245.2	-25	-16	-17	Resolvins (Rv)	1	1
	AT-RvD1	LMFA04030005	5.7	375	215	-50	-26	-11	Resolvins (Rv)	1	1
	RvD1	LMFA04030011	5.6	375.1	215	-50	-26	-11	Resolvins (Rv)	1	1
	RvD2	LMFA04030001	5.3	375.1	277.1	-60	-18	-15	Resolvins (Rv)	1	1
	RvE1	LMFA03140003	3.8	349.1	195	-95	-22	-13	Resolvins (Rv)	1	1
	RvE2	LMFA03140011	6.1	333.1	114.9	-35	-18	-15	Resolvins (Rv)	1	1
	TXB2	LMFA03030002	4.6	369.1	169	-55	-24	-15	Thromboxanes (Tx)	1	1

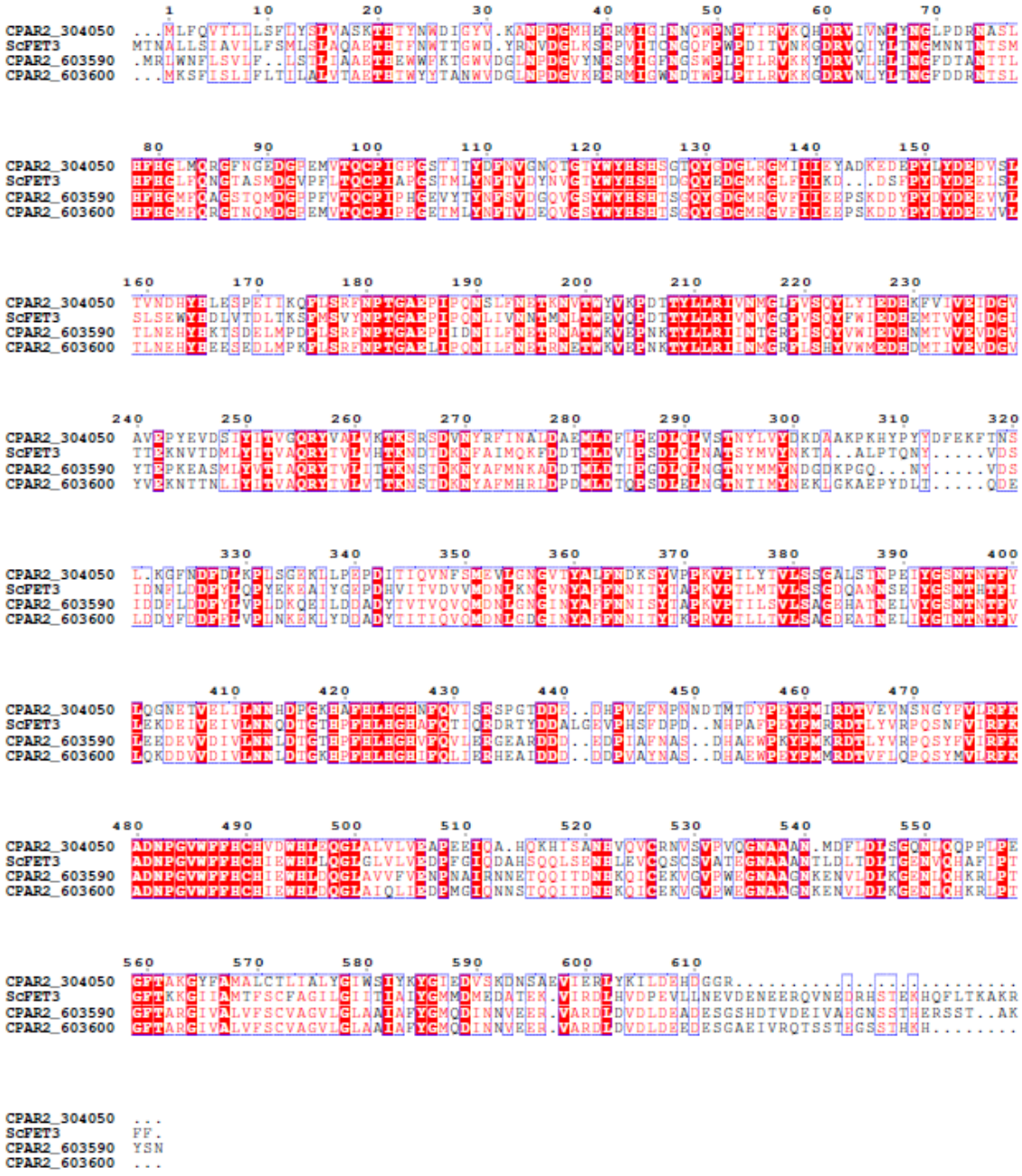

Fig S1: *In silico* analysis of multicopper oxidase genes in *C. parapsilosis*
Using *Sc*Fet3p as a query sequence, three putative multicopper oxidases were identified by *in silico* data analysis.